Inter-cell Coordination for Interference Mitigation in Multi-tier Wireless Networks

AKINDELE SEGUN AFOLABI

(Degree)
博士（学術）

(Date of Degree)
2012-09-25

(Date of Publication)
2012-10-22

(Resource Type)
doctoral thesis

(Report Number)
甲5625

(URL)
https://hdl.handle.net/20.500.14094/D1005625

Doctoral Dissertation

Inter-cell Coordination for Interference Mitigation in Multi-tier Wireless Networks

マルチ階層無線ネットワークにおける与干渉軽減のためのセル間協調

July 2012

Graduate School of Engineering
Kobe University

Akindele Segun Afolabi

INTER-CELL COORDINATION FOR INTERFERENCE MITIGATION IN MULTI-TIER WIRELESS NETWORKS

By

Akindele Segun Afolabi

SUBMITTED IN PARTIAL FULFILLMENT OF THE
REQUIREMENTS FOR THE DEGREE OF
DOCTOR OF PHILOSOPHY
AT
KOBE UNIVERSITY
KOBE, JAPAN
JULY 2012

KOBE UNIVERSITY

Date: **July 2012**

Author: **Akindele Segun Afolabi**

Title: **Inter-cell Coordination for Interference Mitigation in Multi-tier Wireless Networks**

Department: **Computer Science and Systems Engineering**

Degree: **Ph.D.**

To my parents

Table of Contents

List of Tables

List of Figures

Abstract

Recently, the demand for higher data rate from wireless devices has been experiencing an exponential growth, and this growth is attributable to the proliferation of sophisticated devices such as smart-phones and tablet computers that are enabled for broadband services. In order to cope with this traffic demand trend, operators and service providers are considering integrating OFDMA-based (Orthogonal Frequency Division Multiple Access) femtocells on the existing cellular network. A femtocell is a low-power, user-deployed indoor base station that backhauls users' data to the core network through a broadband connection. Base station deployment in current cellular systems is usually preceded by a detailed network planning and optimization procedure. Femtocells, however, will be deployed in an ad hoc manner, thus making planning and optimization in femtocell networks challenging, and consequently leading to coordination and interference problems.

This thesis addresses some of the major technical problems that are delaying the widespread deployment of femtocells. One of these problems is that, it is very difficult to coordinate a large number of femtocells in a network centrally. It is even more difficult when the femtocells are randomly deployed by end-users that lack RF (Radio Frequency) technical skills. Femtocells are, however, devices envisaged to address the difficulties involved in delivering true broadband services to end-users in the current cellular age. Hence, resolving the technical issues delaying femtocell's widespread deployment is inevitable and it is the focus of this thesis. In this thesis, we provide feasible solutions to coordination problems in multi-tier cellular networks, and the proposed coordination techniques have proven effective at mitigating interference.

The extent of the effectiveness of the proposed coordination techniques have been demonstrated through system level simulations.

Chapter 1 of this thesis describes cellular technology history and the current cellular trend. It also contains our contributions and the outline of this thesis.

Chapter 2 of this thesis describes coordination techniques for interference mitigation in multi-tier networks. Coordination is necessary for appropriate resource distribution among co-tier and cross-tier base stations, and if effectively done, mitigates interference. Interference is tightly linked to coordination such that, poor inter-cell coordination between base stations that closely located results in interference. Coordination can either be achieved in a centralized manner or in a distributed manner. Due to the expected large number of femtocells that will be deployed, distributed coordination will be more applicable to the femtocell case than its centralized counterpart.

Chapter 3 of this thesis treats inter-cell coordination from the perspective of a resource partitioning problem. A good resource partitioning method ensures that each user in a network receives a fair portion of the network resources. We solve resource partitioning problem using FFR (Fractional Frequency Reuse) scheme and mathematical tools. Our method focuses on modeling network resource partitioning parameters in a way that jointly achieves macrocell user fairness and femtocell user maximum throughput. The partitioning method adopted ensures that femtocells use frequency sub-bands that are orthogonal to those used by the macrocell in the regions where they (femtocells) are deployed; hence interference between the macrocell tier and the femtocell tier is substantially reduced. The partitioning results obtained serve as important references for the deployment of OFDMA-based multi-tier systems.

Chapter 4 of this thesis discusses inter-cell coordination in the context of femtocell-to-femtocell interference mitigation. We have proposed a distributed solution to femtocell interference mitigation that relies on cooperation among closely located femtocells. In our scheme, femtocells are grouped into clusters and the cluster-heads of each cluster coordinate network resource usage by their cluster-members. Simulation results show that the throughput performance of our proposed cooperative scheme is superior to that of the autonomous scheme under various network densities and various user-to-base station separation distances.

Chapter 5 of this thesis considers inter-cell coordination for femtocell-to-macrocell interference mitigation. We focus attention on how to minimize femto-to-macro interference through a macrocell batch scheduling and femtocell power control method. In particular, we develop a proportional fair scheduling framework for the macrocell in which macrocells are able to assign multiple TTIs (Transmission Time Intervals) to their scheduled users. This helps to improve femtocell's interference avoidance capability. System level simulations are conducted, and throughput results show the effectiveness of our scheme at mitigating interference. Our scheme also improves network-wide fairness while conforming with the 3GPP-LTE (3rd Generation Partnership Project - Long Term Evolution) standard specification that prohibits macrocell-femtocell direct coordination.

Chapter 6 of this thesis contains the general conclusions and future work. The inter-cell coordination schemes proposed in Chapters 3 to 5 work well in OFDMA-based multi-tier networks. All the schemes have followed a distributed coordination approach which is very attractive for femtocell networks (ad hoc-like networks) in which detailed RF planning and optimization is challenging.

Acknowledgements

The successful completion of this research is as a result of the kindness and support that I received from some people, and I would like to express my appreciation to them.

This research was carried out in Professor Hisashi Tamaki's laboratory (CS14), the Emergent Computing laboratory of the Department of Computer Science and Systems Engineering, Kobe University.

First, I would like to thank my main Adviser, Professor Hisashi Tamaki, for guiding me towards the successful completion of this doctoral research. I also thank him for providing all the necessary facilities used during the course of the research, and most importantly for the technical advice I received from his rich bank of knowledge. For these, I want to express my profound gratitude by saying a big thank you. Special thanks go to Professor Toshiya Kaihara and Professor Masakatsu Morii, my co-advisers, for the highly valuable comments I received from them which have improved the quality of this dissertation. Finally, I want to express deep appreciation to Professor Chikara Ohta, my principal adviser, for all he has done for me towards ensuring that this research ends successfully. I really thank him for helping to deepen my knowledge on wireless communications and also for helping to polish my research and technical writing skills.

I would like to thank all the members of CS14 laboratory for sharing ideas with me in various ways and also for introducing me to the beauty of the Japanese Culture. I say a big thank you to you all.

This research has been possible as a result of the financial support I received from the Japanese Government under the *MEXT* scholarship programme from 2009 to 2012. I really thank the Japanese Government for the magnanimosity.

I want to thank my bosses, Professor Tunji Samuel Ibiyemi and Dr. Jayeola Femi Opadiji, for their kindness. Many thanks goes to Mrs. Adenike Bamise, Mrs. Folashade Oladoja, Ms. Rolake Afolabi, and Ms. Gbemisola Afolabi for being loving sisters to me. My parents, Late Barrister Rufus Ajibola Afolabi and Mrs Janet Idowu Afolabi, have been sources of inspiration, support and encouragement to me. I really appreciate your parental love, and for this, I say, "thanks a million".

Lastly I want to thank God for the wisdom and understanding that he has given to me which has made this research work to see the light of the day.

Akindele Segun Afolabi
Kobe, Japan
July 25, 2012

Chapter 1

Introduction

1.1 Preliminaries

Cellular communication technology has experienced tremendous changes over the years due to the ever changing volume and nature of traffic it carries. Since cellular communication technology constitutes one of the most important communication technologies in today's wireless systems, the need to study it in order to improve its efficiency can not be overemphasized.

1.1.1 Cellular network evolution

The radio resources of wireless networks are limited. This limitation therefore has been motivating the planning and design of wireless networks to focus on improving the 3Cs of wireless communication, i.e., cost, coverage, and capacity; it is generally desired to have a large radio coverage and a high capacity at the minimum possible cost. The cellular concept provides a way of partly addressing this resources limitation issue. For example, if a single transmitter is assigned to serve all the users located in a large geographical area, a significantly high amount of power would be required to serve each of the users that are separated by large distances. Moreover, the size of bandwidth assigned to each of the users shrinks as the users' population size grows, leading to a low spectral efficiency. Improved spectral efficiency can be achieved through the cellular concept which exploits the power falloff with distance of signal propagation to reuse the same frequency channel at spatially separated locations [1].

In cellular systems, the associated challenge of serving a large geographical area is addressed by dividing the service area into multiple cells with a base station deployed in each cell. Hence, mobile networks adopted the cellular concept which began with the 1G (First Generation) cellular systems that were deployed before 1990. The 1G systems were based on FDMA (Frequency Division Multiple Access) PHY (physical) layer technology.

In FDMA, the frequency spectrum is split into a number of channels and each user is assigned a channel pair for downlink and uplink communication. To prevent adjacent channel interference, a guard band in inserted in between adjacent channels; this makes FDMA to be spectrum inefficient. The 1G cellular systems were succeeded by the 2G (Second Generation) cellular systems which were based on TDMA (Time Division Multiple Access) PHY layer technology. In TDMA, the time component is divided into slots which each user accesses in a periodic manner. Following the 2G cellular system is the 3G (Third Generation) cellular system which employs the CDMA (Code Division Multiple Access) PHY layer technology. In CDMA, orthogonal codes are used to spread signal energy over the frequency to allow multiple users to be separated at the receiver. The *near-far* problem in which high power users close to the base station drowns the signals of the other users located at farther distances from the base station is a major challenge of CDMA systems.

The ever growing traffic demand has necessitated the migration to the next generation cellular network. More recently, the wireless traffic demand growth has been exponential which is attributable to the proliferation of data dongles, tablet computers with 3G radio modules, and smart phones with rich multimedia content. In fact, the global mobile data has been projected to increase by a whopping 26-fold between 2010 and 2015 [2]. A higher area spectral efficiency is therefore necessary to cope with this evolving traffic demand trend.

In light of this, the next generation cellular networks will employ OFDMA (Orthogonal Frequency Division Multiple Access) [3] PHY layer technology. This is because OFDMA can provide additional capacity gain through frequency domain diversity as well multiuser diversity exploitation. This contrasts earlier PHY layer technologies.

Table 1.1: Comparison of femtocell and other wireless devices [4].

	Wi-Fi access point	**Cordless telephone**	**Repeater stations**	**Outdoor cellular base station**	**Femtocell**
Operates in licensed spectrum	No	No	Yes	Yes	Yes
Supports power control	No	No	Yes	Yes	Yes
Robust security	No	Yes	Not applicable	Yes	Yes
Provides voice and data services	Yes	No	Yes	Yes	Yes
Provides wide area mobility	No	No	Not applicable	Yes	Yes
Supports existing personal devices	No	No	Yes	Yes	Yes
Consumer device and consumer purchase	Yes	Yes	No	No	Yes
Consumer installation	Yes	Yes	No	No	Yes

1.1.2 Multi-tier network

Since 1957, shrinking cell size has yielded a 1600× gain in wireless capacity [5]. Hence, a further reduction in cell size is envisaged since frequency reuse provides a more efficient use of the limited available spectrum. In particular, femtocells, which are small-size cells that provide a cost effective means of achieving ubiquitous connectivity, will play major roles in future cellular networks. A femtocell is a low-power cellular access point envisioned for indoor placement to extend macrocell coverage. It can be installed by the end-user in a plug-and-play mode (zero-touch install). The user data is backhauled from the femtocell access point to the core network over a broadband connection such as DSL (digital subscriber line) [6], optical fiber, etc. It is expected that the legacy macrocell tier will be overlaid on the femtocell tier to yield a multi-tier network, thus enabling spectrum reuse. Some similarities and differences between the femtocell and other wireless devices are illustrated in Tab. 1.1. A lot of benefits are associated with the introduction of femtocells in cellular networks. To mention a few, the indoor placement of femtocells brings the user and the base station transceiver closer to each other, thereby reducing path loss (including the undesired penetration losses due to the external walls of buildings). Also, part of the macrocell traffic can be offloaded to the femtocell, which promotes increased bandwidth per macrocell user (since doing so reduces the number of users attached to the macrocell). Increased bandwidth per user is not seen by the macrocell users alone but also by the femtocell users as well, leading to a *win-win* experience.

In addition, the femtocell users' battery life gets extended due to their (femtocell users) close proximities with their serving femtocell base stations; this is so because the required transmission power for a low-range transmission is usually small. Some

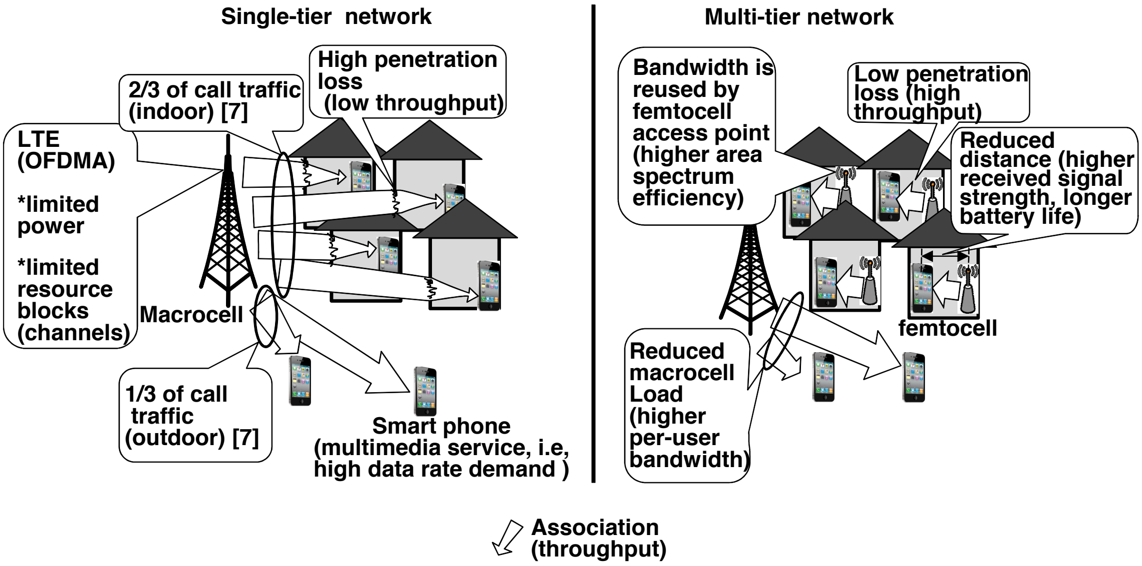

Figure 1.1: Some merits of multi-tier networks.

merits of multi-tier networks are highlighted in Fig. 1.1. Although, while frequency-reuse by the femtocell provides a more efficient usage of the limited available spectrum, it also introduces unwanted co-channel interference which must be addressed [1].

1.1.3 Interference

Depending on the nature and source of interference, interference can be classified as [8]:

- By nature: Co-channel or Adjacent-channel interference

  When two different signals are being transmitted on the same channel, co-channel interference occurs. If the two signals are being transmitted on different channels but the guard band is not sufficiently large, adjacent-channel interference occurs.

- By source: Inter- and Intra-cell interference

  When two different signals are being transmitted by the same sector, intra-cell interference occurs. If, however, they are carried by different but neighboring sectors, inter-cell interference occurs.

The inter-cell interference problem associated with the coexistence of femtocell and macrocell tiers has sparked extensive discussion by the 3GPP (Third Generation Partnership Project) [9]–[16]. The 3GPP, which was created in 1999 to harmonize the worldwide 3G WCDMA (Wideband CDMA) standardization effort, and the Broadband Forum (BBF) are the two main SDOs (Standard Development Organizations) involved in shaping the UMTS (Universal Mobile Telecommunications System)-related femto technology [17]. Other non-SDOs involved in seeking ways of achieving a successful integration of the femtocell on the existing cellular network include the Femto Forum and the NGMN (Next Generation Mobile Network).

Traditional approaches to interference mitigation between transmitted signals have focused on either ensuring orthogonality between transmitted signals in time, frequency as well as spatially, or by actively removing the desired signal if orthogonality between the desired signal and potential interfering signals cannot be achieved [18]. In early 2G cellular systems, such orthogonality was achieved primarily through static pre-planned allocations of radio resources. On the other hand, 3G systems introduced interference cancellation techniques based on a combination of blind information gathering at a base station such as spectrum usage monitoring and coarse exchange of interference indicators such as RoT (Rise over Thermal) indicator [18]. Other ways of interference mitigation include antenna tilting, power control and the use of distributed antennas in which a subscriber is served by its closest antenna.

1.2 Research goal

Since the introduction of femtocells in the existing macrocell networks brings with it an added challenge of interference, it is imperative to focus attention on the mitigation of interference in co-existing femtocell and macrocell networks. This thesis aims at developing schemes for the mitigation of inter-cell interference between macrocells and femtocells, and also among collocated femtocells. Although, downlink communication is the main focus of this thesis, channel reciprocity, however, makes the downlink schemes applicable to the uplink case as well. Hence, we focus on the mitigation of downlink interference using methods such as power control, frequency domain separation, and time domain separation techniques which are introduced in Chapter 2.

1.3 Contributions

Below is a summary of the contributions of this thesis:

We address the problem of fair resource partitioning in multi-tier wireless networks through mathematical formulation in Chapter 3. The macrocell resources are partitioned based on FFR (Fractional Frequency Reuse) in order to ensure an easy coordination procedure at the femtocell (i.e., a simplified spectrum sensing and spectrum access procedure). The formulation takes into consideration the power decay problem which cell-edge macrocell users suffer. A numerical search procedure is used to find the per-user capacity region that ensures a cell-wide throughput fairness among macrocell users. Since it is desired that femtocells should cause as little degradation as possible to the existing macrocell network, the values of resource partitioning parameters that maintains the established cell-wide throughput fairness at the macrocell as well as maximizes the femtocell throughput are obtained. The formulation shows that under a fair macrocell user throughput condition, the relationship between cell-area partitioning and bandwidth partitioning is largely dependent on the path loss exponent of the network considered.

A cooperative channel assignment scheme is developed for inter-cell coordination among femtocell base stations in Chapter 4. The scheme shares the attractive better solutions of centralized systems and the low complexity of distributed control systems. Simulation results show that capacity gain is achievable if neighbor femtocell base stations intelligently and cooperatively select channel resources with a common goal of minimizing interference. Precisely, neighboring femtocells are grouped together under a *cluster-head* (the *cluster-head* is also a femtocell) that assumes the responsibility of a local controller for radio resource management. Two variants of the scheme are investigated, namely, *fair cluster* and *greedy cluster* schemes, respectively. We compare their throughput performances with the existing *autonomous* scheme, and results show that *cluster* scheme always achieve superior throughput performances under low to medium network load conditions. We also show that in high density networks, *greedy cluster* scheme achieves only a little performance improvement on *autonomous* scheme, revealing that inter-cluster cooperation is necessary at such network density if the benefit of clustering is to be realized.

A batch-based proportional fair scheduler is developed in Chapter 5 for inter-cell coordination between macrocells and femtocells. The scheduler allocates resource blocks (i.e., channels) to mobile nodes for a time duration that spans multiple consecutive subframes of an LTE (Long Term Evolution) system. This scheduling approach easily addresses the femtocell-macrocell resource scheduling collision problem common in existing dynamic resource block allocation method of the LTE standard. A mathematical formulation for appropriately updating the average throughput in a batch proportional-fair scheduling framework is developed. Through system level simulations, we show that batch-based proportional fair scheduling offers substantial throughput gain to public users that are trapped in the coverage area of femtocells that operate in the CSG (Closed Subscribers Group) mode. The proposed scheme requires no direct coordination between the femtocell and the macrocell, hence, conforms with the LTE standard requirement. In addition, batch-based proportional fair scheduling improves the network-wide throughput fairness through the mitigation of femto-to-macro interference.

1.4 Outline of thesis

This thesis is organized as follows:

Chapter 1 of this thesis discusses cellular evolutionary trend. Some physical layer technologies are discussed, and the concepts of multi-tier network and interference are introduced.

Chapter 2 discusses background on interference mitigation and inter-cell coordination. In particular, we describe various interference mitigation techniques and discus inter-cell coordination techniques used in coexisting femtocell and macrocell networks.

Chapter 3 addresses the problem of radio resource partitioning. The chapter discusses how to analytically find the values of radio resources partitioning parameters that considers both macrocell users throughput fairness and femtocell throughput maximization.

In Chapter 4, we introduce the proposed cooperative channel assignment scheme for inter-cell coordination among femtocells. The concept of channel assignment is discussed alongside related works. The performance of the proposed scheme is evaluated and conclusions are provided.

In Chapter 5, batch resource scheduling for interference reduction between macrocell and femtocell is discussed. Theoretical background on scheduling is provided. The implementation feasibility of batch scheduling is discussed, and simulation results are presented after which conclusions follow.

Finally the thesis ends with conclusions and future works in Chapter 6. In the chapter, we generally discus the performance of the proposed schemes, and explain how to merge them together for coexistence in the same network. At the end of the chapter, we explain our future works.

Chapter 2

Background on interference mitigation and inter-cell coordination

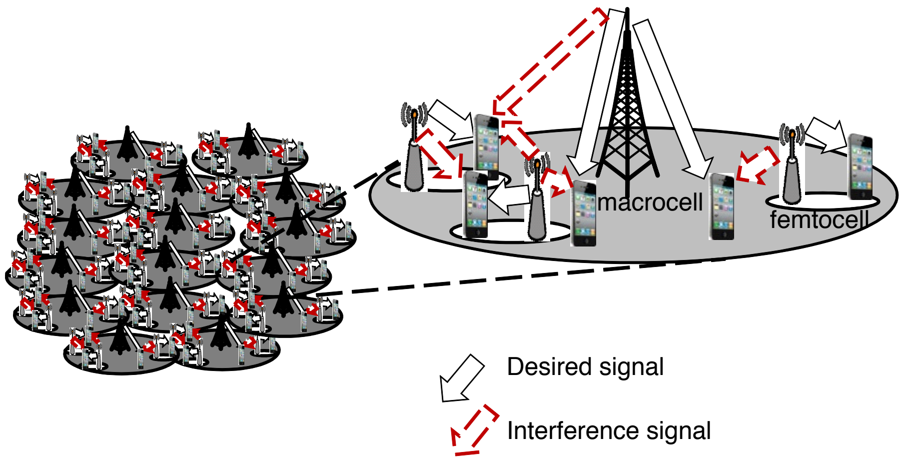

Figure 2.1: A multi-tier network showing a typical interference scenario.

2.1 Interference mitigation

Consider the network illustrated in Fig. 2.1, which comprises of a set $\mathcal{M}$ of macrocell BSs (base stations) of cardinality M such that a femtocell BS set $\mathcal{F}_m$ of cardinality F_m

are deployed in each macrocell BS. All the cells share channel set $\mathcal{B}$ of cardinality B with full frequency reuse. The cardinality of the set of macrocell users, $\mathcal{U}_m$, associated with macrocell BS $m \in \mathcal{M}$ is denoted as U_m, while the set of users, $\mathcal{U}_{f,m}$, associated with femtocell base station $f \in \mathcal{F}_m$ is of cardinality $U_{f,m}$. Let $\psi = \mathcal{U}_1 \cup \cdots \cup \mathcal{U}_M \cup \cdots \cup \mathcal{U}_{1,1} \cup \cdots \cup \mathcal{U}_{1,F} \cup \cdots \cup \mathcal{U}_{M,1} \cup \cdots \cup \mathcal{U}_{M,F}$ be the set of all users in the network, while $\Omega = \mathcal{M} \cup \mathcal{F}_1 \cup \cdots \cup \mathcal{F}_M$ denotes all the BSs in the network. Denote the serving base station of a served user $k \in \psi$ that is served on channel $b \in \mathcal{B}$ as s, and the power assigned to the user on channel b as $p_{b,s}$. The maximum total power constraint at s is

$$\sum_{b=1}^{B} p_{b,s} \leq \mathrm{P_T}, \quad \forall s, \tag{2.1.1}$$

where $\mathrm{P_T}$ is a constant which denotes the total power available at each base station s. Let the complex channel gain between base station s and user k on channel b be denoted as $h_{s,k}(b)$. The received signal at k on channel b is:

$$y_k(b) = \sqrt{p_{b,s}} \cdot h_{s,k}(b) x_s(b) + \sum_{i \in \Omega, i \neq s} \sqrt{p_{b,i}} \cdot h_{i,k}(b) x_i(b) + n_k(b), \tag{2.1.2}$$

where $x_s(b)$ denotes the data symbol of serving base station s, $x_i(b)$ is the interfering data symbol of neighbor base station i, and $n_k(b)$ is the Gaussian noise of variance N_0. The SINR (Signal to Noise plus Interference Ratio) of user k on channel b is given by:

$$\gamma_{s,k}(b) = \frac{p_{b,s} \cdot |h_{s,k}(b)|^2}{I_k(b) + N_0}, \tag{2.1.3}$$

where $I_k(b)$ is the out of cell interference written as:

$$I_k(b) = \sum_{i \in \Omega, i \neq s} p_{b,i} \cdot |h_{i,k}(b)|^2. \tag{2.1.4}$$

Let $\gamma_{\max}$ and $\gamma_{\min}$ denote the system-configured maximum and minimum values of SINR such that $\gamma_{\min} \leq \gamma_{s,k}(b) \leq \gamma_{\max}$ is necessary for a successful decoding of $x_s(b)$.

The corresponding received interference at $\gamma_{\min}$ is:

$$I_{\max} = \frac{p_{b,s} \cdot |h_{s,k}(b)|^2}{\gamma_{\min}} - N_0, \tag{2.1.5}$$

while the corresponding received interference at $\gamma_{\max}$ is:

$$I_{\min} = \frac{p_{b,s} \cdot |h_{s,k}(b)|^2}{\gamma_{\max}} - N_0, \tag{2.1.6}$$

and the achievable rate by user k on channel b according to *Shannon*'s capacity equation is [19],[20]:

$$R_{s,k}(b) = \begin{cases} 0 & \text{for } \gamma_{s,k}(b) < \gamma_{\min}, \\ \log_2(1 + \gamma_{s,k}(b)) & \text{for } \gamma_{\min} < \gamma_{s,k}(b) < \gamma_{\max}, \\ \log_2(1 + \gamma_{\max}) & \text{for } \gamma_{s,k}(b) > \gamma_{\max}, \end{cases} \tag{2.1.7}$$

Eqs. (2.1.3) through (2.1.7) indicate that when the interference is high (e.g., $I_k(b) = I_{\max}$), the achievable capacity, $R_{s,k}(b)$, will be low, and vice versa. Hence, it is important to either subtract the interference through interference cancellation techniques or ensure that $I_{\min} \leq I_k(b) \leq I_{\max}$ is always satisfied through the use of interference mitigation techniques. Several approaches to interference mitigation exist, and some of them are discussed in subsequent sections.

2.1.1 Frequency orthogonalization

Frequency orthogonalization can be classified as SFO (Static Frequency Orthogonalization) and DFO (Dynamic Frequency Orthogonalization).

2.1.1.1 Static frequency orthogonalization

In SFO, the frequency spectrum is fixed-partitioned between the member tiers of the network, i.e., the femtocell and the macrocell. Co-channel interference between

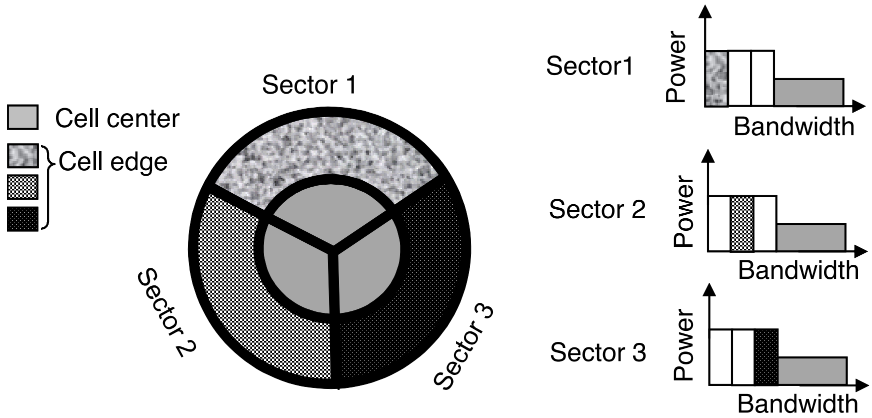

Figure 2.2: Power and bandwidth partitioning in Fractional Frequency Reuse

the tiers is completely eliminated, although, adjacent channel interference, which is beyond the scope of this work, may exist. Albeit, this interference control method may be attractive from the perspective of the ease of interference mitigation, a loss in spectral efficiency is, however, incurred. Examples of SFO are:

1. Fractional Frequency Reuse:

   Fractional Frequency Reuse (FFR), which was first proposed for GSM (Global System for Mobile Communication), is one way of statically orthogonalizing frequency usage. The whole spectrum of the macrocell is divided into two bands, namely, edge band and center band. In order to avoid inter-cell interference between cell edge users of adjacent macrocells, the edge band is further divided into three non-overlapping bands, one for each sector as illustrated in Fig. 2.2. It can be observed that cell center users can be assigned channels within $\frac{1}{2}$ of the spectrum, while cell edge users can only be assigned within $\frac{1}{6}$ [21]. If the transmission power at the cell edge is denoted as P_e, then the transmission

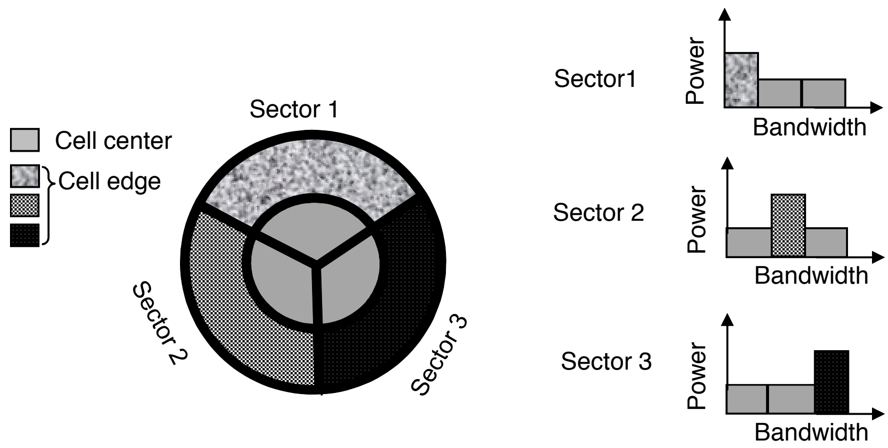

Figure 2.3: Power and bandwidth partitioning in Soft Frequency Reuse.

power at the cell center is $\alpha \cdot P_e$, where $0 < \alpha < 1$ denotes the power masking factor. Hence, lower power is transmitted at the cell center relative to the cell edge. With the well-defined bandwidth usage per region illustrated in Fig. 2.2, a femtocell only needs to use sub-bands not used by the macrocell in its region.

2. Soft Frequency Reuse:

   A variant of FFR, which is illustrated in Fig. 2.3, is known as SFR (Soft Frequency Reuse). In SFR, reuse-1 is assigned to the cell center region while reuse-3 is assigned to the cell edge region. Just like FFR, a lower transmission power is used at the cell center while full power is used at the cell edge. Compared to FFR, SFR has a higher spectral efficiency. However, in a multi-tier scenario, one of the shortcomings of SFR is that, the cell center femtocells are liable to interference since the entire bandwidth can used by the macrocell users located at the cell center region (reuse-1).

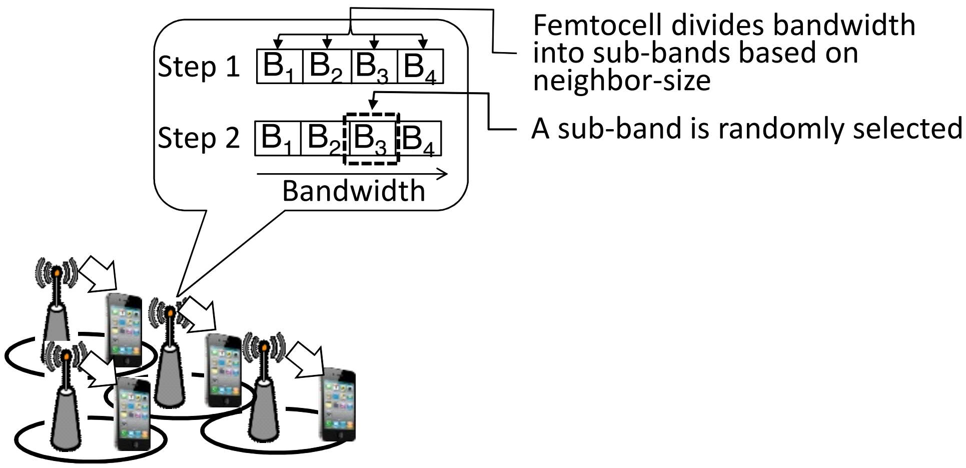

Figure 2.4: Dynamic frequency orthogonalization for interference mitigation.

2.1.1.2 Dynamic frequency orthogonalization

In DFO on the other hand, the member tiers of the network dynamically access the frequency spectrum. DFO can be generally classified under random-based and sensing-based orthogonalization [22].

1. Random spectrum access: In this approach, access to the spectrum by each base station is random, and the absence of collision is not guaranteed. Each base station divides the bandwidth into a number of sub-bands based on the neighbor-size as illustrated in Fig. 2.4. A sub-band can then be randomly selected and the selection can be done based on a hashing function [23]. If the randomly selected sub-band does not collide with that of a strong interfering neighbor, the femtocell reserves such sub-band for subsequent transmission. Frequency hopping [24] in which the sub-band is not reserved is one variation of Random-based DFO. The hopping artificially makes the interference scenario to

fluctuate along the transmission of a reference user. This fluctuation of interference leads to an interference diversity gain [25]. When used in OFDMA-based femtocell, the probability of persistent channel collision between neighboring femtocells and macrocells is reduced [5].

2. Network Listening-based spectrum access: This is a sensing-based approach in which femtocells use the NLM (Network Listening Mode) for channel orthogonalization. The femtocell senses the air-interface and identify which cells and channels are active within its range. Based on this information, the femtocell selects channels that are orthogonal to those used by neighboring nodes.

3. Message sharing-based spectrum access: In this approach, femtocells exchange messages with neighboring femtocells about their channel usage and traffic load. Hence, a femtocell becomes aware of its neighbors' future resource usage and can organize spectrum access in a way that minimizes interference.

4. Measurement report-based spectrum access: This approach relies on the *measurement reports* that are periodically exchanged between a femtocell and its associated users. The report contains information on the received signal strength and active channels of the serving and strongest neighboring cells (both macros and femtos). If post-processed, interference relationships and *forbidden channel list* can be established and used in spectrum access in a manner that reduces interference.

2.1.2 Time orthogonalization

Just like frequency orthogonalization, time orthogonalization can be classified into STO (Static Time Orthogonalization) and DTO (Dynamic Time Orthogonalization).

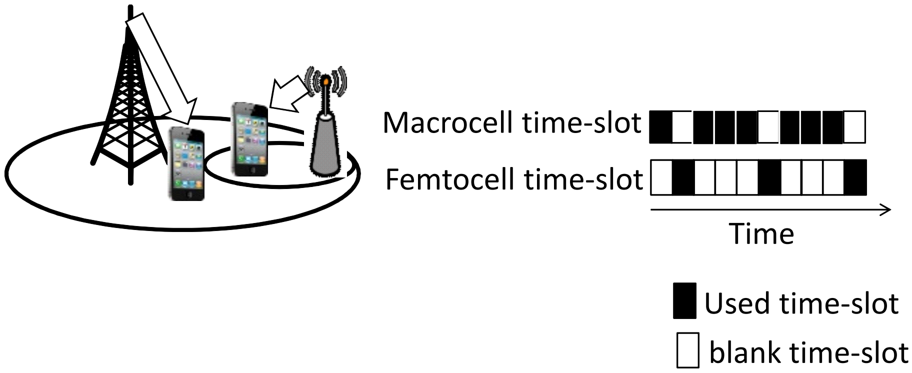

Figure 2.5: Static time orthogonalization for interference mitigation

2.1.2.1 Static time orthogonalization

In this interference mitigation approach, the partitioning of the time resources between neighboring base stations is fixed as illustrated in Fig. 2.5. As can be seen in Fig. 2.5, the femtocell accesses the spectrum only when the macrocell is silent. The partitioning pattern is known to the femtocell a priori (e.g., it can be decided by the macrocell and communicated to the femtocell. Alternatively, the femtocell may observe the RF (Radio Frequency) environment for a series of time-slots and then select the optimum slots for transmission as discussed in [26]). STO interference mitigation technique has been adopted in the LTE-advanced standard in which it is used to create interference free tunnels and it is termed *almost blank sub-frame* [27], [28] in the standard.

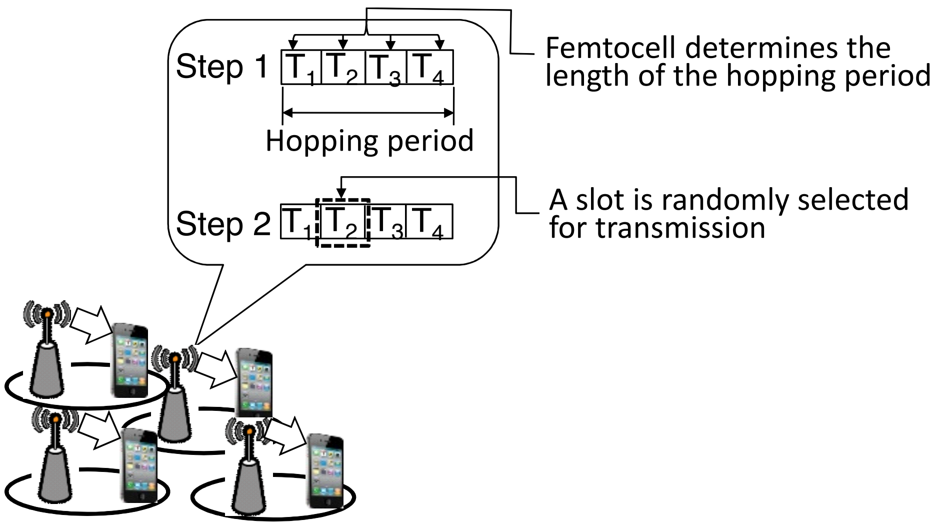

Figure 2.6: Dynamic time orthogonalization for interference mitigation

2.1.2.2 Dynamic time orthogonalization

In this interference mitigation approach, the partitioning of the temporal resources is randomized as illustrated in Fig. 2.6, and this may be achieved through time-hopping (e.g., [24]). The transmission period is divided into a number of time-slots known as the hopping slots. During each hopping period, each base station randomly picks a transmission slot (hopping slot). Although, the absence of slot collision between neighboring base stations is not guaranteed, this inference mitigation technique has been proven effective [29] at reducing interference in TH-CDMA (Time Hopped-CDMA) systems between different femtocells and also between femtocell and macrocells by a factor of $\frac{1}{N_{\text{hop}}}$, where N_{hop} is the number of slots in a hopping period. Previous works [25],[30] have developed collision models for a critical analysis of the performance of these randomized schemes.

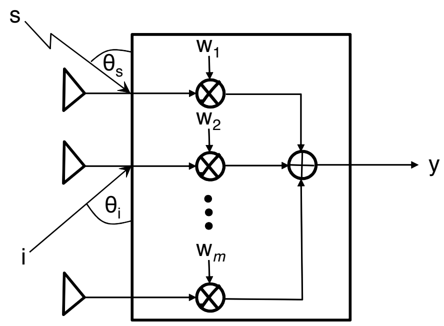

Figure 2.7: Spatial orthogonalization through beam forming [7].

2.1.3 Spatial orthogonalization

This technique takes advantage of the spatial separation between an aggressor (i.e., the interferer) and the victim (i.e., the interference recipient). In this approach, antenna array is used such that different weights are assigned to the antenna elements to selectively attenuate signals from unwanted directions as illustrated in Fig. 2.7. The femtocell receiver in Fig. 2.7 attenuates the interfering signal, i, and amplifies the desired signal, s, through optimum estimation of the set of weights $w_1, w_2, \ldots, w_m$ so that the SINR of the output signal is maximized [7].

2.1.4 Power control

The interference mitigation techniques discussed in the previous sections completely or almost completely eliminate interference either through frequency domain separation, time domain separation, or space domain separation. Another interference mitigation technique is the power control technique which, in contrast to earlier discussions, reduces the amount of interference received by the interference victim. Some existing power control techniques are as follows:

1. Target Radius Based Power Control [31]:

   The power settings depends on the target radius of the femtocell. Hence, each femtocell sets its transmit power, P_{femto}, to be equal to the power received from the closest macrocell at the target femtocell radius:

$$P_{\text{femto}} = \min\left(\underbrace{P_{\text{macro}} + G(\theta) - L_{\text{macro}}(d)}_{\text{estimate of received macro cell power}} + L_{\text{femto}}(r), P_{\max}\right), \tag{2.1.8}$$

   where $L_{\text{femto}}(r)$ is the line of sight path loss at the target cell radius r (excluding any wall losses), while P_{macro} is the transmit power of the macrocell sector in which the femtocell is located, and $G(\theta)$ is the antenna gain in the direction of the femtocell. The angle to the femtocell with respect to the sector angle is denoted as θ, while $L_{\text{macro}}(d)$ denotes the average macrocell path loss at the femtocell distance d.

2. Target Signal to Noise Ratio-based Power Control [32]:

   In this case the power settings depends on the target SNR (Signal to Noise Ratio). The transmit power P_t is set to:

$$P_t = \min\left(P_{\max}, SNR_{\text{target}} \times \frac{P_{\text{noise}}}{g}\right), \tag{2.1.9}$$

   where P_{noise} is the noise power level, SNR_{target} is the targeted received power level relative to the noise floor, and g is an estimate of the path loss to the base station (based on wideband downlink estimates).

3. Fractional Power Control [33]:

   The uplink transmit power P_{t} of a user is determined as :

$$P_{\text{t}} = \min\{P_{\max}, 10\log_{10} M + P_0 + \alpha \cdot L + \Delta_{\text{mcs}} + f(\Delta_i)\}, \tag{2.1.10}$$

where $P_{\max}$ is the maximum transmit power of the user, P_0 is a user specific (optionally cell-specific) parameter, M is the number of channels assigned to the user, α is the cell-specific path loss compensation factor that can be set to 0.0 or from 0.4 to 1.0 in steps of 0.1, L is the path loss (including distance-dependent path loss, shadowing and antenna gain), Δ_{mcs} is a power control parameter, and $f(\Delta_i)$ is the closed loop power control correction transmitted by the base station.

4. Femtocell Measurement-based Power Setting [34]:

   The femtocell adjusts its maximum downlink transmit power as a function of air interface measurements to avoid interfering with macrocell users. The downlink transmit power, P_{t}, of the femtocell is set as

$$P_{\mathrm{t}} = \max\left(\min\left(\alpha \times \left(R + 10\log\left(N_{\mathrm{CH}}^{\mathrm{DL}} \times N_{\mathrm{SC}}^{\mathrm{CH}}\right)\right) + \beta, P_{\max}\right), P_{\min}\right), \quad (2.1.11)$$

   where $P_{\max}$ and $P_{\min}$ are the maximum and minimum femtocell transmit power settings, respectively, R(dBm) is the measured received signal reference power received from the strongest co-channel macrocell, $N_{\mathrm{CH}}^{\mathrm{DL}}$ is the number of downlink channels, while $N_{\mathrm{SC}}^{\mathrm{CH}}$ is the number of sub-carriers per channel (typical value of $N_{\mathrm{SC}}^{\mathrm{CH}}$ is 12). Parameter α is a linear scalar that allows altering the slope of power control mapping curve, β is a parameter expressed in dB that can be used for altering the exact range of R covered by dynamic range of power control. Parameters $P_{\min}, \alpha$, and β are considered to be femtocell configuration parameters and $P_{\max}$ corresponds to the femtocell maximum transmit power capability.

In the uplink, the femtocell can power-control-up or power-control-down the associated users as expedient in order to meet a desired SNR. If the total energy received at the receiver of the femtocell access point is beyond the receiver's dynamic range, it can lead to receiver amplifier saturation. For example, if an associated femtocell user is too close to the femtocell and cannot be power-controlled-down because it is already transmitting at the minimum possible transmission power, other solutions has to be sought. Another example is when high power users that are not associated with a femtocell base station (e.g., cell border macrocell users that have to transmit at high power levels due to their far distances from their serving macrocell base station) are located near the femtocell base station, such that, the users cause significant uplink interference to the femtocell, leading to high noise rise levels and a degradation in the femtocell users' performance. Since the high power users are not associated with the femtocell, the femtocell can not power control them down. These cases can be addressed by a technique known as uplink attenuation [35], [36]. In this technique, the femtocell raises its receiver noise figure to bring the received signal down to an appropriate level so it can be comparable to thermal noise. If the femtocell user's SNR target is not attained, the user can be power-controlled-up adaptively to meet the SNR target.

2.2 Coordination in multi-tier networks

Studies have shown that 2/3 of calls and over 90% of data services occur indoors [7]. However, the high carrier frequency employed in 3G systems makes penetration of signal transmitted from outdoor macrocell to an indoor user a challenge. Besides, current cellular wireless systems are only capable of providing true 3G services, which require high-bandwidth, when the users are located near the cell transceiver (i.e., high signal strength) and the number of simultaneous users is low (low interference from other cell users, i.e., low CDMA MAI (Multiple-access Interference)). Bringing the outdoor cell tower indoors will go a long way to addressing the indoor coverage challenges facing current 3G systems, and this is achievable through femtocell deployment. Hence, it is believed that femtocell is the next step in the evolutionary path of cellular technology. Femtocells are deployable by end-users who may lack technical skills regarding wireless systems. Hence, conventional detailed network planning and optimization will be impracticable in femtocell networks. Due to the unplanned manner of femtocell deployment, a number of unresolved technical problems emerge which include [5]:

1. How will femtocell allocate spectrum in the presence of inter- and intra-tier interference?
2. How will femtocells provide timing and synchronization?
3. How will backhaul provide acceptable QoS (quality of service)?
4. How should femtocells provide open or closed access?
5. How will handoff be performed in open access?
6. How will femtocells provide location tracking for emergency call, and should they serve nearby macrocell users with poor coverage?

The list goes on and on. Among all these challenges, the most important one is the inter- and intra-tier interference. Interference mitigation has been discussed in the previous section. However, in order to implement the mitigation techniques in a

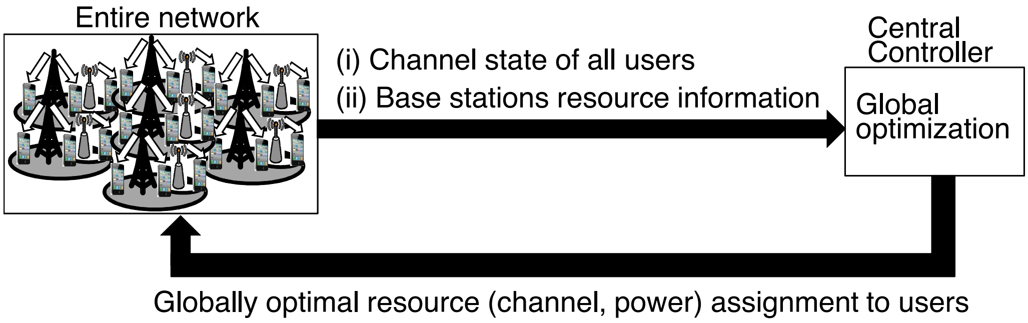

(a) Centralized coordination

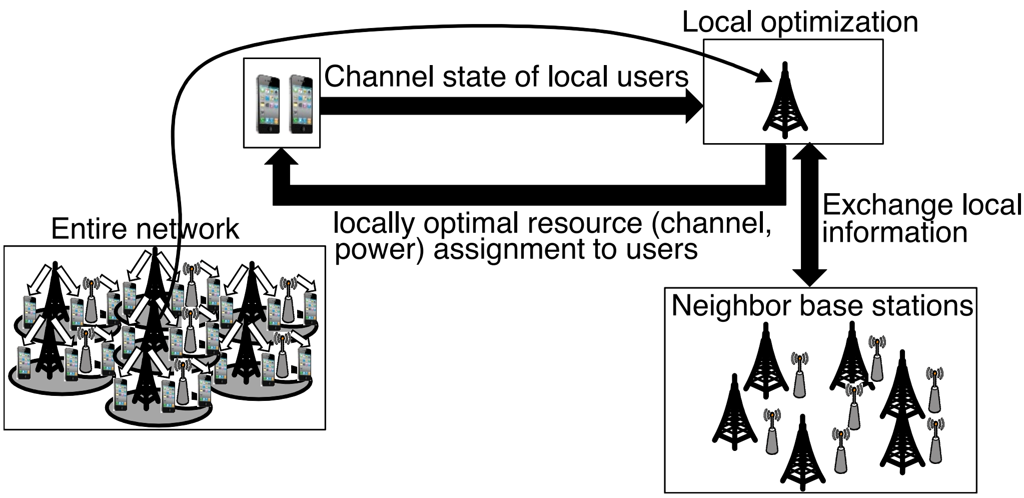

(b) Distributed coordination

Figure 2.8: Categories of inter-cell coordination.

network comprising of multiple base stations such as macrocells and femtocells, coordination among these base stations is inevitable. This coordination may be a direct coordination where control instructions (restrictions and permissions) are exchanged among base stations. It may also be an indirect coordination where actions at a base station are taken after observing the actions of neighbor base stations. The unplanned manner of femtocell deployment, however, makes coordination a challenging task in multi-tier networks comprising of macrocells and underlaid femtocells. That notwithstanding, coordination must be realized somehow so as to achieve an efficient RRM (Radio Resource Management) which is vital for the success of femtocell technology. Coordination schemes for RRM can be categorized into two types: centralized and distributed [37].

In centralized coordination, a center node collects information about the global radio condition and makes decision on how to manage them among multiple cells as illustrated in Fig. 2.8(a). In distributed coordination on the other hand, each base station manages its radio resources based on limited information about the radio resource usage by neighbor cells as illustrated in Fig. 2.8(b). Centralized coordination yields a globally optimal resource allocation solution but the associated computational complexity can be prohibitive in a multi-tier network comprising of a large number of femtocell nodes. The high complexity problem results in large computational times which consequently leads to increased latency that may be unacceptable in traffic classes with stringent delay constraints. Considering the shortcomings of centralized coordination, distributed coordination suffices since it offers a lower computational complexity compared to its centralized counterpart. The shortcoming of distributed coordination, however, is that resource allocation solution is locally optimal.

2.2.1 The 3GPP femto-macro coordination methods

The 3GPP has been very active in the development of coordination techniques for efficient coexistence of femtocell and macrocell tiers. Extensive work has been done by the 3GPP in this area and some of them will be discussed briefly [34].

2.2.1.1 Semi-static resource partitioning by the macrocell

In this approach, the coverage area of the macrocell is partitioned into regions. Radio resources (e.g., channels) are then classified as high priority and low priority resources in each region and location information is communicated to the femtocells. Depending on their (femtocells) locations, femtocells use low priority resources of the macrocell with high priority while the high priority resources of the macrocell are used with low priority by the femtocells.

2.2.1.2 Controller-based coordination

In this coordination method, a centralized controller (e.g, femtocell gateway) is used. Each femtocell determines its temporal resources which is based on the traffic and channel conditions. It forwards information on this resources to a centralized controller which develops an adjacency graph for grouping all femtocells based on

1. Sub-band: femtocells grouped together in a sub-band use such sub-band simultaneously

2. Sub-frame: femtocells grouped together in a sub-frame use such sub-frame simultaneously. In this case, the DRX (discontinuous reception) configuration of the user should, however, be set during the silent sub-frames for power saving.

2.2.1.3 Closed subscriber group alternation

The CSG (Closed Subscriber Group) [5],[22] status of a femtocell determines whether access to the femtocell is restricted to a group of registered subscribers only or it is available for public access. Since the interference received by the macrocell users grows with increasing number of CSG femtocells, the number of CSG femtocells in simultaneous operation is controlled by a centralized entity (e.g., femtocell gateway or femtocell management server) based on a pre-determined threshold. The femtocells are made to dynamically alternate between their default CSG status and a network determined status, e.g., some femtocells may be made to use their default CSG status for the first 30 minutes of every hour, while during the remaining 30 minutes of every hour, they may be made to operate as open access femtocells. This method helps keep the number of CSG femtocells in simultaneous operation within an acceptable limit in order to moderate the interference footprint that results from their operation.

2.2.1.4 Transmission pattern to physical cell identity mapping

Each femtocell reports its PCI (Physical Cell Identity) to a centralized controller (e.g., femtocell gateway) which creates an adjacency graph of femtocells and their users based on the received report. The controller then develops a set of transmission patterns (e.g., maximum transmission power) which it maps to PCIs. The mapping is communicated to the femtocells, e.g., through S1-signaling. A femtocell user that is interfered can report the RSRP (Received Signal Reference Power) of the interferer to its serving femtocell. Using the transmission pattern to PCI mapping information already received from the controller, the serving femtocell can know the allocation pattern of the interferer and can allocate downlink resources to its interfered user in a way that minimizes the received interference.

Chapter 3

Radio resource partitioning

3.1 Introduction

The partitioning of radio resources in a multi-tier network comprising of macrocell and femtocell tiers can be viewed from two aspects. The first aspect entails co-layer resource partitioning, i.e., how radio resources should be shared among users that belong to the same tier, e.g., different categories of users (for example, Inner Zone (IZ) cell users and Outer Zone (OZ) [1] cell users) served by the macrocell. The second aspect involves cross-layer resource sharing, i.e., sharing radio resources between the macrocell and the femtocell tiers. Research works in the literature have considered co-layer resource sharing from a short-term perspective, e.g., scheduling [38], and also from a long-term perspective, e.g., frequency reuse such as SFR [39]. This chapter considers the latter in the context of OFDMA PHY layer technology and aims at reducing interference between the macrocell and femtocell tiers using FFR [21].

[1] OZ and IZ are illustrated in Fig. 3.4

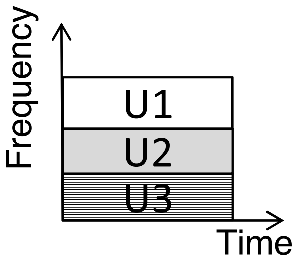

(a) FDMA: coarse scheduling granularity

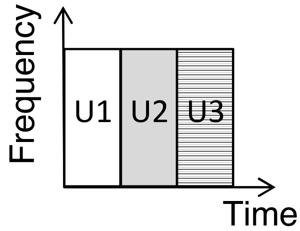

(b) TDMA: coarse scheduling granularity

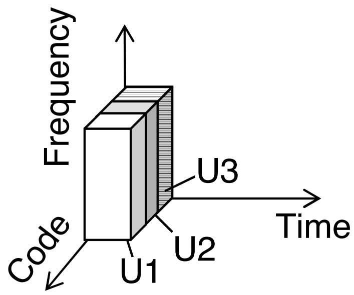

(c) TDMA: coarse scheduling granularity

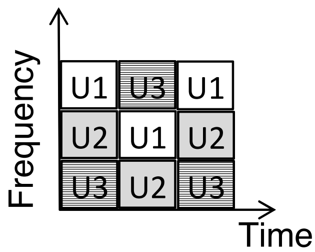

(d) OFDMA: fine scheduling granularity

Figure 3.1: Scheduling granularity of multi-access technologies (U1, U2, and U3 denotes user 1, user 2, and user 3, respectively).

3.2 Theoretical background

The type of air-interface technology used in a network contributes to the method through which radio resources are shared among the users of the network. For example, in FDMA each user is assigned two 200 kHz bandwidth channels, one for uplink and the other for downlink transmission. This technology and other subsequent technologies such as TDMA and CDMA all permit coarse granularity radio resource distribution as illustrated in Fig. 3.1(a)–(c). On the other hand, OFDMA supports a finer resource distribution granularity as shown in Fig. 3.1(d) . Hence, the current evolutionary path of air-interface technologies of cellular networks points at

OFDMA as potentially the next flag bearer.

3.2.1 OFDMA air-interface

The structure of an OFDMA transmitter-receiver block is illustrated in Fig. 3.2. In OFDMA, the bandwidth is sub-divided into multiple orthogonal frequency sub-carriers. The input data streams of multiple users are divided into multiple sub-streams of reduced data rate. The data sub-streams of the users are then separately modulated on the data sub-carriers in parallel for transmission. Sub-dividing the users' data into sub-streams helps increase the symbol length and thus reduces the complexity of the receiver circuitry. Also, subdividing the bandwidth into multiple sub-carriers helps to artificially reduce the transmission bandwidth-size compared to the coherence bandwidth, thus resulting in a flat fading channel. The cyclic prefix

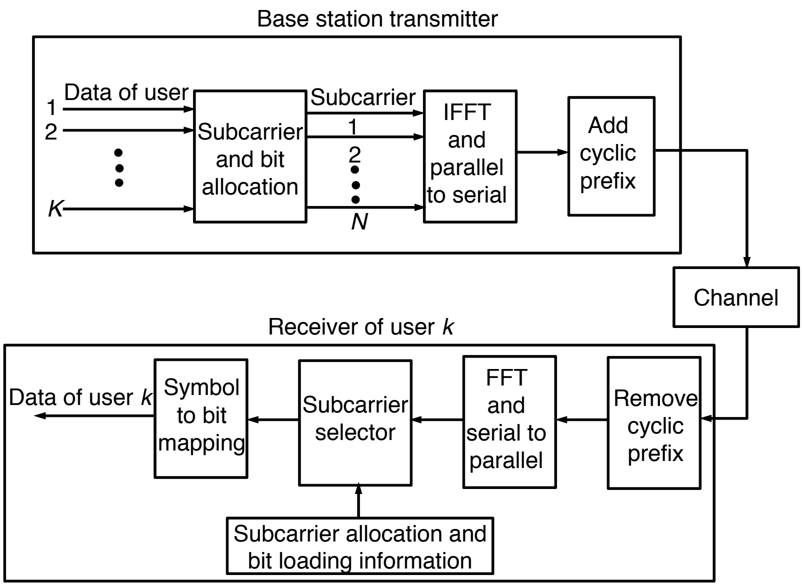

Figure 3.2: Structure of OFDMA block.

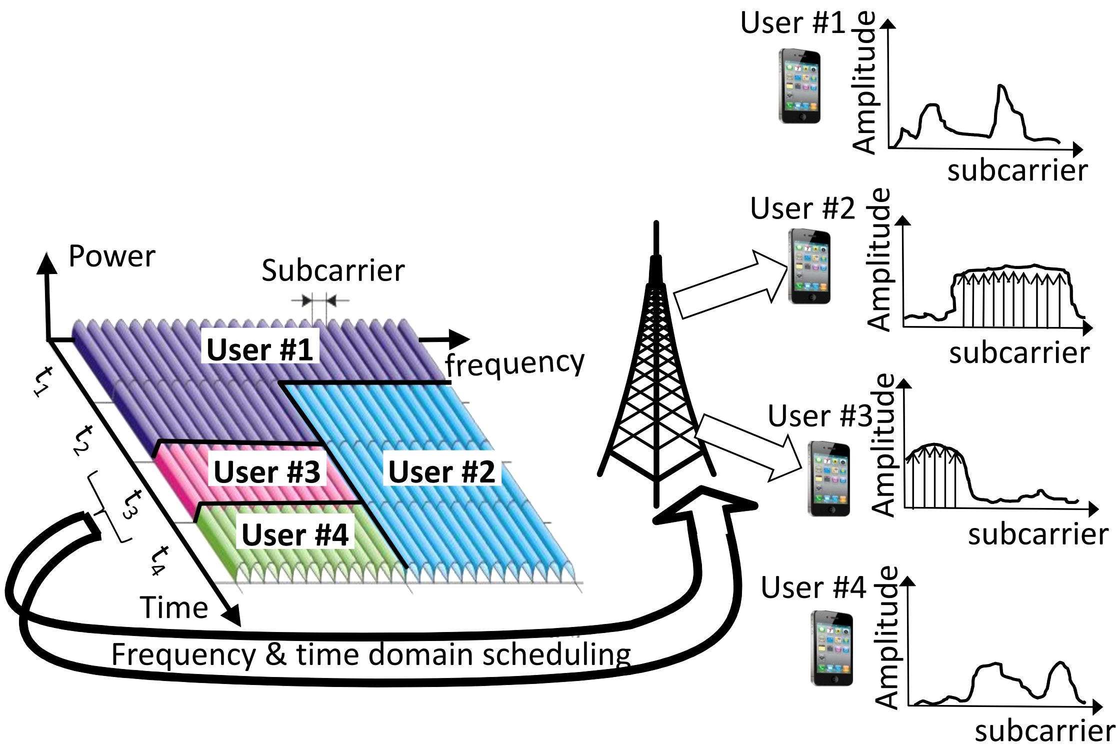

Figure 3.3: Frequency and time domain scheduling in OFDMA.

helps to eliminate ISI (Inter Symbol Interference) if the cyclic prefix length is longer than the channel delay spread.

Compared to its predecessors, OFDMA PHY layer technology permits finer scheduling granularity through a joint time-frequency domain scheduling. This fine granularity scheduling support combined with opportunistic scheduling can yield substantial capacity gain in a multi-user setting where the channels of each user undergo independent fading as exemplified in Fig. 3.3. In Fig. 3.3, it is observable that at time t_3, user #2 shows high gain channel response in the upper part of the frequency spectrum, while user #3 shows high gain channel response in the lower part of the frequency spectrum. Users #1 and #4, however, are in poor channel conditions at time t_3. Hence, the scheduler takes advantage of the independent fading behavior of the sub-carriers (channels) of the users by scheduling only users #2 and #3 on their respective high gain channels at time t_3. The time and frequency resources can be organized into sub-channels (as in WiMAX [40]) or resource blocks (as in LTE [41]).

3.2.2 Co-layer resource partitioning

As mentioned previously, this can be viewed from a short-term perspective or from a long-term perspective, but only the long-term perspective will be considered.

3.2.2.1 Frequency reuse in OFDMA based network

One of the promising tools for interference avoidance in OFDMA networks is the careful exploitation of different frequency reuse schemes (FRS) in different regions of a cell. These FRSs can be described by the notation $N_c \times N_s \times N_f$, where N_c denotes the number of channels, N_s denotes the number sectors per base station, and N_f denotes the number of fragments in which each channel is divided [8]. Common FRS are [8]:

1. FRS $1 \times 3 \times 1$:

   This is the easiest FRS scheme and it simply means the network employs reuse-1 in all sectors. Jia et al. [42], however, showed through simulations that this FRS scheme is infeasible in practical OFDMA systems since outage probability, according to their simulation results, is in excess of 0.5.

2. FRS $1 \times 3 \times 3$:

   This scheme divides the channel into three segments and assigns each channel segment to a sector. Hence, the FRF (Frequency Reuse Factor) of the cell is 3. The technical overhead of the scheme is low due to its simplicity.

3. Fractional Frequency Reuse Scheme:

   In this scheme, a sector is assigned more than one reuse factor. For example, if two regions are defined in the cell, i.e., IZ and OZ, respectively, and α denotes the ratio of the IZ area to the area of the cell, then the aggregate cell reuse factor, CRF, is computed as [42] :

   $$\text{CRF} = \alpha \cdot IRRF + (1 - \alpha)ORRF, \tag{3.2.1}$$

   where ORRF and IRRF denote OZ Region Reuse Factor and IZ Region Reuse Factor, respectively. The size of channel segment assigned to each sector may be asymmetrical and can be dynamically set to adapt to different user densities in different parts of the cell. However, in a multi-tier system, a static settings may be more preferred to its dynamic [43] counterpart considering interference issues. Time Division-FFR (TD-FFR) has also been considered [42],[44] in which access to sector bandwidth is timeshared between OZ and IZ users.

3.3 Related works

Many of the existing works on resource partitioning based on FFR have considered a single-tier scenario where macrocell tier is considered in the absence of femtocell tier [45],[46],[47]. However, it is important to consider the coexistence scenario of macrocell and femtocell so as to find an optimal way of partitioning the common radio resources in order to ensure that none of them is seriously disadvantaged. One of the major shortcomings of existing research works on FFR is that most works have not considered how to optimally partition the cell area into the IZ and OZ regions. For example, [45],[46],[47],[48],[49] have arbitrarily selected cell partitioning parameters without following any design procedure. However, one of the most important issues in cellular systems is the maintenance of fairness among users during resource allocation. Hence, in FFR network design, special attention ought to be given to cell area partitioning, as well as the size of radio resources assigned to each region of the cell that maintains cell-wide fairness.

Zhao et al. [50] have used a stochastic procedure to analyze the throughput performance of the macrocell tier when spectrum access of the femtocell tier is not determined a priori but is, instead, based on a random access mechanism. Specifically, the macrocell periodically broadcasts a message to the femtocells and the message contains information about the region factor, bandwidth partitioning factor, and power ratio factor. Using this information, femtocells access sub-bands of the spectrum by employing a uniform probability distribution technique. The authors revealed that optimal spectrum access by the femtocell is achieved when the path loss control factor (which is the same as fractional power control discussed in Sect. 2.1.4) tends towards 1.0. Analytical results of the authors' work were corroborated by simulation results. However, the authors' work have shortcomings; for example, femtocell spectrum access has been based on a random process (F-ALOHA). This could have serious interference implication when a macrocell user is trapped in the coverage area of multiple femtocell base stations. In such a situation, static spectrum access is more preferred to dynamic spectrum access. Also, the periodic message broadcasted by the macrocell-tier contrasts the direction of evolution of cellular technology due to the ensuing capacity degradation that additional control bits incur.

Jia et al. [42] have compared a reuse-1 network with a reuse-3 network, and have concluded that reuse-1 is practically infeasible in real networks if there is no coordination among the base stations. Unlike previous works, Jia et al. [42] have obtained optimal FFR parameter value for partitioning the coverage area of OFDMA-based macrocell into the IZ and the OZ regions. However, the shortcoming of their is that, the result obtained applies to single-tier networks alone. Moreover, the authors have focused on the maximization of the IZ throughput, disregarding cell-wide fairness issue. Inspired by the achievement of Jia et al. and also by the shortcomings of their work, we are motivated to go one step further to obtain FFR partitioning parameter values, but unlike Jia et al., our focus is on a multi-tier network scenario that comprises of macrocell and underlaid femtocells. In particular, we are interested in obtaining the partitioning parameter values that maximizes femtocell throughput. Also, another important focus of this research is to maintain fairness among different categories of macrocell users.

3.4 Proposed scheme

In spite of the anticipated throughput gain enabled by recent technologies such as femtocells, etc., ensuring that all users receive a fair share of the network resources is another important issue; greedy users must be prevented from consuming excessive network resources and thus starving the other users. It is therefore imperative to ensure a proper network resource partitioning which can jointly reduce inter-cell interference in multi-tier networks (e.g., femtocell underlaid macrocells) and also ensure fairness among the served macrocell users. Fractional Frequency Reuse simplifies spectrum sharing between the femtocell and the macrocell tiers and will therefore be used in the radio resource partitioning process of this work. To the best of the authors' knowledge, previous studies on FFR have not critically modeled the mutual relationship between the cell area partitioning parameter and the network resource partitioning parameter in a multi-tier network settings. We consider a resource partitioning approach, which has been presented in part in [51], that employs mathematical formulation and exhaustive search procedure to obtain optimal resource partitioning values from the perspectives of macrocell user fairness and femtocell throughput maximization. We are focusing on improving the macrocell users' fairness and not the femtocell users fairness due to the following reasons.

1. A macrocell's coverage area is usually large, such that, the separation distance between an IZ user and the base station compared to the separation distance between an OZ user and the base station can be large, hence increasing the chances of unfairness between these two classes of users.

2. Macrocells usually serve many users using limited radio resources; hence, the chances of having an unfairly served user is higher compared to femtocells.

In this study, we have chosen to maximize femtocell throughput because femtocells are deployed in the coverage area of the macrocell and are not given free access to the network resources but are instead allowed to use only the unused macrocell resources in the zones where they (femtocells) are deployed.

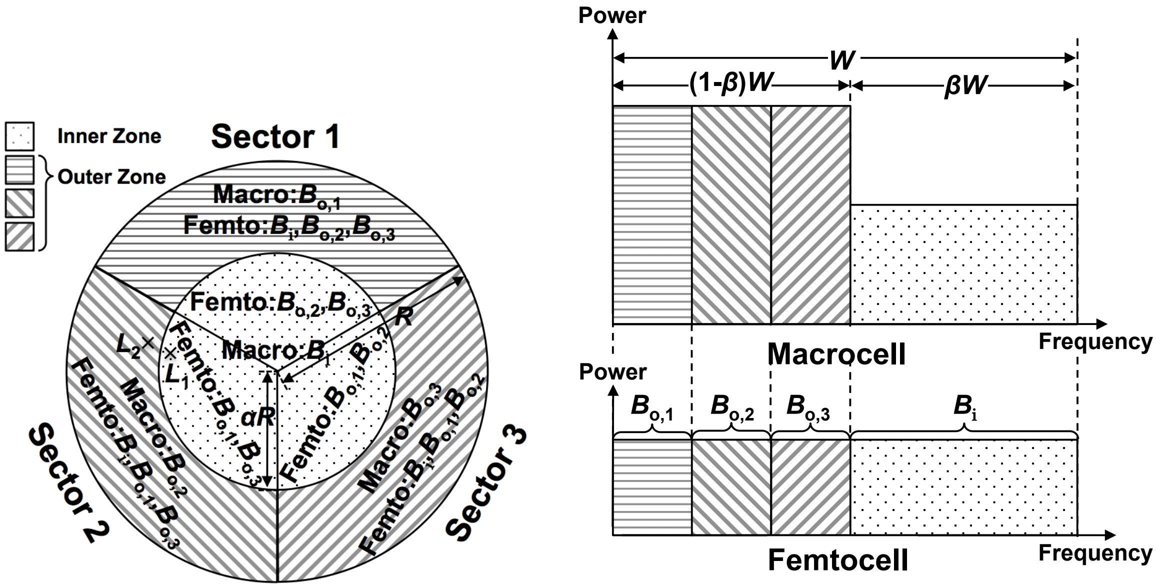

(a) Cell structure (b) Network resource partitioning architecture

Figure 3.4: Cell structure and the network resource partitioning architecture.

3.4.1 System model

We consider the downlink of an OFDMA-based macrocell system illustrated in Fig. 3.4(a), and assume that network resources are partitioned based on FFR-scheme as illustrated in Fig. 3.4(b). At the macrocell, the whole bandwidth is divided into two parts and one of the two parts is further divided into three parts, such that, the entire bandwidth is made up of sub-bands $B_{\mathrm{o},1}$, $B_{\mathrm{o},2}$, $B_{\mathrm{o},3}$, and B_{i} as illustrated in Fig. 3.4(b). The coverage area of the macrocell is divided into the IZ and the OZ, and sub-band B_{i} is assigned to the IZ. The OZ of the macrocell is further divided into three parts and the remaining sub-bands ($B_{\mathrm{o},1}$, $B_{\mathrm{o},2}$, and $B_{\mathrm{o},3}$) are shared among the parts, such that, Sectors 1, 2, and 3 of the OZ are assigned sub-bands $B_{\mathrm{o},1}$, $B_{\mathrm{o},2}$, and $B_{\mathrm{o},3}$, respectively, as illustrated in Fig. 3.4(a). Although, the OZ of the macrocell can be divided into any number of sectoral regions, we have, however, divided it into three sectoral regions just to follow the typical convention adopted in many existing works on FFR (e.g., [49]). Moreover, the division helps to increase the overall network frequency efficiency since more unused sub-bands of the macrocell becomes available to the several femtocells located in the sectorized regions of the macrocell as will be explained shortly.

The patterns in Fig. 3.4(b) represent the sub-bands that constitute the bandwidth. The amount of power used by the macrocell and the femtocells on each sub-band is also shown in Fig. 3.4(b). It can be observed in Fig. 3.4(a) that the sub-bands used by the femtocells that are located in macrocell sub-areas are orthogonal to those sub-bands used by the macrocell in those sub-areas. For example, the femtocells located in the OZ of Sector 2 are prevented from using sub-band $B_{\mathrm{o},2}$ since sub-band $B_{\mathrm{o},2}$ is used by the macrocell users in that region. These femtocells are, however, allowed to use sub-bands B_{i}, $B_{\mathrm{o},1}$, and $B_{\mathrm{o},3}$ which are not used by the macrocell users in that region as illustrated in Figs. 3.4(a). Note that the access of these femtocells to sub-bands $B_{\mathrm{o},1}$ and $B_{\mathrm{o},3}$ is possible due to the sectorization of the macrocell OZ and this improves the overall network frequency efficiency as mentioned previously. The coverage area of the macrocell has a radius denoted as R, and there are N_{m} macrocell users uniformly distributed in the coverage area of the macrocell. P_{T} denotes the overall macrocell downlink transmission power per Hz, P_{c} and P_{e} are the transmission power per Hz at the IZ and the OZ of the macrocell, respectively, while the system bandwidth is denoted as W.

3.4.2 Macrocell network resource partitioning

In this section, we establish mathematical relationship between resource partitioning parameters and determine the throughput-fair capacity region of the macrocell. In cellular networks, if network resources are not adequately shared between the OZ and IZ of a cell, there will be non-uniformity in the per user data rate of UEs (User Equipments) located at the OZ and the IZ of the cell. This may stem from the fact that UEs at the IZ of the cell experience low path loss and are also more robust against inter-cell interference compared to those at the OZ who suffer from high interference as well as high path loss. For this reason, it is necessary to determine the optimal resource partitioning ratio that minimizes the margin between the per user capacities of UEs located at the IZ and the OZ of a macrocell. In order to address this radio resource partitioning problem, we start by expressing the total power available at the macrocell base station as:

$$P_{\mathrm{T}}W = P_{\mathrm{c}}\beta W + P_{\mathrm{e}}(1-\beta)W, \tag{3.4.1}$$

where β is the fraction of the system bandwidth alloted for IZ transmission. Since received power decays with distance according to a path loss exponent n [19], then, inter-zone received power fairness can be realized based on Eq. (3.4.2):

$$\frac{P_{\mathrm{c}}}{(\alpha R)^n} = \frac{P_{\mathrm{e}}}{R^n}, \tag{3.4.2}$$

where the left and right terms of Eq. (3.4.2) are the received powers per Hz of the macrocell users located at the edge region of the IZ and the OZ of the macrocell, respectively, while α is the fraction of R representing the IZ radius. Equation (3.4.2) ensures that the received power per Hz of a macrocell user located at the edge of the IZ of the macrocell is equal to the received power per Hz of a macrocell user located at the edge of the OZ of the macrocell. From Eqs. (3.4.1) and (3.4.2),

$$P_{\mathrm{T}} = P_{\mathrm{c}}\beta + P_{\mathrm{e}}(1-\beta) = P_{\mathrm{e}}(\alpha^n\beta + 1 - \beta), \tag{3.4.3}$$

$$P_{\mathrm{e}} = \frac{P_{\mathrm{T}}}{\alpha^n\beta + 1 - \beta}, \tag{3.4.4}$$

and

$$P_{\mathrm{c}} = \alpha^n P_{\mathrm{e}} = \frac{\alpha^n P_{\mathrm{T}}}{\alpha^n \beta + 1 - \beta}. \tag{3.4.5}$$

Let $\gamma_{\mathrm{c},u}$ and $\gamma_{\mathrm{e},u}$ denote the SNR (signal to noise ratio) of IZ and OZ macrocell UE, u, respectively, then

$$\gamma_{\mathrm{c},u} = \frac{\alpha^n P_{\mathrm{T}} G_{\mathrm{c},u}}{(\alpha^n \beta + 1 - \beta)\sigma}, \tag{3.4.6}$$

while $\gamma_{\mathrm{e},u}$ is

$$\gamma_{\mathrm{e},u} = \frac{P_{\mathrm{T}} G_{\mathrm{e},u}}{(\alpha^n \beta + 1 - \beta)\sigma}, \tag{3.4.7}$$

where $G_{\mathrm{c},u}$ and $G_{\mathrm{e},u}$ denote the signal gain (antenna gain and path loss) of the IZ and OZ UE, respectively, while σ denotes the additive white Gaussian noise power per Hz.

Let μ denote macro UE density which can be written as

$$\mu = \frac{N_{\mathrm{m}}}{\pi R^2}, \tag{3.4.8}$$

the system bandwidth can be expressed as

$$W = \int_0^{2\pi} \int_0^R W_u \mu r \partial r \partial \theta, \tag{3.4.9}$$

where W_u is the per UE bandwidth. Based on *Shannon*'s capacity equation, W_u can be expressed as

$$W_u = \frac{C_u}{\log_2(1 + \gamma_u)}, \tag{3.4.10}$$

where C_u is the capacity achieved per UE, while γ_u is the corresponding signal to noise ratio of the UE. Substituting for μ and W_u in Eq. (3.4.9),

$$\begin{aligned} W &= \int_0^{2\pi} \int_0^R \frac{C_u}{\log_2(1 + \gamma_u)} \frac{N_{\mathrm{m}}}{\pi R^2} r \partial r \partial \theta \\ &= \frac{2 N_{\mathrm{m}} C_u}{R^2} \int_0^R \frac{1}{\log_2(1 + \gamma_u)} r \partial r. \end{aligned} \tag{3.4.11}$$

Re-arranging Eq. (3.4.11), we have

$$C_u = \frac{WR^2}{2N_\mathrm{m}\displaystyle\int_0^R \frac{1}{\log_2(1+\gamma_u)} r\partial r}. \tag{3.4.12}$$

Since β denotes the fraction of the system bandwidth alloted for IZ transmission, the capacity per UE at the IZ, $C_{\mathrm{c},u}$, can be expressed as

$$C_{\mathrm{c},u} = \frac{\beta WR^2}{2N_\mathrm{m}\displaystyle\int_0^{\alpha R} \frac{1}{\log_2(1+\gamma_{u,\mathrm{c}})} r\partial r}, \tag{3.4.13}$$

while $C_{\mathrm{e},u}$, which denotes the capacity per UE at the OZ, is

$$C_{\mathrm{e},u} = \frac{(1-\beta)WR^2}{2N_\mathrm{m}\displaystyle\int_{\alpha R}^{R} \frac{1}{\log_2(1+\gamma_{u,\mathrm{e}})} r\partial r}. \tag{3.4.14}$$

The total macrocell capacity, C_T, is then

$$C_\mathrm{T} = N_\mathrm{m}\alpha^2 C_{\mathrm{c},u} + N_\mathrm{m}(1-\alpha^2)C_{\mathrm{e},u}. \tag{3.4.15}$$

Consider Eqs. (3.4.13) and (3.4.14), if α is decreased and β is simultaneously increased, $C_{\mathrm{c},u}$ increases while $C_{\mathrm{e},u}$ decreases. Conversely, if α is increased and β is simultaneously decreased, $C_{\mathrm{e},u}$ increases while $C_{\mathrm{c},u}$ decreases. Therefore, α and β can be tuned to achieve any desired level of fairness at the macrocell. In the next section, we discuss how to determine α and β and establish a relationship between them from the perspective of macrocell UE fairness.

3.5 Numerical evaluation

In this section, we are interested in obtaining the values of parameters α and β under the conditions that macrocell user fairness is achieved, and at the same time, femtocell throughput is maximized.

Table 3.1: Configuration Parameters

Parameter	**Setting**
Sub-carrier spacing	8 kHz
Number of sub-carriers	600
Carrier frequency	2.14 GHz
Transmit power (macrocell, femtocell)	43 dBm, 20 dBm
Antenna gain (macrocell, femtocell, UE)	8 dBi, 3 dBi, 3 dBi
Path loss exponent	3.5
Thermal noise (density, figure)	−134 dBm/Hz, 7 dB
Macro-eNB cell radius	1,000 m
Number of Macro UEs	1,000

3.5.1 Macrocell throughput fairness

It can be observed in Eqs. (3.4.13) and (3.4.14) that $C_{\mathrm{c},u}$ and $C_{\mathrm{e},u}$ are functions of α and β, hence, they can be represented as $C_{\mathrm{c},u}(\alpha,\beta)$ and $C_{\mathrm{e},u}(\alpha,\beta)$, respectively. Let $f(\alpha,\beta)$ denote the magnitude of the difference between them as shown in Eq. (3.5.1):

$$f(\alpha,\beta) = \left|C_{\mathrm{c},u}(\alpha,\beta) - C_{\mathrm{e},u}(\alpha,\beta)\right|. \tag{3.5.1}$$

In order to achieve fairness between the IZ macrocell UEs and the OZ macrocell UEs, we need to find the values of α and β which satisfies

$$f(\alpha,\beta) = 0. \tag{3.5.2}$$

It is, however, hard to solve Eq. (3.5.2) with respect to α and β explicitly. Therefore, we solve Eq. (3.5.3), which is a modified form of Eq. (3.5.2), numerically:

$$f(\alpha,\beta) \leq \epsilon, \tag{3.5.3}$$

where ϵ is an infinitesimal small number. More precisely, we monotonically increase β in the interval $(0,1)$, and a corresponding α is selected as α_{f} from the α space for each

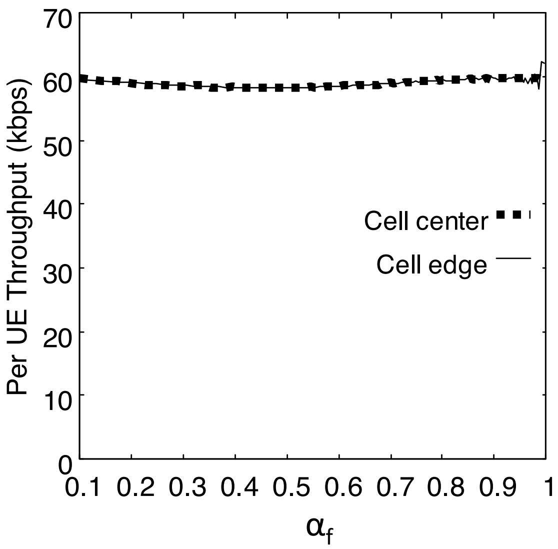

Figure 3.5: Per user throughput of macrocell

β subject to the condition in Eq. (3.5.3). The numerical problem (i.e., Eq. (3.5.3)) is solved using *Simpson*'s numerical method. Based on *Simpson*'s numerical procedure, the values of $C_{\mathrm{c},u}$, $C_{\mathrm{e},u}$, and C_{T} are computed according to Eqs. (3.4.13), (3.4.14), and (3.4.15), respectively, using the configuration parameters in Table 3.1. Figure 3.5 shows the throughput graphs of the macrocell IZ and OZ UEs (i.e., $C_{\mathrm{c},u}$ and $C_{\mathrm{e},u}$, respectively) plotted against α_{f}. As shown in Fig. 3.5, it can be observed that $C_{\mathrm{c},u}$ and $C_{\mathrm{e},u}$ are approximately equal to each other and are constant regardless of α and β. This demonstrates a high level of fairness among the macrocell UEs. Figure 3.6 illustrates the graph of total macrocell throughput plotted against α_{f}, while Fig. 3.7 shows the graph of β plotted against α. An interesting deduction that can be made is that, at $\alpha = \alpha_{\mathrm{f}}$ (i.e., throughput-fair region),

$$\beta = f(\alpha) \approx \alpha^2, \tag{3.5.4}$$

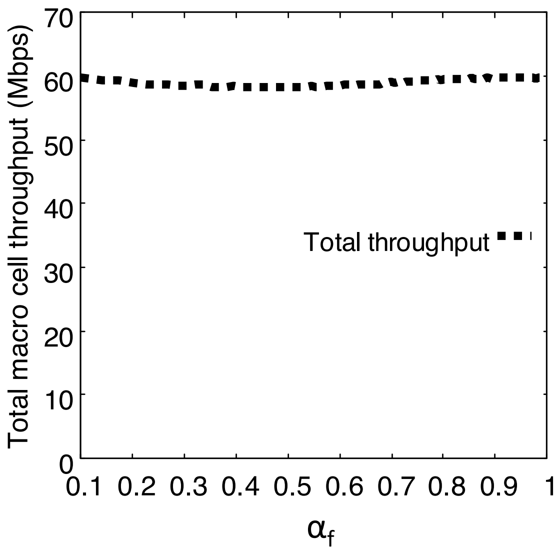

Figure 3.6: Total throughput of macrocell

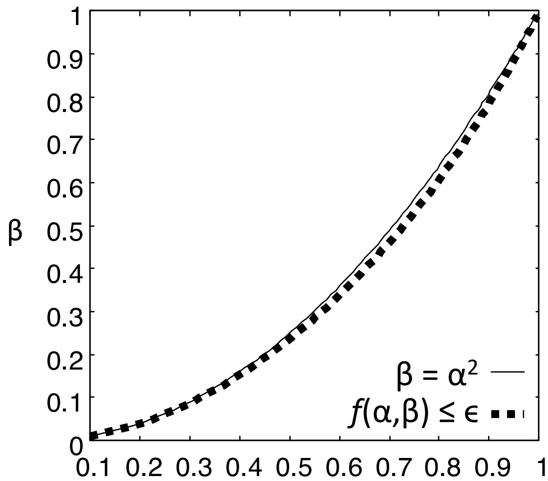

Figure 3.7: Comparison between the graph of the function $f(\alpha, \beta) \leq \epsilon$ and the graph of the quadratic equation $\beta = \alpha^2$.

as shown in Fig. 3.7. This relationship between α and β holds for the path loss exponent, $n = 3.5$, used in this study. If n is varied, the shape of the graph in Fig. 3.7 changes and so also the representative function. Such function can be determined through a curve fitting procedure (e.g. least square method) and can be used in place of Eq. (3.5.4) in the next section. The next section considers a femtocell underlay scenario and discusses how to maximize femtocell throughput while still maintaining macrocell fairness by using Eq. (3.5.4).

3.5.2 Femtocell throughput maximization

In this section, we assume that a grid network of femtocell is integrated on the macrocell as underlay, and the structure of FFR resource partitioning adopted is as illustrated in Fig. 3.4(b). We also assume that only one femtocell UE is attached to each femtocell. It can be observed in Figs. 3.4(a) and (b) that the bandwidth resources used by the inner zone femtocells overlap that used by outer zone macrocell UEs which could result in interference. However, the interference affects only a small subset of the total number of macrocell UEs and femtocell UEs (i.e., UEs at the border region between the IZ and the OZ and also UEs at inter-sector border regions, e.g., Sector 1/Sector 2 border region). For example, mutual interference exists between a macrocell UE using sub-band B_{i} at location L_1 and a femtocell at location L_2 that is also using sub-band B_{i}. Actually, the femtocell at this border region (i.e., the femtocell at location L_2) should sense the resources that are occupied by macrocell UEs in its surrounding so that reuse of such resources by this femtocell can be avoided, but we ignore this in our analysis due to the low number of affected UEs.

From Figs. 3.4(a) and (b), the size of bandwidth used by each femtocell UE located at the IZ of Sector 1 of the macrocell is

$$\frac{2}{3}\left(1-\beta\right)W. \tag{3.5.5}$$

In the case of the femtocell UEs located at the OZ of Sector 1 of the macrocell, the bandwidth used by each femtocell UE is

$$\frac{2}{3}\left(1-\beta\right)W+\beta W=\frac{(2+\beta)W}{3}. \tag{3.5.6}$$

It is noteworthy that we have considered only Sector 1 in Eqs. (3.5.5) and (3.5.6). This is because symmetry is assumed among the three sectors; hence, the computational results obtained for one of the sectors are applicable to the other sectors. The power transmitted by a serving femtocell (or interfering femtocell), s (or j), to femtocell UE, i, is $P_{s,i}$ (or $P_{j,i}$), while $G_{\mathrm{f},s,i}$ (or $G_{\mathrm{f},j,i}$) denotes the signal gain (antenna gain and the pathloss) between femtocell UE i and its serving femtocell (or interfering femtocell), while N_{J} denotes the number of neighbor interfering femtocells. Due to the way the bandwidth resources are partitioned and due to the equal distances between adjacent nodes of the grid network, the SINR (signal to interference plus noise ratio) seen at each femtocell is similar. The SINR, γ_i, of UE i can be expressed as

$$\gamma_i=\frac{P_{s,i}G_{\mathrm{f},s,i}}{\displaystyle\sum_{j=1,j\neq s}^{N_{\mathrm{J}}}P_{j,i}G_{\mathrm{f},j,i}+\sigma}. \tag{3.5.7}$$

The total number of femtocells at the IZ is

$$N_{\mathrm{f}}\frac{\pi(\alpha R)^2}{\pi R^2}=N_{\mathrm{f}}\alpha^2, \tag{3.5.8}$$

where N_{f} is the total number of femtocells deployed in the network, while the total number of femtocells at the OZ is

$$N_{\mathrm{f}}-N_{\mathrm{f}}\alpha^2=(1-\alpha^2)N_{\mathrm{f}}. \tag{3.5.9}$$

Combining Eqs. (3.5.5), (3.5.6), (3.5.7), (3.5.8), and (3.5.9), the total femtocell capacity, C_{f}, is computed as

$$\begin{aligned} C_{\mathrm{f}} &= \frac{2(1-\beta)W\alpha^2 N_{\mathrm{f}}}{3}\log_2(1+\gamma_i) + \frac{(2+\beta)(1-\alpha^2)WN_{\mathrm{f}}}{3}\log_2(1+\gamma_i) \\ &= \frac{2+\beta-3\alpha^2\beta}{3}N_{\mathrm{f}}W\log_2(1+\gamma_i). \end{aligned} \tag{3.5.10}$$

In order to ensure fairness at the macrocell layer, we replace β with α^2 (i.e., Eq. (3.5.4)) in Eq. (3.5.10):

$$C_{\mathrm{f}} = \frac{2+\alpha^2-3\alpha^4}{3}N_{\mathrm{f}}W\log_2(1+\gamma_i). \tag{3.5.11}$$

The maximum total throughput of the femtocells, $C_{\mathrm{f,max}}$, is:

$$C_{\mathrm{f,max}} = C_{\mathrm{f}}|_{\frac{\partial C_{\mathrm{f}}}{\partial \alpha}=0 \text{ and } \frac{\partial^2 C_{\mathrm{f}}}{\partial \alpha^2}<0}. \tag{3.5.12}$$

Solving Eq. (3.5.12), $\alpha = \sqrt{\frac{1}{6}}$ and $\beta = \alpha^2 = \frac{1}{6}$. These values of α and β ensure UE fairness at the macrocell layer and at the same time maximizes the total femtocell throughput.

3.6 Concluding remarks

In this chapter, we used an analytical technique to optimally partition radio resources in a multi-tier network scenario. In particular, we mathematically established the relationship between base station-to-user distance and radio resource partitioning variables. By applying an exhaustive search procedure on the developed formulation, we determined the optimal radio resource partitioning parameter values from the perspectives of macrocell user fairness and femtocell throughput maximization. The formulation revealed that the path loss exponent of a wireless system influences the relationship between partitioning parameters such as the distance factor and bandwidth factor at the throughput-fair region. Even though, the results presented were obtained for a certain network model, they, however, serve as important references in the deployment of OFDMA-based multi-tier systems.

Chapter 4

Cooperative channel assignment

4.1 Introduction

The frequency spectrum is a costly and scarce radio resource which requires proper usage plan in order to achieve an efficient network performance. Radio resource usage efficiency is improved if network interference is minimized. Therefore, channel assignment is usually done in order to orthogonalize, as much as possible, the channels used by collocated potential interferers.

This chapter discusses channel assignment for the mitigation of femto-to-femto interference. The existing channel assignment techniques used in fixed-position base stations such as macrocell base stations (MBSs) may have little performance efficiency when used in nomadic user-deployed base stations such as femtocell base stations (FBSs). Hence, channel assignment techniques for these classes of base stations will be discussed separately in this chapter.

4.2 Theoretical background

Channel assignment dates back to the days of GSM systems which employed fixed-position base stations.

4.2.1 Channel assignment in fixed-position base stations

For this type of base station, channel assignment is classified into FCA (Fixed Channel Assignment), DCA (Dynamic Channel Assignment), and HCA (Hybrid Channel Assignment) [52].

4.2.1.1 Fixed channel assignment in fixed-position base stations

In FCA technique, the cells are permanently assigned channels based on some reuse pattern and SINR requirement. Due to traffic temporal variation and spatial variation, the performance of FCA often becomes degraded as a result of high blocking probability. To address this, a type of FCA known as NCPA (Non-uniform Compact Pattern Allocation) assigns channels using a pattern that minimizes the overall system blocking probability. Furthermore, various channel borrowing schemes are used with FCA to keep blocking probability low. These include SBR (Simple Borrow From the Richest), BA (Basic Algorithm), BAR (Basic Algorithm with Reassignment), and BFA (Borrow First Available).

4.2.1.2 Dynamic channel assignment in fixed-position base stations

In DCA, the channels are not permanently assigned to the cells, but instead are kept in a common pool and are made available to the cells as calls arrive. At the end of the call, the channel is returned to the pool. In networks where traffic condition fluctuates, DCA are more preferred to FCA. The implementation of DCA can either follow a centralized or distributed manner. Existing centralized DCA algorithms include FA (First Available) and LODA (Locally Optimized Dynamic Assignment). In distributed DCA, channel is assigned autonomously by the each cell. Existing distributed

DCA schemes include LP-DDCA (Local Packing Dynamic Distributed Channel Assignment), SSMD-DDCA (Signal Strength Measurement-based Distributed DCA), MV-DDCA (Moving Direction Distributed DCA) etc. Although, DCA is more suitable than FCA for networks whose traffic varies, the system complexity of DCA is, however, higher.

4.2.1.3 Hybrid channel assignment in fixed-position base stations

HCA is a mixture of the FCA and DCA schemes. The channels are grouped into two sets, one set is used in the FCA mode while the other set is used in the DCA mode. The ratio of Fixed channel to Dynamic channel is an important design parameter in HCA systems.

4.2.2 Channel assignment in nomadic base stations

Most of the channel assignment schemes discussed in the previous sections have been implemented for MBSs and microcell base stations which are fixed-position infrastructures usually planned and deployed by technical experts. FBSs on the other hand are classified as nomadic base stations since they can be moved around, and a change in the geographical location of the base station can render the RF settings of the station inefficient if fixed-configured. Therefore, in this case, an adaptive configuration mechanism is inevitable, and for this reason, FBSs self-organize (adjust transmission configuration according to the current RF condition of the surrounding) usually in the UE (User Equipment) mode at power-on and also during normal operation. Hence, in the case of FBS, only dynamic channel assignment is realistic.

4.2.2.1 Dynamic channel assignment in nomadic base stations

In order to enable FBSs to adapt themselves appropriately to changing RF environments, specialized channel assignment algorithm is necessary. Some channel assignment algorithms have been proposed for FBS [53]. Let $\mathcal{J}$ denote the set of sub-channels from which ρJ sub-channels are to be selected by an FBS (where $0 < \rho \leq 1$ and J is the cardinality of $\mathcal{J}$). Each sub-channel $j \in \mathcal{J}$ has M sub-carriers, and the channel gain of sub-carrier m belonging to sub-channel j is denoted as $h_{j,m}$.

1. Channel-gain oriented channel assignment [53]

   a) Max-min channel-gain channel assignment

   - step 1: For all sub-carriers in each sub-channel, find the minimum subcarrier gain

   $$h_j = \min_m \{h_{j,m}\} \quad \forall j \in \mathcal{J} \tag{4.2.1}$$

   - step 2: Sort h_j as $h_1 \geq h_2 \geq \cdots \geq h_J$
   - step 3: Select the first ρJ sub-channels with higher link gain, $h_j > h_{j+1} \quad \text{for } j = 1, \ldots, \rho J$

   b) Max-avg channel-gain channel assignment

   This algorithm selects sub-channels that have higher average sub-carrier gain

   - step 1: Compute the average sub-carrier gain of each sub-channel

   $$h_j = \frac{1}{M} \sum_{m=1}^{M} h_{j,m} \quad \forall j \in \mathcal{J} \tag{4.2.2}$$

   - step 2: Follow step 2 and step 3 in 1(a)

2. Interference oriented channel assignment [53]

   a) Min-max interference-avoidance channel assignment

   In this algorithm, sub-channel selection is based on the interference on the sub-carrier

   - step 1: For all sub-carriers in each sub-channel, find the minimum interference, I_j, on the sub-carrier

$$I_j = \max_m \{I_{j,m}\} \quad \forall j \in \mathcal{J}, \tag{4.2.3}$$

     where $I_{j,m}$ is the total interference received by all sub-carriers m in sub-channel j

   - step 2: Sort I_j as $I_1 \leq I_2 \leq \cdots \leq I_J$
   - step 3: Select the first ρJ sub-channels with lower interference, such that $I_j < I_{j+1}$ for $j = 1, \ldots, \rho J$

   b) Min-avg interference avoidance channel assignment

   This algorithm selects sub-channels that have lower average sub-channel interference

   - step 1: Compute the average sub-carrier interference for each sub-channel

$$I_j = \frac{1}{M} \sum_{m=1}^{M} I_{j,m} \quad \forall j \in \mathcal{J} \tag{4.2.4}$$

   - step 2: Follow step 2 and step 3 in 2(a)

3. SINR oriented channel assignment

   a) Max-avg channel SINR channel assignment

This algorithm selects sub-channels that have higher average sub-carrier SINR. This channel assignment technique is by far the most widely used method since it is a hybrid of channel-gain oriented and interference oriented methods.

- step 1: Compute the average[1] sub-carrier SINR of each sub-channel as [54]

$$\gamma_j = -\beta \ln\left(\frac{1}{M}\sum_{m=1}^{M} \exp^{-\frac{\gamma_m}{\beta}}\right) \quad \forall j \in \mathcal{J}, \tag{4.2.5}$$

  where β is a parameter that must be optimized from link-level simulation results for every modulation and coding rate combination.

- step 2: Sort γ_j as $\gamma_1 \geq \gamma_2 \geq \cdots \geq \gamma_J$
- step 3: Select the first ρJ sub-channels with higher average SINR such that $\gamma_j > \gamma_{j+1}$ for $j = 1, \ldots, \rho J$

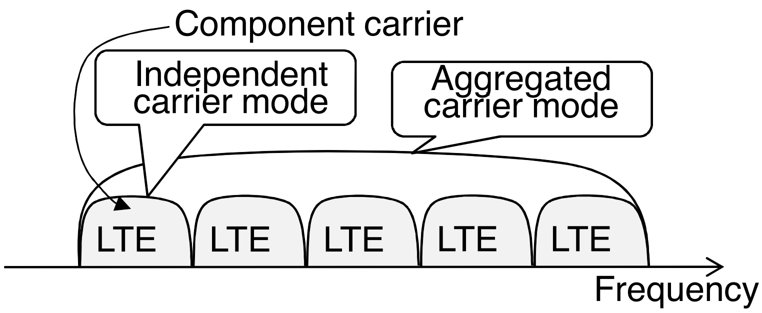

Figure 4.1: Bandwidth structure of LTE-advanced.

[1]This SINR averaging technique is known as EESM (Exponentially Effective SINR Map). Note that the MIC (Mean Instantaneous Capacity) method may also be used. In the case of MIC, the average sub-carrier SINR is computed as [55] $\gamma_j = 2^{\left(\frac{1}{M}\sum_{m=1}^{M} \log_2(1+\gamma_m)\right)} - 1$

4.2.3 LTE-advanced

LTE-advanced (Long Term Evolution-advanced) is an evolution of the standard LTE. It supports wide bandwidth for the purpose of achieving higher peak data rates. The LTE-advanced comprises of multiple component carriers that can operate in two modes namely, independent carrier mode, and aggregated carrier mode as illustrated in Fig. 4.1. A component carrier is made up of a standard LTE bandwidth. If the component carriers of an LTE-advanced system are treated as separate bandwidths, it is referred to as independent carrier mode. If, however, the component carriers are combined and treated as a single bandwidth, it is referred to as aggregated carrier mode. The support for these two modes makes LTE-advanced backward compatible with standard LTE, since in the independent carrier mode, each component carrier can be used in the same way as a standard LTE system. Carriers intended for aggregation should not be constrained to adjacent carriers in frequency bands, i.e., both contiguous and non-contiguous spectrum aggregation should be supported [56].

4.3 Related works

The network density has a significant impact on the availability of interference-free channels in an FBS network scenario. How to assign channels in an optimal manner in such networks is crucial in order to fully reap the capacity gain benefits promised by FBSs. From the perspective of channel assignment optimality, a centralized assignment approach is most attractive. Its attractiveness, however, dwindles when the associated computational complexity, control signaling overhead, and scalability drawbacks are considered in large networks. For these reasons, many decentralized schemes have been proposed in the literature.

In [8], the authors propose a frequency assignment technique in which sub-channel usage probability message is broadcasted periodically by every FBS in the network. Each FBS then prioritizes sub-channels usage based on usage probability at neighboring cells in order to reduce interference received by its own users. The work focuses on self-received interference mitigation and disregards own-radiated interference. This could impact the channel assignment efficiency at neighboring cells, leading to a reduced network-wide throughput. Also, due to the periodic information broadcast that this approach relies upon, a trade-off exist between signaling overhead and outdated information. This is because lengthening the broadcast interval leads to a desired low signaling overhead, but it also leads to an undesired broadcast of outdated information, whereas, shortening it desirably avoids the broadcast of outdated information but also leads to an undesired high signaling overhead.

The authors in [37] proposed a joint sub-channel and power allocation scheme for indoor base stations and showed that in dense networks, optimal BPA (Binary Power Allocation) outperforms IWF (Iterative Water Filling) scheme in terms of system capacity. In BPA, only one base station is allowed to transmit at full power on a given channel at a given time while other neighboring base stations remain silent. Hence, interference does not occur. Since in BPA, power allocation problem is substantially reduced, the main problem that remains is channel allocation which the authors addressed by assigning a channel only to the user that has the best channel state. Issues regarding which base station should transmit, at what time should it transmit, and which user should receive are decided by a central node which has a backhaul link to all base stations. Since the central node has to acquire channel information from all base stations by exchanging signaling messages with the base stations, this can be a serious burden on the backhaul and poses a major drawback. In addition, the channel assignment is an opportunistic one which is not in favor of users experiencing poor RF conditions. Hence, users located in particular cell regions such as cell-edge region gets starved while users closer to the base station are greedily served. Moreover, this approach is based on centralized coordination of both base stations and users, it therefore suffers scalability issues.

Successive interference cancellation approach has been used to address femtocell-to-macrocell interference problem [57]. In this approach, the supposed uplink interference from a nearby macrocell user is treated as a wanted signal at a serving FBS. Through successive interference cancellation technique, the serving FBS decodes the nearby macrocell user alongside the uplink signal from its own users. Other users belonging to other base stations (e.g, neighbor FBSs) are, however, additional sources of interference if scheduled on the same channel used at serving FBS, and their signals have to be canceled as well. In this case, the cancellation burden is non-trivial since all the interference signals have to be regenerated through estimation by base station f and subsequently subtracted successively. Hence, high computational complexity attributable to channel estimation task, and also interference estimation error are the major drawbacks of this approach.

Interference management through power control has been proposed in [58]. The interference problem is addressed through a mathematical framework that compels each FBS to ensure that after power is loaded on sub-channels, the neighboring users' SINR does not fall below a pre-determined threshold value. The burden of exchanging FBS user's received interference between an FBS and its user is avoided through interference estimation at the FBS which is based on the separation distances between the FBS and the surrounding base stations. The formulation however neglects femto-to-femto interference which is a highly significant problem in enterprise FBSs where multiple FBSs may coexist in the same building e.g., in a shopping mall, airport, etc. This reduces the generality of the approach. In addition, the formulation disregards the actual interference received by the FBS user from surrounding base stations and simply assume it to be equal to the interference received at the FBS itself. This assumption has a significant performance implication in sectorized networks where the received interference from a directional antenna does not only depend on a receiver's linear distance from the transmitting antenna alone, but also on the angular distance between them as well. Also, a mathematical formulation is used in the estimation of base station-to-base station distances which are used in place of actual distances for channel gain computation. This, together with the previously mentioned sectorized antenna case raises the probability of interference estimation error. Also, additional supporting devices such as GPS (Global Positioning System), etc. may be necessary for neighbor base station position estimation which means additional capital cost.

Autonomous component carrier selection scheme has been proposed for FBSs [59]. In this scheme, each FBS autonomously selects component carriers. The selection process ensures that a serving FBS selects with low priority, a component carrier that is being used by a neighboring FBS with which it shares high mutual path loss coupling. In addition, the selection procedure ensures that FBSs minimizes the interference caused to neighbor FBSs. This selection is attractive due to its fully distributed channel selection mechanism and also due to the channel usage fairness among neighboring FBSs. However, the drawback of this scheme is that an active negotiation between FBSs for channel usage is lacking. Channel usage negotiation can yield higher channel assignment efficiency in situations where after negotiation, an FBS leaves a channel for another adjacent FBS to occupy if the adjacent FBS has a higher utility for the channel.

Inspired by the shortcomings of previous research works on interference management in FBS networks, we develop a channel assignment scheme that has the following properties.

1. The channel assignment scheme is decentralized in order to avoid the high computational complexity of centralized channel assignment
2. The channel assignment scheme does not require excessive control signaling
3. The channel assignment scheme is scalable with network-size growth
4. The channel assignment scheme does not rely on pure spectrum sensing alone but is supported by additional cooperative channel usage processing
5. The channel assignment scheme does not need additional infrastructure (e.g., GPS) other than existing ones for practical implementation
6. The channel assignment scheme jointly considers femtocell self-throughput maximization and neighbor throughput implication as well

4.4 Proposed scheme

Before explaining schemes, we should clarify the problem. The problem we are considering is a channel assignment problem, but the word channel has several notations. In this chapter, we use the word “channel” to represent “bandwidth”. If closely located BSs (base stations) use different channels, the problem of interference does not arise; but, if the same channel is used by very close BSs, interference is introduced and this could result in a poor network performance. We propose a scheme that is based on the grouping together of FBSs that are close to one another for the purpose of joint assignment of channels.

4.4.1 System model

The downlink of an LTE-Advanced system is considered in this chapter. The 100 MHz LTE-Advanced system consists of five component carriers (CCs), each with a bandwidth of 20 MHz. We assume that each FBS uses only one of the 20 MHz bandwidth CCs for transmission. Each CC contains 100 resource blocks (RBs) and each RB has a bandwidth of 180 KHz. Our BS deployment technique follows the approach discussed in [60] where a 5×5 grid model was used to simulate FBS deployment. This simulation assumption represents a realistic case in which an apartment may or may not have a FBS deployed in it. The deployment of FBSs follows a random and uniform manner such that FBSs are deployed with a probability p in each of the 25 apartments being considered and the FBSs are placed at the centre of the apartments. Each apartment has a dimension of 10×10 m^2 and whichever one contains an FBS also contains exactly one associated user equipment (UE). The UE is dropped randomly and uniformly at a specified minimum separation distance of 0.2 m [60] and a maximum separation distance r metres from its serving BS which operates in the closed access mode [22],[61]. In this consideration, the closed access mode ensures that a UE connects to its serving FBS only, notwithstanding its closeness to other neighbor FBSs. In order to compute the useful/interfering signal, a simplified pathloss model recommended in [60] for the 5×5 grid deployment in LTE-advanced

Table 4.1: Link to system mapping parameters

Parameter	**Value**	**Note**
α	0.6	Implementation losses
$\gamma_{\min}$[dB]	-10	QPSK
$\gamma_{\max}$[dB]	19.5	64 QAM
β[bps/Hz]	4.4	Maximum spectral efficiency

is used such that pathloss is calculated as:

$$L(\mathrm{dB}) = 127 + 30\log_{10}\left(\frac{d}{100}\right), \tag{4.4.1}$$

where d is the distance between the UE and the FBS expressed in meters. This simplified LTE-Advanced model avoids the need to model wall penetration loss. A realistic link level model suggested by the 3GPP for LTE link level simulation [20] is used to model the link adaptation:

$$R_u = \begin{cases} 0 & \text{for } \gamma_u < \gamma_{\min}, \\ \alpha \cdot B \cdot A(\gamma_u) & \text{for } \gamma_{\min} < \gamma_u < \gamma_{\max}, \\ \beta \cdot B & \text{for } \gamma_u > \gamma_{\max}, \end{cases} \tag{4.4.2}$$

where

$$A(\gamma_u) = \log_2(1 + \gamma_u), \tag{4.4.3}$$

and R_u is the capacity achieved by user u in bps at SINR γ_u. The channel bandwidth is denoted as B in Hz, α is the attenuation factor representing implementation losses, while β is the maximum throughput of the ACM (Adaptive Coding and Modulation) codeset in bps/Hz. The minimum SINR of the codeset is denoted as $\gamma_{\min}$, while $\gamma_{\max}$ is the SINR at which maximum throughput is reached. These parameters are summarized in Tab. 4.1.

4.4.2 Proposed cooperative channel assignment scheme

In this section, we describe how cluster scheme can be beneficial in a network that comprises of many user-deployed FBSs. Cooperative coordination among closely located FBSs is vital due to the unplanned nature of their deployment. This coordination helps to improve the network radio resource distribution pattern at high activation ratio. The activation ratio is the percentage of active FBSs in a network at any particular time [60]. One way of achieving this type of automatic coordination is through the formation of clusters which we will now explain.

4.4.2.1 Cluster concept

In conventional cellular networks, handover is often done when the signal strength received from the serving BS becomes significantly weaker than the strength received from a neighbor BS. Handover functionality may, however, not be enabled in the case of FBSs depending on the access mode of the BS such as, closed access mode. Since FBSs are deployed by end users, conventional network planning prior to deployment is impracticable, owing to the fact that the position of each BS is usually not previously known. Moreover, the BS is not a fixed structure and a user can move it to a new

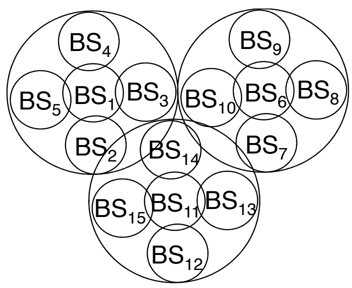

Figure 4.2: Typical base station clusters.

location, thereby disrupting initially configured RF parameters. Figure 4.2 illustrates a typical cluster structure. In the proposed cluster system, one BS assumes the duty of a CH (cluster-head), and this BS is responsible for making final decision regarding the radio resource usage (for example, channel utilization, optimum pilot strength, time-slot usage, joint scheduling coordination etc.) by members of its cluster. If a CM (cluster-member) is being restricted to use a channel on which it is experiencing high interference, the CH can re-organize spectrum usage in the cluster, thus achieving a better user experience at each BS.

The CH will normally communicate with its CMs over radio or DSL (or X2 interface in the case of LTE networks), so that it is not necessary for other members of the cluster to communicate directly with each other since resource sharing will be centrally coordinated by the CH. In order to realize an effective resource assignment procedure by the CH, we divide the whole process into three major steps, which are:

1. cluster formation
2. interference coordination
3. channel assignment.

4.4.2.2 Cluster formation

We propose two types of cluster formation techniques, which are, *choose first request* and *choose best request schemes*. These two schemes differ by the way in which the CM candidate selects its CH. In the *choose first request scheme*, the CM candidate waits for the first request to come from a CH candidate and it immediately sends a response when it receives the request. This scheme is particularly useful in a network in which there are no existing clusters or in a network in which few clusters have been formed. It ensures that the expected minimum allowed cluster size is guaranteed throughout the network, since a CH candidate that nominates itself will certainly get responses from all the CM candidates it sends requests to. However, in the *choose best request* scheme, the CM candidate does not send response after receiving the first request from a CH candidate. Instead, it waits for a pre-configured time delay before it chooses one of the several requests it receives from multiple CH candidates. This is particularly useful in a network in which several clusters have been formed. It gives the CM candidate the opportunity to send response to the CH to which it could possibly cause the highest interference.

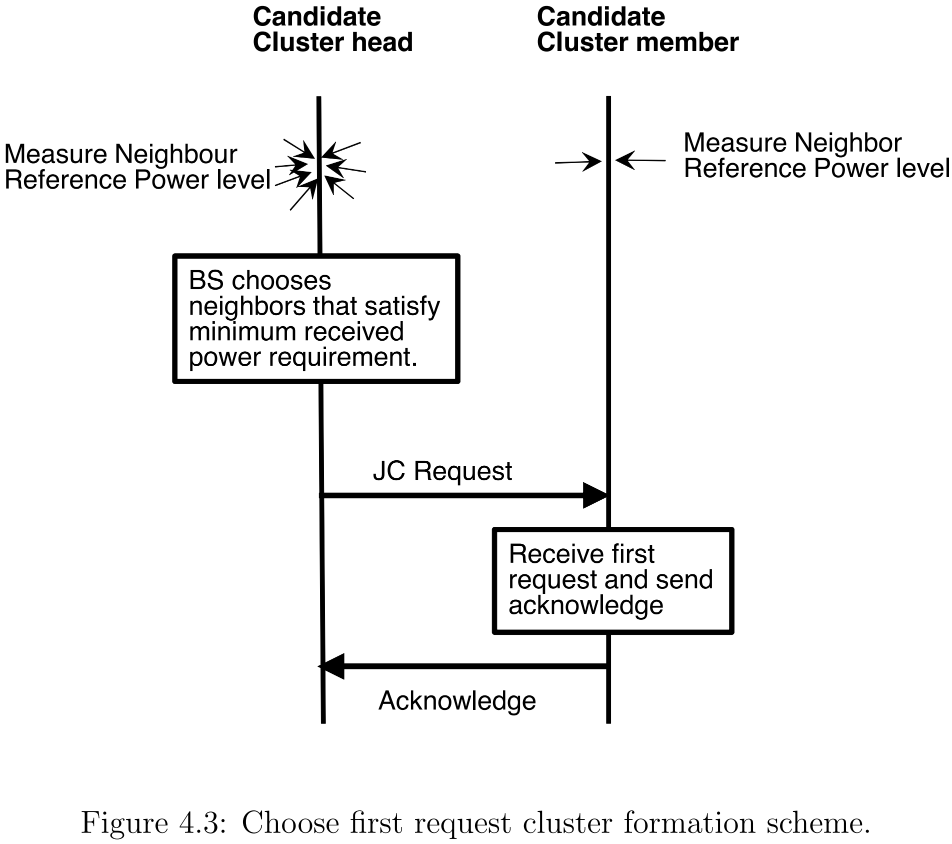

Figure 4.3: Choose first request cluster formation scheme.

Choose first request The choose first request scheme is illustrated in Fig. 4.3. When a *form cluster instruction* is initiated, all BSs in the network use UE-assisted measurements to determine the reference power received from their neighbor BSs. Due to the random positions of BSs and user equipments, the measured values at individual cells follow a random pattern; hence, some stations receive stronger power from more neighbors than others. These BSs become CH candidates because they are in higher interference regions compared to others. The CH candidates send Join Cluster (JC) requests to a predetermined number of neighbor BSs from which strongest powers are measured. These neighbors immediately send acknowledgment messages in response to the request.

Choose best request The choose best request scheme is illustrated in Fig. 4.4. Assuming in a network, a number of BSs have already formed clusters before a new BS is turned-on, it is possible for this newly switched-on BS to receive JC requests from more than one CH. Since the CHs are at different distances away from the newly switched-on BS, their path losses are also different. In this situation, the best CH for this newly switched-on BS is the CH to which it could possibly cause the highest interference. Hence, only the CH whose UE measures the strongest pilot strength from the CM candidate receives an acknowledgment message as illustrated in Fig. 4.4.

4.4.2.3 Interference coordination

The CH classifies its CMs according to the pilot strength that each CM receives from other same cluster CMs. If two or more CMs mutually measure low pilot strength

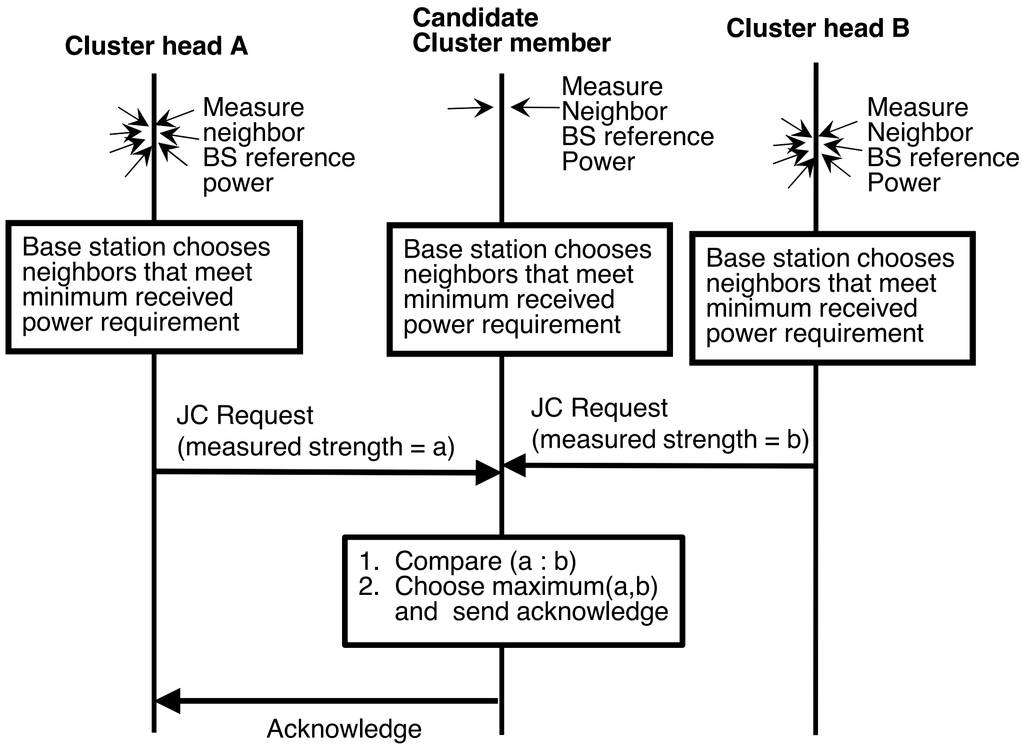

Figure 4.4: Choose best request cluster formation scheme.

from one another, they are grouped together for co-channel operation. Also, each CM classifies all the channels according to the carrier to interference ratio (C/I). Channels with a value of C/I below a given threshold value are classified as unusable channels while channels with a C/I value greater than or equal to this threshold value are classified as usable channels. The C/I classification information is sent by the CMs to their respective CHs which in return assign channels to the CMs after processing the received information.

Table 4.2: Channel assignment table with reuse.

Pattern	BS_1	BS_2	BS_3	BS_4	BS_5
P_1	R_a	R_b	R_b	R_d	R_e
P_2	R_a	R_b	R_b	R_e	R_d
P_3	R_a	R_c	R_c	R_d	R_e
P_4	R_a	R_c	R_c	R_e	R_d
$\vdots$	$\vdots$	$\vdots$	$\vdots$	$\vdots$	$\vdots$
P_{120}	R_e	R_d	R_d	R_b	R_a

Table 4.3: Channel assignment table without reuse.

Pattern	BS_1	BS_2	BS_3	BS_4	BS_5
P_1	R_a	R_b	R_c	R_d	R_e
P_2	R_a	R_b	R_c	R_e	R_d
P_3	R_a	R_b	R_d	R_c	R_e
P_4	R_a	R_b	R_d	R_e	R_c
$\vdots$	$\vdots$	$\vdots$	$\vdots$	$\vdots$	$\vdots$
P_{120}	R_e	R_d	R_c	R_b	R_a

4.4.2.4 Channel assignment

The CH refers to the channel assignment table to determine how best the usable channels of cluster members can be permuted with each other in order to achieve the highest reuse at the shortest possible distance. The CA table contains a permutation of all the usable channels in such a way that avoids intra-cluster interference. Without loss of generality, we develop typical CA tables for a 5-channel system as the case of LTE-Advanced standard, and we illustrate them in Tabs. 4.2 and 4.3. Assuming the available channels are "R_a," "R_b," "R_c," "R_d," and "R_e," Tabs. 4.2 and 4.3 illustrate some possible permutations with different reuse levels. In order to explain the usage of these tables, we describe a typical channel distribution in a cluster with Figs. 4.5 and 4.6. In Fig. 4.5, all the CMs classify the channels as either usable or unusable

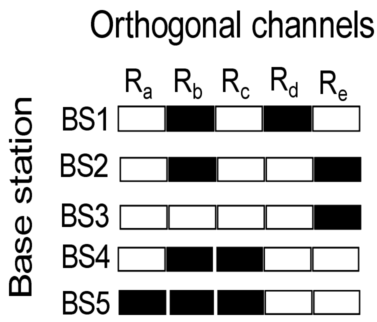

Figure 4.5: Cluster-members group channels into usable and unusable channels.

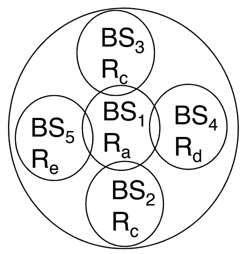

Figure 4.6: Cluster uses pattern P_3 of Tab. 4.2.

according to earlier discussion, and make this information available to the CH.

Also, according to earlier discussion, they inform the CH about the pilot strength measured from other BSs that are members of the same cluster. In Fig. 4.6, BS_1 is the CH and it uses the channel state information and mutual pilot strength measurement information it receives from its CMs to search the resource allocation table for an interference-free pattern. In this particular case, the CH chooses pattern P_3 of Tab. 4.2 which ensures that all the CMs are able to use the channels that they classified as usable. Both BS_2 and BS_3 use the same channel "R_c" because they have been grouped together by the CH owing to the fact that they mutually receive low pilot strength from each other. It should be noted that we can have more CA tables with different reuse factors such that each CH makes effort to choose patterns having highest re-use first.

4.5 Numerical evaluation

In this section, we consider 3 CA methods namely, *autonomous*, *greedy cluster*, and *fair cluster* CA methods:

autonomous CA method is used by BSs that does not belong to any cluster, and the the channel selection method is similar to the primary component carrier selection CA method discussed in [59]. In this channel selection method, BSs independently pick their best channels based on measurement reports received from their UEs.

greedy cluster CA method is when a CH selects high-gain channels for the CMs without considering the interference that the selection may cause to neighbor clusters. The CH picks a CA pattern from the CA table that yields the highest cluster throughput. There is a trade-off between increasing own cluster throughput and avoiding causing interference to neighbor cluster BSs. This CA method disregards inter-cluster interference.

fair cluster CA method is when a CH selects channels for the CMs after first considering the interference that the selection may cause to neighbor clusters. The CH selects a pattern from the CA table that increases the current network throughput the most. This CA method balances the throughput-interference trade-off.

4.5.1 System level simulation setup

We evaluate the CA scheme with a 5×5 grid model. Our simulator is setup to feature the following:

1. *autonomous*: In this setup, no cluster is formed by the FBSs. Each FBS autonomously assigns channel based on the measurement report it obtains from its UE. This setup is used as a comparative scheme.

2. *fair cluster (size: 4 to 5)*: In this setup, the FBSs are allowed to cooperate to form clusters such that each cluster contains a minimum of 4 FBSs and a maximum of 5 FBSs. FBSs that cannot join any cluster are first allowed to select channels using autonomous method after which the CHs use the fair cluster CA method to allocate channels to their CMs.

3. *fair cluster (size: 3 to 5)*: This is exactly the same as *fair cluster (size: 4 to 5)* except that in this case, each cluster is allowed to contain a minimum of 3 FBSs.

4. *greedy cluster (size: 4 to 5)*: In this setup, the FBSs are allowed to cooperate to form clusters such that each cluster contains a minimum of 4 FBSs and a maximum of 5 FBSs. FBSs that cannot join any cluster are allowed to pick channels using autonomous method after which the CHs use the *greedy cluster* CA method to allocate channels to their CMs.

5. *greedy cluster (size: 3 to 5)*: This is exactly the same as *greedy cluster (size: 4 to 5)* except that in this case, each cluster is permitted to have minimum of 3 FBSs.

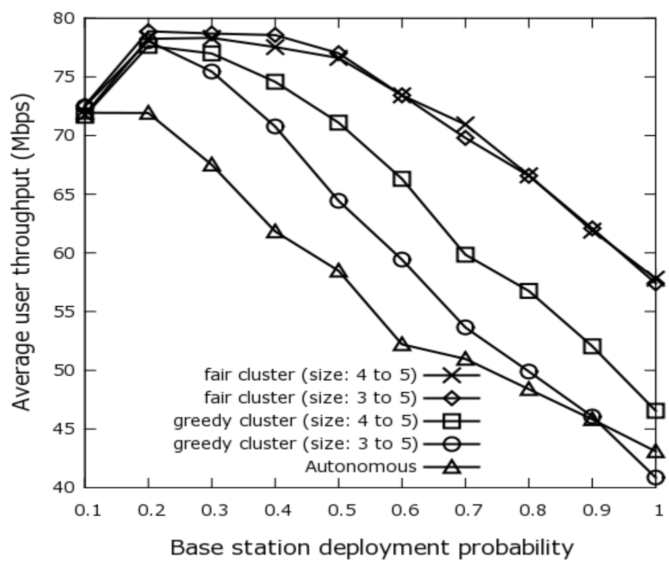

Figure 4.7: Average user throughput when user is placed at a maximum separation distance of 8 m from the serving BS.

4.5.2 Simulation results

Figure 4.7 compares the average UE throughput performance of the discussed CA methods when the FBS deployment probability is varied from 0.1 to 1.0 while the maximum separation distance between an FBS and its UE is fixed at 8 m. It can be seen from Fig. 4.7 that all the *cluster* schemes outperform the *autonomous* scheme in terms of average user throughput. This is because in the *autonomous* scenario, each FBS is a candidate source of interference to the UE of any of the FBSs around it. In the *greedy cluster* scenario on the other hand, the cluster members reduce intra-cluster interference but do not consider inter-cluster interference.

In the *fair cluster* scenario, however, all the CHs ensure that their CMs make effort to reduce the interference caused to the UEs of neighbor FBSs and at the same time selecting high-gain channels. This makes the *fair cluster* scenario to result in

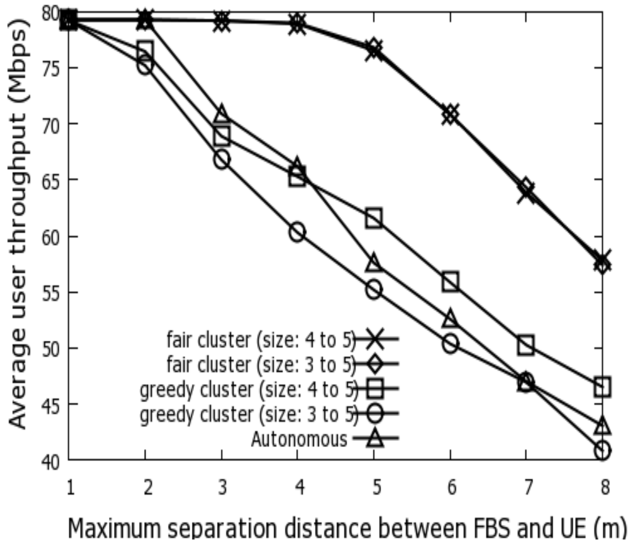

Figure 4.8: Average user throughput with BS deployment probability fixed at 1.0.

a higher average user throughput in all levels of network congestion compared to other CA methods. Higher throughput is achieved in the *greedy cluster (size: 4 to 5)* compared to *greedy cluster (size: 3 to 5)* because in the case of *greedy cluster (size: 4 to 5)*, more FBSs are able to reduce interference caused to neighbor BSs belonging to the same cluster due to larger cluster size

Figure 4.8 compares the average user throughput for the CA methods at a high deployment probability of 1.0. Again the fair cluster CA scheme performs best. The *greedy cluster* schemes do not significantly perform better than the *autonomous* scheme because the clusters are close to one another due to high deployment density such that, inter-cluster interference becomes worse. Considering Fig. 4.9, where deployment probability is set to 0.5, all *cluster* schemes perform better than the *autonomous* scheme as the UE moves farther away from its serving BS. This is because the impact of interference becomes significant when a receiver moves away from its

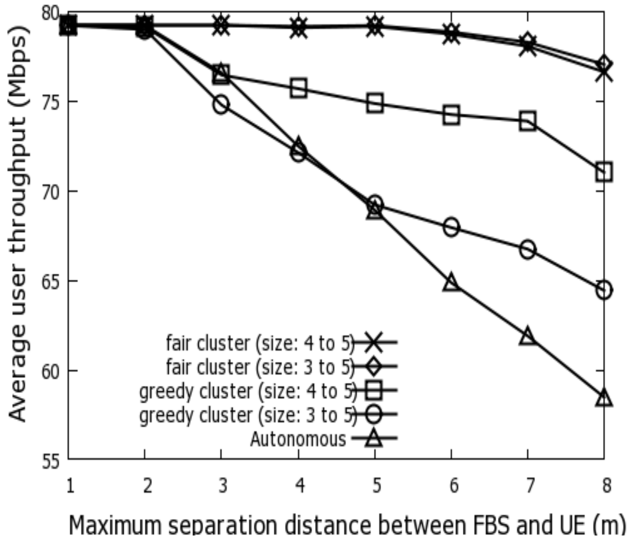

Figure 4.9: Average user throughput with BS deployment probability fixed at 0.5.

serving BS but closer to the interfering BS. In our proposed schemes, the supposed interfering BS is usually a co-operating BS, hence, uses a channel that causes little interference to the UE.

In summary, it is observed from our simulations that the *fair cluster* CA scheme yields the best average user throughput performance in all deployment density cases. Also, *greedy cluster* CA yields a higher average user throughput than *autonomous* CA under low and medium deployment density conditions. Finally, high cluster size is better than low cluster size in the case of *greedy* cluster CA method.

4.6 Conclusion

A novel inter-cell coordination scheme (co-operative channel assignment) for addressing femto-to-femto interference has been presented in this chapter. The performance of the proposed scheme has been compared with autonomous-based reference scheme available in the literature. It has been observed from simulation results that the proposed co-operative channel assignment scheme, compared to the autonomous scheme, yields higher throughput performance when a user is separated at a relatively long distance from the base station. The improvement in performance achieved by our proposed scheme is as a result of a combination of interference reduction and the use of high-gain channels which is realized through co-operation among neighboring base stations.

Chapter 5

Batch resource allocation

5.1 Introduction

In this chapter, we focus attention on how to mitigate the interference that femtocell causes to macrocell on a short-term scale. The adopted standard in this chapter is the LTE, and therefore, henceforth, we will refer to the femtocell as HeNB (Home Enhanced Node B), and to the macrocell as macro-eNB (macro-evolved Node B) since these are the terminologies used for these base stations in the 3GPP parlance.

5.2 Theoretical background

Deploying multiple HeNBs in the coverage area of the macro-eNB has the potential of increasing network throughput manifold. However, a trade-off exists between throughput gain and the flexibility of HeNB spectrum access. As a first step towards achieving interference mitigation, the 3GPP have considered five deployment configurations [62] for the HeNB, namely, (1) Configuration A, (2) Configuration B, (3) Configuration C, (4) Configuration D, and (5) Configuration E.

5.2.1 HeNB deployment configuration

(1) Configuration A: CSG, Dedicated channel, fixed power

In this mode, the HeNB uses a spectrum different from that used by the macro-eNB. The HeNB is configured as a closed subscriber group. This method is spectrally inefficient since the HeNB cannot use the part of the spectrum assigned to the macrocell even when there is no macro-eNB user in the vicinity of the HeNB that could receive interference.

(2) Configuration B: CSG, Dedicated channel, adaptive power

This is the same as Configuration A except that, in this case, the power of the HeNB is not fixed-configured but adaptive.

(3) Configuration C: CSG co-channel, adaptive power

In this mode, the HeNB uses the same spectrum as the macro-eNB. The HeNB operates in the CSG mode and the transmission power is dynamically adjustable. This mode has the chances of achieving high network throughput but it can lead to a degradation in the performance of the macro-eNB tier if interference is not adequately checked.

(4) Configuration D: Partial co-channel

In this case, only a portion of the spectrum is shared by both the HeNB and the macro-eNB, while the remaining part of the spectrum is accessible by the macro-eNB alone. Since a restriction is placed on the HeNB regarding the usage of a part of the spectrum, the spectral efficiency is lower than what is achievable in Configuration C.

(5) Configuration E: Open access, dedicated or co-channel

In this mode, the whole spectrum is accessible by both the HeNB and the macro-eNB. The HeNB, however, operates like a macro-eNB by providing access to macro-eNB users in its vicinity. Since the HeNB is usually owned by users (purchased and managed by the user - Tab. 1.1), additional incentives may have to be provided for the HeNB owner since access of public users to a privately owned HeNB could lead to a reduction in the owner's throughput and could also raise privacy concerns as well.

In this research, Configuration C has been adopted due to the associated throughput gain that can be realised when interference issues are properly addressed.

5.2.2 OFDMA-based and CDMA-based femtocell

OFDMA-based femtocell stands a higher chance of wide-spread deployment than the CDMA-based one. This is because, femtocell, if deployed in a 3G CDMA network, has a more complicated interference management challenge. For example, in the uplink, the *near-far* problem that is usually addressed through a fast closed-loop power control at the macrocell base station will be difficult to manage. This is because femtocells constitute a separate tier, hence, multiple loud femtocell users that are not under the control of the macrocell can degrade the performance of the macrocell. Also, in the downlink, the issue of dead-zone becomes practically difficult to solve since in CDMA, the bandwidth is not sub-channelized. Hence, in a situation whereby the base station operates only on a single carrier, intracell handover [63] for interference mitigation is not possible. In this chapter, it is assumed that HeNBs are deployed in an LTE network whose physical layer is based on OFDMA in the downlink. Therefore, we provide a brief overview on the LTE PHY layer in the next section.

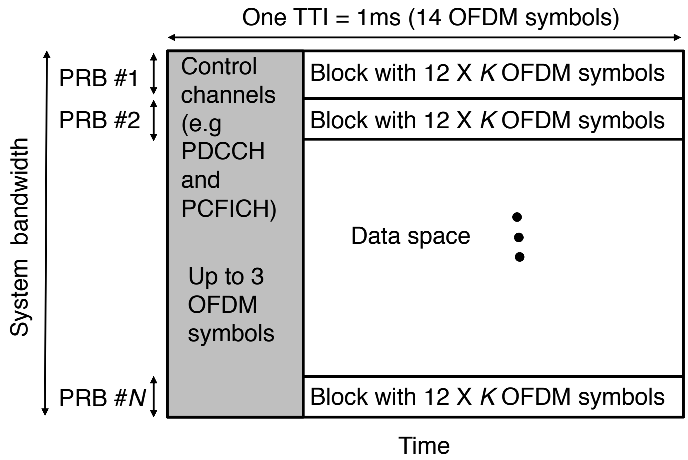

Figure 5.1: Structure of the LTE physical layer resource space for one TTI [41]. Note that PRB denotes Physical Resource Block.

5.2.3 LTE PHY layer

The LTE is characterized by high spectral efficiency, robust multi-path tolerance, and scalable bandwidth (1.4, 3, 5, 10, 15, and 20 MHz are supported). In LTE, both FDD (Frequency Division Duplex) and TDD (Time Division Duplex) modes are supported. Since its PHY layer is based on OFDMA, orthogonal sub-carriers of OFDMA makes LTE immune to intra-cell interference. The smallest radio resource unit that can be assigned to a user is the resource block which spans 180 kHz (12 sub-carriers) in the frequency domain and 1 ms (6 or 7 OFDM symbols depending on whether normal or extended cyclic prefix is used) in the time domain. The structure of the LTE physical layer resource space for one TTI is illustrated in Fig. 5.1. The data and control information are sent within a 1 ms TTI (Transmission Time Interval). The first

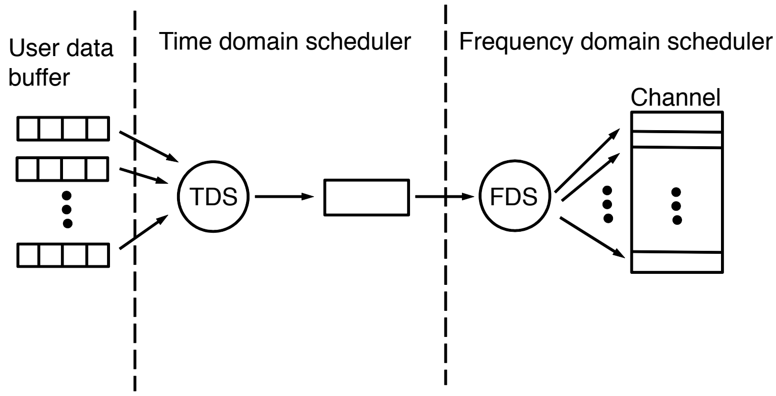

Figure 5.2: Joint time domain and frequency domain scheduling.

three OFDM symbols in a TTI are reserved for the transmission of downlink control channels such as the PDCCH (Physical Downlink Control Channel) and the PDFICH (Physical Control Format Indicator Channel). The remaining OFDM symbols in the TTI are used for the transmission of user data and reference signals. During each TTI, users are scheduled based on a scheduling policy of choice, and each user can be scheduled on multiple resource blocks. CQI (Channel Quality Indicator) report is periodically sent by the users to the base station to enhance scheduling decision and link adaptation.

5.2.4 Time domain/frequency domain scheduling

In a multi-user scenario, the base station bears the task of maximizing the utility of the radio resources through the selection the best user for a particular resource block. A typical user scheduling diagram is illustrated in Fig. 5.2. The scheduler is a combined time domain and frequency domain scheduler. The TDS (Time Domain Scheduler) selects a set of users that will be passed to the FDS (Frequency Domain Scheduler). The selected users must have non-empty buffers and there must be sufficient control channel capacity to schedule all the users selected. If the control channel capacity is insufficient for scheduling all the selected users, then, only a fraction of them will be passed to the frequency domain scheduler. The assignment of a user to a resource block is usually based on some scheduling policy.

5.2.5 Scheduling policy

Several scheduling schemes for assigning channels to users exist. Among them are round robin, maximum SINR, Earliest deadline first, PF (proportional fair), etc. The proportional fair is commonly used since it finds a balance between round robin and maximum SINR. It aims at ensuring fairness among MUEs (macro-eNB users), while at the same time considers the channel condition of the prospective MUEs before channel assignment. In particular, the PF scheduler computes the scheduling priority metric, λ_m, of each macro-eNB user, $m \in \mathcal{M}$, which is the ratio of the achievable capacity of MUE, m, to the long-term throughput of m. The MUE with the highest computed value of λ_m gets the channel. The average throughput $\bar{R}_m$ of a user that has been assigned a channel is updated as:

$$\bar{R}_m(t+1) = \frac{T-1}{T}\bar{R}_m\left(t\right) + \frac{1}{T}r_m\left(t\right), \tag{5.2.1}$$

where T denotes the time window, t is the current scheduling time, while $t+1$ is the next scheduling time.

5.2.6 Fairness

When multiple users coexist and are scheduled by a base station scheduler, it is often necessary to assess the extent of fairness of the scheduler. A commonly used fairness metric for assessing user fairness is the *Jain*'s fairness indicator, JFI. Assuming

$m \in \mathcal{M}$ and $\bar{R}_m$ are as defined in Sec. 5.2.5, the JFI can be computed as [64]:

$$JFI = \frac{\left(\sum_{m=1}^{|\mathcal{M}|} \bar{R}_m\right)^2}{|\mathcal{M}|\sum_{m=1}^{|\mathcal{M}|} \bar{R}_m^2} \tag{5.2.2}$$

The value of the JFI ranges from $\frac{1}{|\mathcal{M}|}$ (i.e., maximum unfairness, a situation in which only one user achieves high throughput while others achieve zero throughput) to 1 (i.e., maximum fairness, a situation in which all users achieve exactly equal throughput).

5.3 Related works

Concerns about the detrimental impact of HeNB-induced interference has resulted in many research works on interference mitigation. One of such works was done by Claussen et al. [65] in which an algorithm for the self-configuration of transmit power level of home base station based on the measured received signal level from the macro cell was developed. Li et al. in [66] used downlink power control to address the co-channel interference problem in a network composed of overlaid macro cell and underlaid home base stations. Han-Shin Jo et al. [67] proposed both open-loop and closed-loop power control strategies that adjust the maximum transmit power of home base station users in order to suppress the cross-tier interference at a macro cell. It is worth mentioning that, the gravity of the necessity to mitigate inter-cell interference has been demonstrated by the 3GPP through extensive discussions in [9],[10],[11]. All the aforementioned previous works ([9],[10],[11],[65],[66],[67]), even though interesting, have not adequately catered for the interference caused to the macro cell layer because the femto cell does not usually have information about the future resource usage plan of the macro cell.

A very interesting scheme is proposed by Lien et al. in [68], where the home base station autonomously mitigate interference after sensing macro cell resource usage pattern. The setback of this scheme is that, in the formulation, the future resource usage plan of the macro cell is not modeled. The home base station therefore relies largely on a probability approach in order to avoid resource allocation collision with the macro cell. If a multi-user macro-eNB scheduling scenario is considered, the set of users scheduled by the scheduler may change frequently due to an attempt to ensure fairness among the macro-eNB users, thereby causing the resource usage pattern of macro cell to vary from LTE frame to LTE frame (assuming an LTE-based network). Consequently, the correlation of resource block (RB) usage by the macro-eNB decreases, causing the performance of the proposed scheme in [68] to degrade to the case of a randomized scheme.

Inspired by cognitive radio technology [68],[69] which enables a station to cognize and adapt to a communication environment to achieve optimum network performance, we provide a new formulation for the resource allocation problem in OFDMA-based networks in order to enable a better cognition among different layers of a multi-layer OFDMA network. We model a scheduling framework in which macro-eNB resources are allocated in batch in such a way that, contrary to the probability approach employed in [68], the home base station is fully aware of future resource usage plan of the macro-eNB.

A dynamic resource partitioning approach is discussed in [70]. In the scheme, each macro-eNB user measures its channel gain towards nearby femto cell base stations.

If the measured gain exceeds a pre-determined threshold, a DL-HII (downlink high interference indicator) message is sent by the macro-eNB to the aggressor femto cell over the wired backbone, and consequently, the femto cell stops transmission on the channels being used by the victim macro-eNB user. One drawback of this approach is that it is not scalable since the number of DL-HII message sent by the macro-eNB grows with increasing number of femto cell base stations and macro-eNB users. Moreover, additional control bits incur capacity loss, hence, this approach may not be applicable in practical LTE systems since it has been agreed in 3GPP release 10 that there shall be no backhaul coordination between macro-eNB and femto cell. It is noteworthy that the batch resource allocation scheme being proposed in this chapter does not suffer from the previously mentioned drawbacks of [70] since it is scalable in large networks and it is void of capacity-reducing macro-femto backhaul coordination.

5.4 Proposed scheme

Considering multi-tier networks such as the case of coexisting macro-eNB (macro evolved Node B i.e macro-eNB) and HeNB, it is necessary to mitigate co-tier interference among HeNBs and also cross-tier interference between HeNBs and macro-eNBs. A severe interference case involves a situation in which an indoor macro-eNB user equipment (MUE) is trapped in the coverage area of a collocated indoor HeNB, and the MUE is disallowed access to the HeNB network resources owing to the fact that the terminal does not belong to the HeNB's closed subscriber group (CSG) (further details on CSG can be found in [22] and [61]). This interference problem must be addressed carefully in order to fully realize the merits of the HeNB when integrated on the existing macro-eNB network.

This chapter, which has been presented in part in [71], focuses on interference mitigation in an HeNB underlaid macro-eNB network using femtocell cognition technique. Although, the downlink case is discussed in this chapter, the formulations, however, are applicable to the uplink case as well.

5.4.1 System model

An LTE network is assumed in which the macro-eNB has a fixed value of total base station power, and there are M MUEs belonging to set $\mathcal{M}$ to which resource blocks are to be assigned. The set of resource blocks available at the macro-eNB which are to be assigned to these M users is denoted as $\mathcal{N}_{\mathrm{M}}$ while the RB index, n, is an identifier that is used to denote a resource block in the frequency domain.

5.4.2 Batch resource allocation at macro-eNB

In this section, we provide details on our proposed *batch* resource allocation scheme.

5.4.2.1 Interference avoidance vs. diversity exploitation

In wireless communication systems, the quality of signal from a transmitting source gets degraded by the time it is received at the receiving end due to large scale and small scale fading effects, Gaussian noise, and interference from other transmitting sources. LTE systems schedule resources both in the time domain (TD) and also in the frequency domain (FD) in such a way that minimizes the detrimental impact of multi-path fading. This scheduling approach contrasts earlier radio access technologies such as HSDPA (High Speed Downlink Packet Access) etc. in which network resources are scheduled in the time domain (TD) alone. In LTE, users are dynamically allocated network resources in each TTI (Transmission Time Interval) based on their instantaneous channel condition. User's channel state, however, is considered to be independent, such that, a channel that is in deep fade for one user may have the highest gain for another user. Hence, LTE systems have the capability of exploiting multi-user channel diversity to achieve substantial throughput gain.

The introduction of CSG in LTE release 8 limits the applicability of conventional interference control through cell handoff in HeNB networks. In view of this, it is imperative for the HeNB to be aware of macro-eNB's resource schedule in order to effectively avoid causing interference to nearby nonmember-CSG MUEs. A simple and effective way of achieving this is for the macro-eNB to pre-determine it's future usage of network resources, and make this information available to neighboring HeNBs. Precisely speaking, resources are allocated to MUEs in batch, meaning that an RB allocated to a user equipment (UE) in the current TTI will continue to be used by the same UE in future consecutive TTIs. We refer to the number of consecutive TTIs allocated to a UE for RB usage as the *batch-length*.

The time varying property of the wireless channel raises the question of what length of time should be allocated to a UE in order to achieve the desired interference reduction merit characterized by batch allocation, and at the same time minimize the detrimental impact of channel fluctuations. Invariably, channel fluctuation places an upper bound on the length of time the scheduling of a UE can be prolonged on the same channel. Further discussion on this will be addressed in a later section of this paper. Compared to dynamic resource allocation, batch allocation reduces the flexibility of multi-user channel diversity exploitation. Hence, a trade-off exists between batch resource allocation for interference coordination and dynamic resource allocation for multi-user channel diversity exploitation. As an illustration, consider

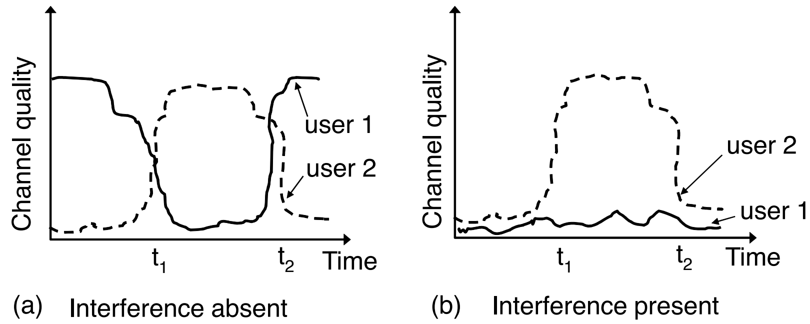

Figure 5.3: Channel quality as a function of time.

Figs. 5.3(a) and 5.3(b). In Fig. 5.3(a), interference has been neglected such that the instantaneous channel quality depends mainly on shadowing and multi-path fading effect. The channel quality has been considered to be i.i.d (independent and identically distributed) for users 1 and 2, such that, the bad channel of user 1 has been assumed to be the best channel of user 2.

A prudent way of achieving multi-user channel diversity gain is to dynamically allocate a channel to the user with the best channel quality at any particular time instance (in this case, at times t_1 and t_2). Let us consider Fig. 5.3(b), where the impact of interference on channel quality has not been neglected. Assuming that user 1 is under the influence of a significantly high interference, it can be observed that the quality of user 1's signal is consistently poor both at times t_1 and t_2 notwithstanding the random nature of channel gain. In reality, this interference situation arises whenever an MUE is collocated indoors with an active HeNB that operates in closed-access mode. In this case, interference coordination should take higher priority than multi-user channel diversity exploitation.

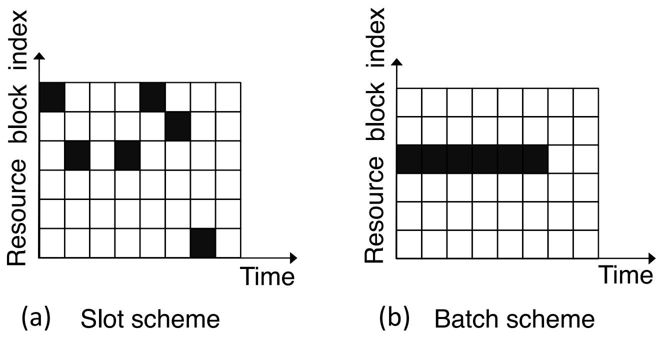

Figure 5.4: Dynamic versus batch resource allocation at macro-eNB.

5.4.2.2 Dynamic resource allocation vs. batch resource allocation

Figures 5.4(a) and 5.4(b) are typical scheduling maps that represent possible time/frequency resource assignment by a scheduler. The shaded blocks in both figures are the time/frequency resources assigned to a particular UE.

While Fig. 5.4(a) represents dynamic scheduling scheme (slot scheme), which is commonly used in the 3GPP/LTE technology, Fig. 5.4(b) on the other hand represents a batch scheduling scheme. If the dynamic scheduling scheme illustrated in Fig. 5.4(a) is used at a macro-eNB to schedule an MUE, a nearby HeNB observes the resource allocation of the MUE to be random both in the frequency and time domains. The random nature of this scheme makes it difficult to achieve effective interference coordination at the HeNB.

Figure 5.4(b) in contrast comprises of consecutive shaded blocks along the time axis which shows that the user's resource schedule follows an organized fashion in the time direction. In this case, an HeNB knows in advance the RBs that will be used by a nearby MUE at a given time, and hence, mitigate interference in such RBs. This paper proposes the batch resource allocation pattern of Fig. 5.4(b), and in the next section, we explain its implementation feasibility.

5.4.2.3 Feasibility of batch resource allocation

(1) Multi-path fading

The channel gain seen at the receiver is time varying, and the rate of variation largely depends on the velocity of motion of the transmitter relative to the receiver. The channel changes faster at a higher velocity and conversely at a lower velocity. It is important to carefully select the *batch-length* in a way that ensures that the channel allocated to a UE does not repeatedly transit to periods of deep fade during the allocated *batch-time* (the period during which an RB is occupied by a UE). In this vain, the *batch-length* should be selected less than or equal to the channel coherence time. For example, a receiver moving at a velocity of 7.0 m/s has a channel coherence time of approximately 9.0 ms as illustrated below:

Assuming the speed of light, v_{c}, is 3.0×10^8 m/s while the speed of motion of the receiver, v, is 7.0 m/s. Assuming the carrier frequency of the LTE system, f_{c}, is 2.0 GHz. The Doppler frequency is

$$f_{\mathrm{D}} = \frac{v}{v_{\mathrm{c}}} f_{\mathrm{c}} = 46.7 \text{ Hz}, \tag{5.4.1}$$

and the coherence time, τ, is computed as [19]

$$\tau = \frac{0.42}{f_{\mathrm{D}}} = 9.0 \text{ ms}. \tag{5.4.2}$$

This implies that the gain of a channel being used by an MUE moving at a velocity of 7.0 m/s changes only a little during a period of 9.0 ms. Hence, multi-path fading will have insignificant impact on the throughput performance of the MUE if the *batch-length* of the channel allocated to the UE is set to 9 TTIs (i.e., 9.0 ms) as compared to the 1 TTI (i.e., 1.0 ms) employed in conventional LTE systems.

(2) Sensing and information exchange

Information about resource usage schedule of the macro-eNB can be delivered to the HeNB either through the backhaul, or wirelessly over-the-air (OTA). Even though, there are a number of ways through which information can be exchanged between the macro-eNB and the HeNB (e.g., OTA, X2-interface, S1-interface), each method, however, has its pros and cons [34]. For example, the OTA approach, which is assumed in this paper, has the benefit of low latency, high scalability (amount of information exchanged does not grow with increasing number of HeNB), little overhead, and predictable timeline (i.e information exchange is independent of backhaul condition). In the batch resource allocation scheme, scheduling decision of the macro-eNB is conveyed to the MUE through the PDCCH (Physical Downlink Control Channel). This information is overheard by nearby HeNB using OTA method, and consequently, the HeNB controls transmission powers in appropriate RBs in order to mitigate the interference introduced to nearby nonmember-CSG MUEs.

If, however, the OTA sensing method is used in LTE, the downlink of the HeNB has to be interrupted each time the scheduling information of the macro-eNB is read. However, technologies that support concurrent transmission and reception already exist, and could be introduced in the LTE radio access technology so as to make concurrent sensing and transmission possible at the HeNB. Another issue worthy of mentioning is that the CRC (Cyclic Redundancy Check) of the DCI (Downlink Control Information) is scrambled with the UE's identity, C-RNTI (Cellular Radio Network Temporary Identity), which is used to address the scheduled message to the UE [72],[73]. Hence, based on the current LTE DCI format, neighboring HeNB will not be able to directly decode the scheduling message of the macro-eNB. Changes to the macro-eNB DCI format is therefore necessary to enable the HeNB to be able to read the scheduling information of the macro-eNB contained in the PDCCH without direct interaction between the macro-eNB and the HeNB.

In the next section, we provide a typical batch resource allocation algorithm for the macro-eNB. We, however, emphasize that the basic idea of batch allocation scheme is not limited to the algorithm provided in the next section. In fact, the algorithm represents just one of many ways of implementing our proposed batch resource allocation scheme.

5.4.2.4 Proposed macro-eNB batch scheduling algorithm

The proposed algorithm is based on the PF (proportional fair) scheduling policy and we use it for the allocation of $n \in \mathcal{N}_{\mathrm{M}}$ resource blocks to members of $\mathcal{M}$. The proposed PF-based macro-eNB batch scheduling algorithm is as follows:

- Step 1 :

  Initialize parameters:

$$\mathcal{M}_{\mathrm{s}} \leftarrow \mathcal{M}, \tag{5.4.3}$$

$$\mathcal{B} \leftarrow \emptyset, \tag{5.4.4}$$

$$\mathcal{B}_m \leftarrow \emptyset, \quad \forall m \in \mathcal{M}_{\mathrm{s}}, \tag{5.4.5}$$

$$L_{m,\mathrm{est}} \leftarrow L_{m,\mathrm{curr}}, \quad \forall m \in \mathcal{M}_{\mathrm{s}}, \tag{5.4.6}$$

  where $\mathcal{M}_{\mathrm{s}}$ is the MUE scheduling list of the current TTI, $\mathcal{B}$ is the set of RB indices of all MUEs in $\mathcal{M}$, and $\mathcal{B}_m$ is the set of RB indices allocated [1] to MUE

[1]If m has been allocated some RB indices prior to the current TTI, $\mathcal{B}_m$ is initialized based on that instead of the initialization to an empty set done in Eq. (5.4.5).

m. $L_{m,\text{curr}}$ is the current size of the backlogged data of MUE m while $L_{m,\text{est}}$ is an estimate of the size of the backlogged data of MUE m after the batch allocation of resources.

- Step 2 :

  Resolve RB index allocation of all MUEs in $\mathcal{M}$ as

$$\mathcal{B} = \bigcup_{m \in \mathcal{M}} \mathcal{B}_m. \tag{5.4.7}$$

- Step 3 :

  Calculate the scheduling priority, λ_m, of MUE m as

$$\lambda_m = \frac{K_{m,n}}{\bar{R}_m}, \qquad \forall m \in \mathcal{M}_\text{s}, n \in \mathcal{N}_\text{M}, \tag{5.4.8}$$

  where $\bar{R}_m$ is the long term throughput of MUE m averaged over a time window T_w, and $K_{m,n}$ is the achievable data rate on one RB index n if allocated to MUE m. Note that $\bar{R}_m$ is updated in Step 8. Inline with Algorithm 1 of [74], the selection of n from $\mathcal{N}_\text{M}$ follows an ordered sequence [2].

- Step 4 :

  From set $\mathcal{M}_\text{s}$, pick an MUE m^* that has the highest value of λ_m,

$$m^* = \arg\max_{m \in \mathcal{M}_\text{s}} \{\lambda_m\}. \tag{5.4.9}$$

- Step 5 :

  Add n to the set of RB indices of MUE m^*,

$$\mathcal{B}_{m^*} \leftarrow \mathcal{B}_{m^*} \cup \{n\}. \tag{5.4.10}$$

[2]We have simply used an ordered sequence approach for the allocation of resource block $n \in \mathcal{N}_\text{M}$ since our major interest in this work is to implement batch resource allocation.

- Step 6 :

Calculate the *batch-length* $X^{(m^*)}_{\text{schedule}}$, i.e., the number of TTIs the selected MUE will be scheduled on the selected RB index n,

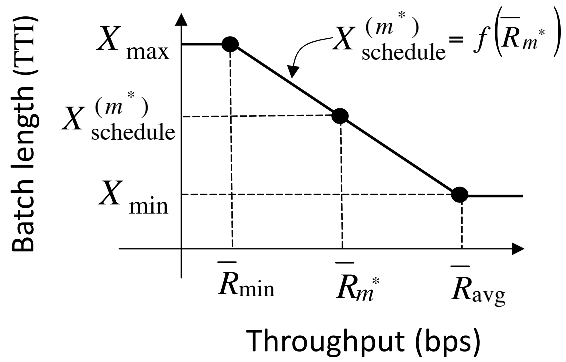

Figure 5.5: Batch resource allocation graph.

$$X^{(m^*)}_{\text{schedule}} = \max(X_{\text{min}}, X_{\text{max}} + \min(0, \lceil \alpha(\bar{R}_{m^*} - \bar{R}_{\text{min}}) \rceil)), \tag{5.4.11}$$

where

$$\alpha = \frac{X_{\text{min}} - X_{\text{max}}}{\bar{R}_{\text{avg}} - \bar{R}_{\text{min}}}, \tag{5.4.12}$$

and

$$\bar{R}_{\text{avg}} = \frac{\sum_{m=1}^{M} \bar{R}_m}{M}, \tag{5.4.13}$$

and

$$\bar{R}_{\text{min}} = \text{S} \cdot \bar{R}_{\text{avg}}, \quad 0 < \text{S} < 1, \tag{5.4.14}$$

where $X^{(m^*)}_{\text{schedule}}$ is the *batch-length* allocated to MUE m^* on RB index n, while X_{min} and X_{max}, respectively, denotes the minimum and maximum allowed *batch-length*. $\bar{R}_{\text{avg}}$ is the average of the long term throughputs of all MUEs in $\mathcal{M}$

while $\bar{R}_{\text{min}}$ is the value of an MUE's average throughput that qualifies the MUE for being allocated the maximum number of TTIs, X_{max}, and S is a constant fraction used for setting the value of $\bar{R}_{\text{min}}$. It can be observed that the corresponding batch allocation graph in Fig. 5.5 shows that an MUE with a high value of long term throughput relative to the network average throughput, $\bar{R}_{\text{avg}}$, will be allocated a few number of TTIs, $X^{(m^*)}_{\text{schedule}}$, and vice versa according to Eq. (5.4.11).

- Step 7 :

  Re-size the *batch-length* if necessary in order to ensure that it commensurates the size of backlogged data of m^* so as to avoid over-allocating the *batch-length* to m^*,

$$V_{m^*,n} = X^{(m^*)}_{\text{schedule}} \cdot K_{m^*,n} \cdot T_{\text{s}}, \tag{5.4.15}$$

  and

$$\begin{aligned} &\text{if} \quad V_{m^*,n} > L_{m^*,\text{est}} \\ X^{(m^*)}_{\text{schedule}} &= \frac{L_{m^*,\text{est}}}{K_{m^*,n} \cdot T_{\text{s}}}, \end{aligned} \tag{5.4.16}$$

  where T_{s} is the time span of one TTI, and $V_{m^*,n}$ is the transmittable number of bits in user m^*'s buffer during period $X^{(m^*)}_{\text{schedule}}$ at a data rate $K_{m^*,n}$ on RB index n.

- Step 8 :

  Update the long term throughput of MUE m^*,

$$\bar{R}_{m^*} \leftarrow \beta^{X^{(m^*)}_{\text{schedule}}} \bar{R}_{m^*} + \left(1 - \beta^{X^{(m^*)}_{\text{schedule}}}\right) K_{m^*,n}, \tag{5.4.17}$$

where

$$\beta = 1 - \frac{1}{T_{\mathrm{w}}}. \tag{5.4.18}$$

Eq. (5.4.17) is explained further in the Sec. 5.4.2.5.

- Step 9 :

Update the expected size of backlogged data, $L_{m^*,\mathrm{est}}$, of m^* based on the batch assignment. If buffer is expected to become empty, then remove MUE m^* from the current TTI scheduling list, $\mathcal{M}_{\mathrm{s}}$,

$$L_{m^*,\mathrm{est}} \leftarrow L_{m^*,\mathrm{est}} - \left(X^{(m^*)}_{\mathrm{schedule}} \cdot K_{m^*,n} \cdot T_{\mathrm{s}} \right), \tag{5.4.19}$$

and

$$\begin{aligned} &\text{if} \quad L_{m^*,\mathrm{est}} \leq 0 \\ &\mathcal{M}_{\mathrm{s}} \leftarrow \mathcal{M}_{\mathrm{s}} \setminus \{m^*\}. \end{aligned} \tag{5.4.20}$$

- Step 10 :

Prevent over-allocation of RBs to m by limiting the maximum acquirable RBs by a single MUE to a predetermined number D,

$$\begin{aligned} &\text{if} \quad |\mathcal{B}_{m^*}| \geq D \\ &\mathcal{M}_{\mathrm{s}} \leftarrow \mathcal{M}_{\mathrm{s}} \setminus \{m^*\}. \end{aligned} \tag{5.4.21}$$

- Step 11 :

If there are unallocated RBs, and the total base station power has not been exceeded, and $\mathcal{M}_{\mathrm{s}} \neq \emptyset$, goto step 2, otherwise, end.

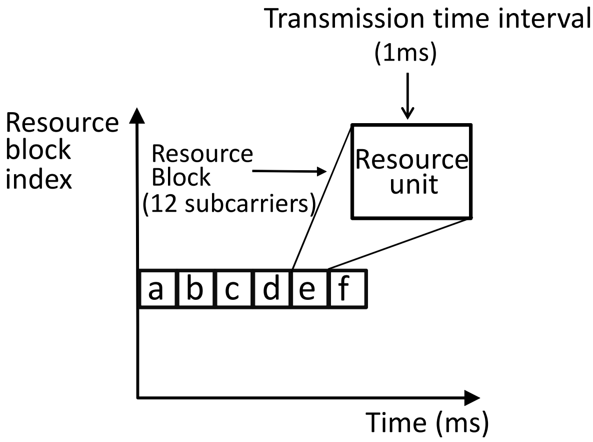

Figure 5.6: LTE resource unit.

5.4.2.5 Updating throughput in batch allocation scheme

If a resource block is allocated to a user such that the assigned usage time spans several TTIs, the traditional average throughput updating equation, Eq. (5.2.1), has to be adapted to this case. Figure 5.6 is an illustration of an LTE resource frame in which resource units a, b, c, d, e and f are allocated in batch to a user. Assuming T_{w} denotes time window, $\bar{R}$ denotes long term throughput while K denotes the instantaneous data rate on one resource unit, then, the moving average throughput for multiple resource units can be determined as follows:

$$\beta = 1 - \frac{1}{T_{\mathrm{w}}} \tag{5.4.22}$$

1. update of $\bar{R}$ for one resource unit "a" is

$$\beta\bar{R} + (1-\beta)K \tag{5.4.23}$$

2. update of $\bar{R}$ for two resource units "a" and "b" is

$$\beta(\beta\bar{R} + (1-\beta)K) + (1-\beta)K = \beta^2\bar{R} + (1-\beta)(1+\beta)K$$

3. update of $\bar{R}$ for three resource units "a," "b," and "c" is

$$\beta(\beta^2\bar{R} + (1-\beta)(1+\beta)K) + (1-\beta)K = \beta^3\bar{R} + (1-\beta)(1+\beta+\beta^2)K$$

4. update of $\bar{R}$ for "n" resource units is

$$\beta^n\bar{R} + (1-\beta)K\frac{1-\beta^n}{1-\beta} = \beta^n\bar{R} + (1-\beta^n)K$$

However, in order to prevent a degradation in the performance of the proposed scheme, the *batch-time* must be less than the coherence time:

$$nT_s < \tau, \tag{5.4.24}$$

where τ can be computed according to Eq. (5.4.2).

5.4.3 Slot-based interference coordination at the HeNB

The interference received by an MUE from an HeNB is usually small if the MUE is located faraway from the HeNB due to the lower transmission power of HeNBs. Moreover, HeNBs are envisioned to be located indoors, and the walls of buildings therefore automatically serve as attenuators for limiting the amount of interference released to the outdoor environment. If however, an MUE is located in the same building with an HeNB, the interference received by the MUE could be severe. It is therefore necessary for the HeNB to tune its transmit power on RBs used by the interfered MUE. However, before interference coordination is triggered at the HeNB, the HeNB first needs to detect the presence of a victim nonmember-CSG MUE. Two possible detection methods have been identified by the 3GPP [34], i.e.,

1. Determination at the eNB or HeNB on the basis of reported UE measurements, and
2. Determination at the HeNB on the basis of detection of uplink transmissions from victim UEs.

5.4.3.1 HeNB power tuning

Once the presence of an interfered nonmember-CSG MUE has been detected, interference coordination procedure is triggered, and the RBs used by the aggressor HeNB (interference-inducing HeNB) are classified into the following categories using a power control algorithm that will be explained later in this section:

1. RBs that can be used at maximum power
2. RBs that should be used at a controlled power, and
3. RBs that are not to be used at all.

The total HeNB base station power is equally distributed among all the RBs such that the maximum power that can be loaded on any RB is given as

$$p_{\max} = P_{\mathrm{T}} - 10 \log \left(|\mathcal{N}_{\mathrm{H}}| \right), \tag{5.4.25}$$

where P_{T} is the total power (in dBm) available at the HeNB, and $\mathcal{N}_{\mathrm{H}}$ is the set of all RBs available at the HeNB. Equation (5.4.25) ensures that the total power P_{T} available at the base station is not exceeded. We assume that the aggressor HeNB can know the uplink transmission power of the victim MUE through the DCI of the PDCCH of the macro-eNB[1], and it is also assumed that channel is symmetric (i.e the

[1] Although we explained in Sect. 5.4.2 that the scheduling information of the PDCCH is scrambled with the MUE's identity, we, however, assume that the scrambled information is decodable by the HeNB.

uplink and downlink channel responses are approximately the same). Each HeNB f controls $p_f^{(n)}$ which is the power it loads on RB index n. The power control is done in such a way that limits the amount of interference received by the MUE m that is scheduled by the macro-eNB on co-channel RB n. In order to achieve this, we introduce an interference threshold I_{th} which denotes the maximum amount of interference an HeNB is allowed to introduce to a nearby MUE. The HeNB determines the channel gain between itself and a nearby MUE m as

$$G_{f,m} = p_{\text{uplink},m} - p_{f,m,\text{measured}}, \tag{5.4.26}$$

where $p_{\text{uplink},m}$ denotes the uplink transmit power of the victim MUE m in dBm, while $p_{f,m,\text{measured}}$ is the power measured at the HeNB f also in dBm. Let $p_{\min}$ denote the minimum power that can support a successful communication between the HeNB and the HUE (HeNB UE) h. Let $\mathcal{Q}$ be the set of HUEs $h \in \mathcal{H}$ that has non-empty data buffers, and l_h, the length of the data buffer of HUE h. The interference control at the HeNB is implemented according to the following algorithm:

- Step 1:

  Update the number of HUEs $h \in \mathcal{Q}$ that has non-empty buffers,

$$\mathcal{Q} = \mathcal{H}, \tag{5.4.27}$$

$$\forall h \in \mathcal{Q} \quad \text{if} \quad l_h = 0$$

$$\mathcal{Q} \leftarrow \mathcal{Q} \setminus \{h\}. \tag{5.4.28}$$

- Step 2:

  If there is an HUE with a non-empty buffer, power is loaded on $\mathcal{N}_{\text{H}}$, otherwise power is not loaded, i.e.,

$$\text{if} \quad \mathcal{Q} \neq \emptyset$$
$$\text{execute step 3.}$$

- Step 3:

  RBs are allocated to HUEs using slot-based PF policy[2], and the transmit power $p_f^{(n)}$ of co-channel RB index n used by victim MUE m is controlled at the HeNB as

$$p_f^{(n)} = \min\left(p_{\max}, I_{\text{th}} + G_{f,m}\right), \quad \forall m \in \mathcal{M}, \forall n \in \mathcal{N}_{\text{H}} \cap \mathcal{B}_m. \tag{5.4.29}$$

- Step 4:

  If $p_f^{(n)}$ is too low for successful communication at the HeNB, the HeNB remains mute on RB n, i.e.,

$$\begin{aligned} \text{If} \quad & p_f^{(n)} < p_{\min} \\ & p_f^{(n)} = -\infty. \end{aligned} \tag{5.4.30}$$

The elements of $\mathcal{N}_{\text{H}} \cap \mathcal{B}_m$ in Eq. (5.4.29) are the RBs in $\mathcal{N}_{\text{H}}$ on which power must be controlled. The macro-eNB resource allocation decision does not necessarily occur at every TTI since the macro-eNB allocates a batch of resource units that spans several TTIs to each selected MUE. This invariably reduces the computational load on the macro-eNB processor.

It is important to note that cell edge HeNBs consider more than one macro-eNB allocation since they are likely to cause interference to MUEs served by different

[2]The slot-based PF scheme is not presented in this work due to limited space. It is however not different from the standard PF scheme in common use.

macro-eNBs. Our HeNB power control formulation does not reflect this case for brevity although it encompasses it. If an MUE is collocated indoors with an HeNB, the signal strength from the collocated HeNB will likely dominate all the other outdoor signals received by this MUE since walls attenuate the outdoor signals received by the indoor MUE. If closed-access mode is considered and the indoor MUE does not belong to the CSG of the collocated HeNB, by selecting an appropriate value of I_{th}, a relatively high throughput can still be enjoyed by this MUE if our proposed power control algorithm is used by the HeNB.

5.5 Simulation setup and results

System level simulation is done to demonstrate the effectiveness of our proposed *batch* resource allocation scheme. The macro-eNB network comprises of a ring of seven cells underlaid with HeNBs which are randomly and uniformly deployed in its coverage area as shown in Fig. 5.7. The location of any HeNB represents the center of a house

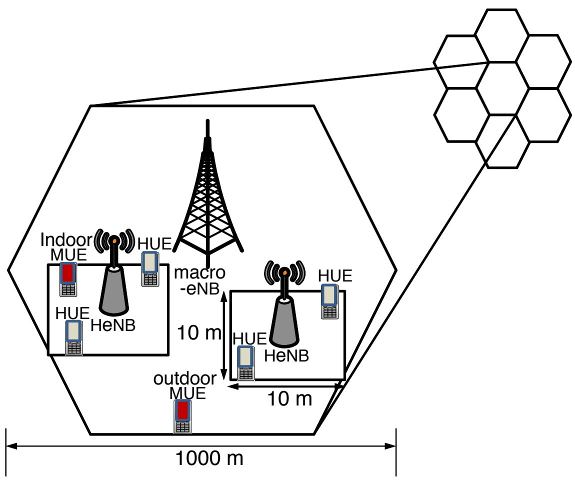

Figure 5.7: Network model.

of dimension 10×10 m^2, and each HeNB is forced to be at least 30 m away from its closest neighbor HeNB. MUEs are randomly and uniformly deployed in the coverage area of the macro-eNB. Indoor MUEs are then relocated and placed in the same house with the HeNB nearest to them while outdoor MUEs are placed between 2 m and 10 m distance away from the external wall of the HeNB nearest to them. Associated with each HeNB are two HUEs.

The placement of HUEs follow a random and uniform manner, and the HUEs are forced to be at least 0.2 m away from their HeNBs [60]. All MUEs connect to the

Table 5.1: System Configuration

Parameter	**Setting**
Bandwidth	5 MHz
Carrier frequency	2 GHz
Transmit power (Macro-eNB, HeNB)	43 dBm, 10 dBm
Interference threshold (I_{th})	-81 dBm
Antenna gain (Macro-eNB, HeNB, UE)	13 dBi, 0 dBi, 0 dBi
Thermal noise density	-174 dBm/Hz
Loss (ext. wall, int. wall, window)	15 dB, 0.7 dB/m, 1 dB
Minimum batch-length ($X_{\min}$)	3 TTIs
Maximum batch-length ($X_{\max}$)	8 TTIs
Macro-eNB cell radius	500 m
House dimension	10×10 m^2
Number of macro-eNB	7
Number of MUE per macro-eNB	15
Number of HeNB BS per macro-eNB	10
Number of HUE per HeNB	2
Traffic model	Poisson arrival
Offered traffic	0–13 Mbps
Packet size	1.5 kbyte
Buffer capacity per UE	125 kbyte
Macro-eNB scheduling	Batch-based proportional fair
HeNB scheduling	Slot-based proportional fair

macro-eNB only (closed-access mode). Link adaptation is modeled by mapping SINR to capacity, using the *attenuated and truncated Shannon bound method* [75], while path-loss is computed using the suburban path-loss model [60]. Power allocation and RB usage coordination at the macro-eNB is done by employing SFR (soft frequency re-use) approach such that cell-edge MUEs are allocated higher power values than cell-interior MUEs. The cell-interior is re-use 1-enabled, while re-use 3 is employed at the cell-edge. The system configuration parameters are as shown in Table 5.1. In this work, we assume accurate time synchronization among all base stations. Resource allocation at the HeNB is done according to slot-based PF scheduling policy. We assume that each HeNB can sense and know the set of RBs that have been allocated to nearby MUEs by reading the PDCCH information.

For reference purposes, we denote our proposed scheme as *batch* scheme. Usually, the PDCCH information is transmitted at the beginning of every sub-frame by both the macro-eNB and the HeNB, but in the case of the *batch* scheme, the HeNB needs to read the PDCCH information of the macro-eNB in order to prepare its own scheduling map. Hence, two variants of the *batch* scheme are considered namely, the *batch-IPC* (Instant Power Control) and the *batch-DPC* (Delayed Power Control). In the *batch-IPC* scenario, it is assumed that an aggressor HeNB controls its transmission power during the same TTI that it reads the scheduling information of a neighbor macro-eNB. This represents an ideal case. In the *batch-DPC* scenario on the other hand, it is assumed that due to some processing delay, power control is done by the aggressor HeNB in the next TTI after reading the scheduling information of the neighbor macro-eNB. Hence, a victim MUE is briefly interfered in the *batch-DPC* scenario, and this represents a more realistic case.

The dynamic resource allocation scheme of the standard LTE in which RBs are allocated during every TTI is used as a comparative scheme to which our proposed scheme is compared. The drawback of this scheme is that it is difficult for the HeNB to avoid interference resulting from the collision of resource tiles (time/frequency) between the two tiers. We refer to this scheme as the *slot* scheme. Both schemes (*batch* and *slot* schemes) are referred to as the two-tier cases and are compared to a single-tier scenario in which macro-eNB operates in the absence of HeNB. The single-tier scenario serves as the baseline case for our assessment. In the baseline case, all UEs connect to the macro-eNB while in the two-tier scenarios, the UEs are split between the macro-eNB and HeNB. Hence, HUEs of the two-tier cases are considered as indoor MUEs in the corresponding single-tier scenario. In the *batch* and *slot* schemes, in addition to the interference received from neighboring macro-eNBs, the interference landscape observed at an MUE terminal is influenced by the buffer status of the HeNB as well. For example, whenever the HUE data buffer is empty, the HeNB remains mute and vice versa.

The performance of our proposed scheme is evaluated under different UE spatial positions (indoor/outdoor), and diverse offered traffic conditions. The arrival of packets is modeled as a Poisson arrival process. The results obtained are illustrated in Figs. 5.8 through 5.15. It can be observed in Fig. 5.8 that when all the MUEs are outdoors, all the considered two-tier cases achieve similar MUE throughput performances. The throughput of the *slot* scheme, however, decreases with an increase in offered load due to interference received from the HeNB although the decrease is not profound. It can be observed that the per-MUE throughput of the baseline case is less than that of the two-tier cases. This is because in the two-tier cases, some UEs (20

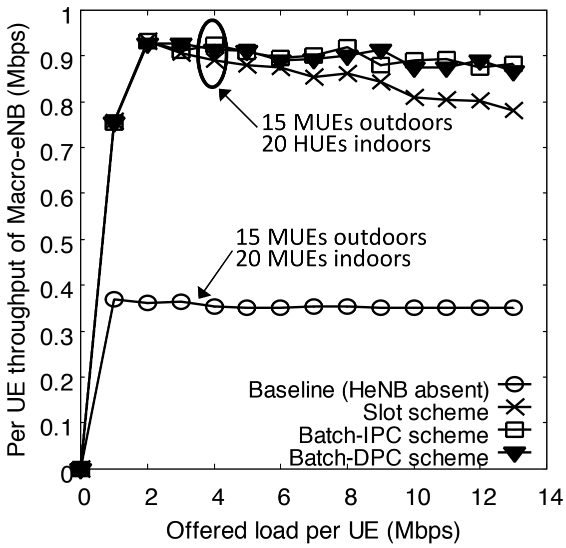

Figure 5.8: Per user macro-eNB throughput as a function of offered traffic (15 UEs outdoors, 20 UEs indoors).

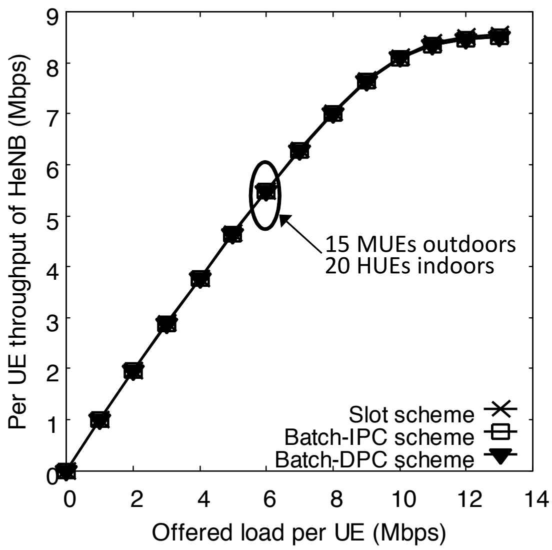

Figure 5.9: Per user HeNB throughput as a function of offered traffic (15 UEs outdoors, 20 UEs indoors).

UEs) have been offloaded to the HeNB, hence, fewer MUEs (15 UEs) of the two-tier case enjoy the same bandwidth size available to many MUEs (35 UEs) of the baseline counterpart. Figure 5.9 shows the corresponding throughput performance of the HeNB when all MUEs are located outdoors. It can be observed that all the schemes achieve similar HeNB throughput performance under all the considered offered load conditions. This is because all the candidate interference victims are outdoors and therefore only receive low level interference, leading to a not-so-significant power reduction at the HeNB in the *batch* scheme. This affords the per-HUE throughput of the *batch* scheme to match up with that of the *slot* scheme.

Figure 5.10 shows the MUE throughput plotted against offered load with all the UEs located indoors. In all the schemes, the MUE throughput progressively rises as the offered load is increased from zero. However, in the case of the batch scheme, the MUE throughput begins to drop when the offered load exceeds 2 Mbps, whereas, it begins to drop at 1 Mbps in the case of the slot scheme. The drop in throughput is as a result of the fact that data arrives at the HeNB more frequently at high offered traffic than at low offered traffic. Therefore, the probability that power is loaded on an RB by an HeNB is higher at high offered traffic case than at low offered traffic, hence, accounting for the fall in MUE throughput at high offered traffic since interference is more imminent. Among the considered two-tier schemes, the *batch-IPC* scheme performs best, and it is closely followed by the *batch-DPC* scheme, while the *slot* scheme shows the worst performance. All the two-tier cases outperform the baseline case in the low offered load region in terms of per-MUE throughput. However, the per-MUE throughput of the baseline case exceeds that of the *slot* scheme and *batch-DPC* scheme at 3 Mbps and 10 Mbps offered traffic, respectively. Only the *batch-IPC*

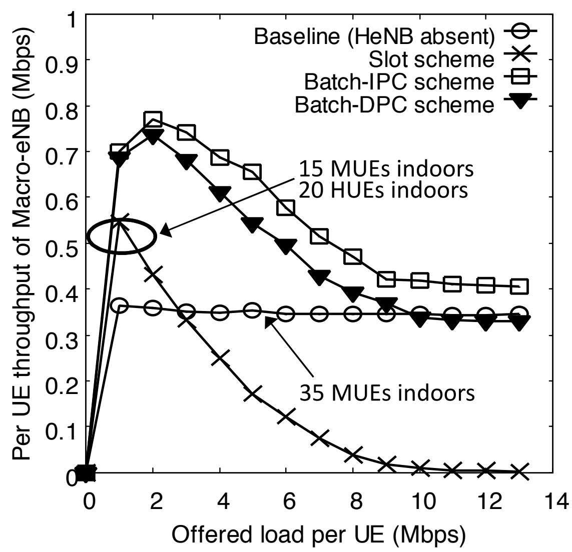

Figure 5.10: Per user macro-eNB throughput as a function of offered traffic (35 UEs indoors).

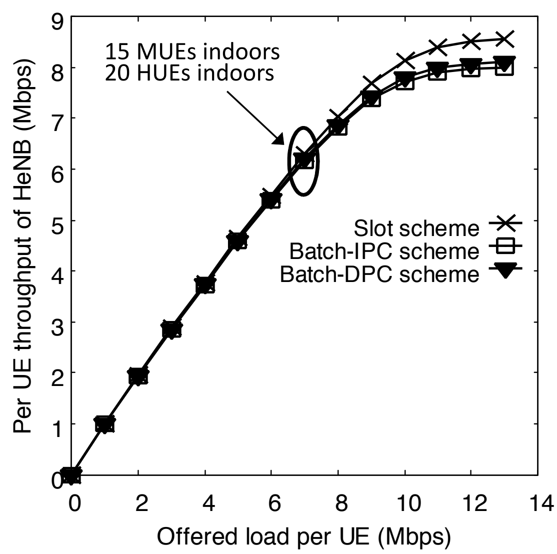

Figure 5.11: Per user HeNB throughput as a function of offered traffic (35 UEs indoors).

scheme achieves a higher per-MUE throughput than the baseline case in all offered traffic conditions. It should be noted that this does not make the baseline case superior to the two-tier cases since in the two-tier cases, there is additional capacity from the HeNB as will be explained next.

The corresponding per-HUE throughput when all UEs are located indoors is illustrated in Fig. 5.11. It can be observed that all the schemes perform alike in terms of per-HUE throughput between 0 Mbps and 7 Mbps offered traffic. However, the *slot* scheme begins to outperform the *batch* scheme when the offered traffic exceeds 7 Mbps, although the performance difference is not large. As a matter of fact, the packets of the HUE are only delayed for a short-while whenever a collocated victim MUE is scheduled for data transmission by the macro-eNB. Moreover, the MUEs are uniformly distributed in the geographic space of the macro-eNB cell, and since RBs are shared among these MUEs, it is unlikely that all RBs simultaneously get occupied by a single nearby MUE such that an aggressor HeNB is prevented from using all the RBs at the same time in our proposed *batch* scheme. In the worst case scenario, the HeNB is prevented from using only a subset of the available RBs. All these bridge the per-HUE throughput margin between the *slot* scheme and our proposed *batch* scheme. It is important to note that in the proposed *batch* scheme, the throughput gain achieved at the macro-eNB due to HeNB power control is relatively much larger than the corresponding throughput loss at the HeNB due to the power control, and this is an attractive feature of our proposed scheme.

Figures 5.12 and 5.13 illustrate the total network throughput plotted against per-UE offered load. Figure 5.12 in which all MUEs are outdoors shows that the total cell throughput of the two-tier cases all outstandingly outperform the baseline case. The

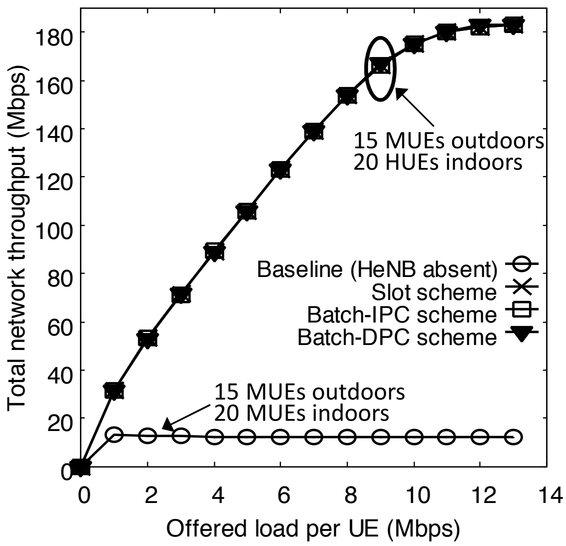

Figure 5.12: Total network throughput as a function of offered traffic (15 UEs outdoors, 20 UEs indoors).

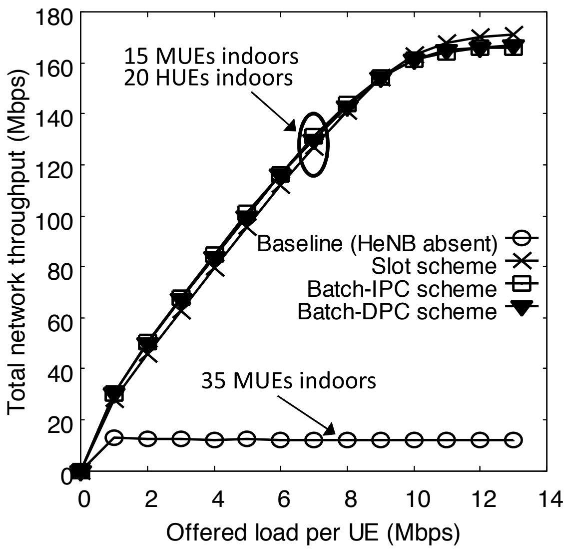

Figure 5.13: Total network throughput as a function of offered traffic (35 UEs indoors).

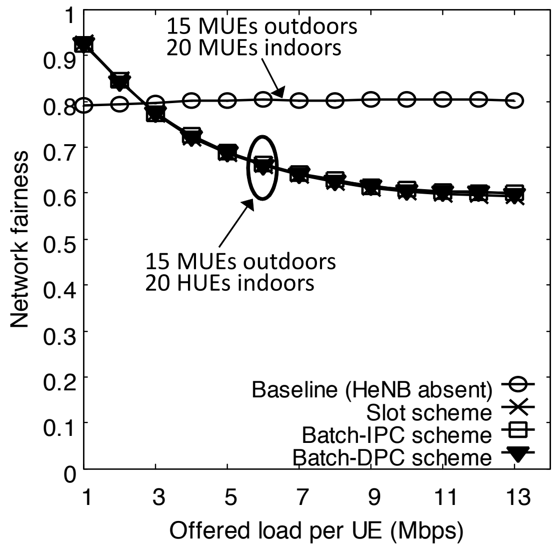

Figure 5.14: Network fairness as a function of offered traffic (15 UEs outdoors, 20 UEs indoors).

enormous throughput gain of the two-tier cases relative to the baseline is as a result of the multiple channel reuse done by the HeNBs. The total network throughput of the two-tier cases are similar because of the fact that the interference received by outdoor MUEs from indoor HeNB is not so significant. In Fig. 5.13 all UEs are indoors, and it can be observed that, beyond 9 Mbps, the *slot* scheme outperforms our proposed *batch* scheme with a small margin. This stems from the fact that in the *slot* scheme, there is higher throughput contribution from the HeNB tier at higher offered load but it is however important to note that the corresponding contribution from the macro-eNB tier at this offered load region is unacceptably small (as seen in Fig. 5.10). The *Jain*'s fairness index [64] is used to evaluate the overall network (HeNB and Macro-eNB combined) fairness as shown in Figs. 5.14 and 5.15. In Figs. 5.14 and 5.15, the network fairness of the two-tier schemes decreases with an increase in offered load due

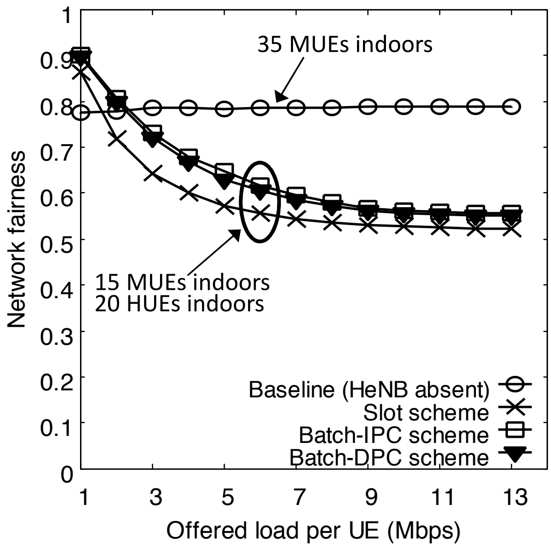

Figure 5.15: Network fairness as a function of offered traffic (35 UEs indoors).

to two reasons; (1) The HUEs are more capable of achieving higher throughput at high offered load than the MUEs due to their close proximity to their serving HeNBs, and also due to their larger per-HUE bandwidth share compared to the MUEs, (2) The probability that an MUE receives interference from an aggressor HeNB increases with an increase in offered load, leading to a corresponding decrease in the MUE's throughput as well as the network fairness.

Figure 5.14 shows that the two-tier schemes have higher network fairness at low offered load region than at high offered load region. This is because within the low offered load range, the per-UE throughput of the macro-eNB is comparable to that of the HeNB since the macro-eNB only deals with a few number of MUEs, hence, a higher per-UE bandwidth share is achievable. However, due to the reasons mentioned earlier, the margin between the per-UE throughput of the macro-eNB and the HeNB widens rapidly as the offered load is increased further thereby reducing the network fairness of the two-tier schemes. In Fig. 5.15, all UEs are indoors. It can be observed in the figure that the *batch* scheme achieves a higher network fairness compared to the *slot* scheme under all offered load conditions thanks to the HeNB power control of the *batch* scheme.

5.6 Concluding remarks

In this chapter, we focused attention on the mitigation of femto-to-macro interference, and we discussed a *batch* resource allocation strategy for a closed-access cellular network in which macro-eNBs allocate resources to macro-eNB users in *batch* in the time domain. In this context, *batch* denotes multiple TTIs which means that the macro-eNB scheduler allocates network resources in such a way that future resources to be used by it are known to the underlaid HeNBs in advance. Based on the knowledge of resources that will be used by the macro-eNB, HeNBs located near macro-eNB users coordinate interference using a power control algorithm in order to limit the amount of interference received by these users.

Simulation results revealed that at various UE offered traffics, the proposed *batch* scheme shows superior throughput performance when compared to the conventional *slot* scheme in which resource allocation decision is made during every TTI. Impressive throughput performance is also achieved by the proposed *batch* scheme when compared to a macro-only network in which HeNB is absent. Sometimes, the power control imposed on the HeNB in the proposed *batch* scheme prevents some resource blocks from being used by the HeNB for a period of time, hence, leading to a delay of packets. However, the ensuing packet backlogging does not necessarily always lead to system performance degradation due to the relatively high instantaneous data rate of the HeNB. Since it has been agreed in 3GPP release 10 that there shall be no backhaul coordination between macro-eNB and HeNB, the *batch* scheme conforms with this requirement to prevent additional control bits from inducing unwanted capacity loss.

Chapter 6

Conclusions and future work

6.1 Conclusions

The alarming rise in the demand for higher data rate by wireless devices has made it necessary to underlay existing cellular networks with femtocells, which are low-power, short-range base stations. In existing cellular networks, inter-cell coordination function is simplified due to the planning and optimization procedures that normally precedes base station deployment. Femtocells are, however, envisioned for plug and play (PnP) mode of deployment in which conventional pre-deployment network planning and optimization is absent. Hence, it is necessary to develop automatic base station coordination algorithm in lieu of the absent conventional pre-deployment procedures. This is necessary because, if a proper coordination mechanism among the base stations of a network is absent, interference, which degrades the network throughput performance becomes imminent.

This research work considers inter-cell coordination for interference mitigation in multi-tier networks that is composed of macrocell and femtocell base stations, and all the networks considered are based on OFDMA PHY layer technology. In particular, Chapter 3 considers OFDMA in its basic form, while in Chapter 4, LTE-advanced, a type of OFDMA PHY layer technology that comprises of OFDM sub-carriers and OFDM symbols grouped together into resource blocks, and then into component carriers is considered. The network considered in Chapter 5 is based on LTE standard in which the minimum allocable resource consists of 12 OFDM sub-carriers and 6 or 7 OFDM symbols grouped together.

The performances of all the proposed schemes have been examined using self-developed simulators that were based on C++ and simulation results have shown that, individually, each of the schemes outperforms comparative schemes. However, combining them together for simultaneous operation in a single network will be highly beneficial. Since they are all based on OFDMA PHY layer technology, merging them together is possible through appropriate planning which is explained in what follows.

Assuming that an LTE-advanced network is considered for the coexistence of the three proposed schemes, the merging can commence with the planning procedure in which the resources (e.g., component carriers) to be used in various cell regions (assuming an FFR-based cell region partitioning is adopted) of the macrocell is decided according to the resource partitioning procedure of Chapter 3. It is recommended that macrocell uses the component carriers in the aggregated mode while femtocell's usage should be based on the independent carrier mode. Aggregated carrier is recommended for the macrocell so as to enable a more flexible spectrum division into segments in which the number of resource blocks contained in each segment is based on the partitioning result obtained through the procedure discussed in Chapter 3.

After FFR-based spectrum segmentation has been done for the macrocell, the channel assignment by femtocells discussed in Chapter 4 follows. Depending on the part of the frequency spectrum being used by the macrocell in a particular cell region, the femtocells in that region of the macrocell classify the LTE-advanced CCs (component carriers) into orthogonal and non-orthogonal CCs. Orthogonal CCs are CCs in the spectrum that are currently not being used by the macrocell in the FFR region where a femtocell is located. Hence, they can be accessed by the femtocells in that region without causing interference to the macrocell. Femtocells' spectrum access is done through the channel allocation procedure of Chapter 4 such that the orthogonal CCs are assigned first by the *cluster-heads*. If, however, the orthogonal CCs are insufficient to meet the throughput requirement of some femtocells, non-orthogonal CCs are assigned to such femtocells in addition to the assigned orthogonal CCs. However, femtocells assigned non-orthogonal CCs must control interference caused to macrocell users according to the discussions in Chapter 5. Since macrocell partitions the spectrum flexibly, such that, from femtocells' viewpoint, it is possible for a CC to be composed of both orthogonal and non-orthogonal parts, such CCs should be treated as non-orthogonal CCs by the femtocells so that interference control can be implemented on such CCs.

6.2 Future works

The radio resource partitioning problem discussed in Chapter 3 can be extended to address a case of non-uniform user density in the macrocell network. Hence, femtocell spectrum usage restriction can be relaxed in regions of low macrocell user density which indicates that such released spectrum can be used by multiple femtocell users in those regions compared to the single macrocell user in the current formulation. This can yield a substantial increase in aggregate network throughput.

The cooperative channel assignment scheme proposed in Chapter 4 can be extended such that the cluster-heads perform additional tasks other than channel allocation alone. These tasks may include NBSs' (Neighbor Base Stations) optimum pilot strength computation, optimization of NBSs' time-slot usage, and MIMO (Multiple Input Multiple Output) coordination among base stations.

The batch resource allocation scheme proposed in Chapter 5 can be extended to address application-oriented scenario whereby macrocell users' traffic are first sorted by a classifier based on the class of flow, e.g., VoIP (Voice over Internet Protocol), HTTP (Hypertext Transfer Protocol), etc. The batch-based proportional fair scheduler can then be modified to treat different user classes with different priorities. By so doing, the QoS of users can be improved in addition to the interference mitigation currently proposed in the thesis.

Finally, in the previous section, we explained how all the schemes proposed in this thesis could be merged for coexistence. Since doing so offers a combination of the individual merits of each of the proposed schemes, we are, therefore, considering the merging of the proposed schemes as part of our future works.

Bibliography

[1] M, -S Alouini and A. J Goldsmith, “Area spectral efficiency of cellular mobile radio systems,” IEEE Trans. on Vehicular Tech., vol. 48, no. 4, pp. 1047–1066, July 1999.

[2] “Global mobile data traffic forecast update 2010-2015,” Cisco Visual Networking Index, White Paper, Feb. 2011.

[3] H. Liu and G. Li ,“OFDMA-based broadband wireless networks: Design and optimization,” John Wiley & Sons, Inc., 2005.

[4] S. R. Saunders, S. Carlaw, A. Giustina, R. J. Bhat, V. S. Rao, and R. Siegberg, “Femtocells–Opportunities and challenges for business and technology,” John Wiley and Sons, Ltd., 2009.

[5] V. Chandrasekhar, and J. G. Andrews, “Femtocell Networks: a survey,” IEEE Commun. Mag., pp. 59–67, Sept. 2008.

[6] S. Lee, “An enhanced IEEE 1588 time synchronization algorithm for asymmetric communication link using block burst transmission,” IEEE Commun. Letters, vol. 12, no. 9, pp. 687–689, Sept. 2008.

[7] J. Zhang and G. de la Roche, “Femtocells: technologies and deployment,” John Wiley and Sons, Ltd., 2010.

[8] D. L.-Perez, A. Juttner, and J. Jhang, “Dynamic frequency planning versus frequency reuse schemes in OFDMA networks,” IEEE VTC Proc., pp. 1–5, April 2009.

[9] 3GPP R4-092498, “Hybrid HeNB interference scenarios and techniques,” Qualcomm Europe, June–July 2009.

[10] 3GPP R4-093092, “Femtocell and macrocell coordination based on SFR,” Motorola, May 2009.

[11] 3GPP R4-092872, “Downlink interference coordination between HeNBs,” CMCC, Aug. 2009.

[12] 3GPP R4-093203, “Downlink interference coordination between eNodeB and home eNodeB,” NTT DOCOMO, Aug. 2009.

[13] 3GPP R4-093556 “HeNB downlink interference avoidance with adaptive frequency selection,” NEC, Oct. 2009.

[14] 3GPP R4-093620, “Network Assisted Interference Coordination between Macro eNodeB and Home eNodeB in Downlink,” Kyocera, Oct. 2009.

[15] 3GPP R4-100051 , “Victim UE aware downlink interference management,” picoChip Designs, Jan. 2010.

[16] 3GPP R1-101453 “Macro+HeNB performance with escape carrier,” Nokia Siemens Networks, Nokia, Feb. 2010.

[17] D. N. Knisely, “Standardization of femtocells in 3GPP,” IEEE Commun. Mag., pp. 68–74, Sept. 2009.

[18] G. Boudreau, J. Panicker, N. Guo, R. Chang, N. Wang, and S. Vrzic, “Interference coordination and cancellation for 4G networks,” IEEE Commun. Magazine, pp. 74–81, April 2009.

[19] A. Goldsmith, “Wireless communication systems,” Cambridge University Press, 2005.

[20] 3GPP TR 36.942 v8.2.0, “Evolved universal terrestrial radio access (E-UTRA); radio frequency (RF) system scenarios,” May 2009.

[21] W. Li, C. Wang, and M. Tao, “User based adaptive joint channel assignment in multi-cell OFDMA systems,” IEEE WPMC Proc., 2009.

[22] D. L-Perez, A. Valcarce, G. de la Roche, and J. Zhang, “OFDMA femtocells: a roadmap on interference avoidance,” IEEE Commun. Mag., pp. 41–48, Sept. 2009.

[23] K. Sundaresan and S. Rangarajan, “Efficient resource management in OFDMA femto cells,” Proc. of the 10th ACM Symposium on MobiHoc, pp. 33–42, May 2009.

[24] M. Andrews, V. Capdevielle, A. Feki, and P. Gupta, “Autonomous spectrum sharing for mixed LTE femto and macro cells deployments,” IEEE Infocom Proc., pp. 1–5, March 2010.

[25] R. Bosisio and U. Spagnolini,"Interference coordination vs. interference randomization in multicell 3GPP LTE system" Proc. the IEEE WCNC, pp. 824–829, March 2008.

[26] K. Chawla and X. Qiu, "Quasi-static resource allocation with interference avoidance for fixed wireless systems," IEEE Journal On Selected Areas in Commun., vol. 17, no. 3, pp. 493–504, March 1999.

[27] A. Damnjanovic, J. Montojo, J. Cho, H. Ji, J. Yang, and P. Zong, " UE's role in LTE advanced heterogenous networks," IEEE Commun. Mag., pp. 164–176, Feb. 2012.

[28] N. Miki, Y. Saito, M. Shirakabe, A. Morimoto, and T. Abe, "Investigation on interference coordination employing almost blank subframesin heterogeneous networks for LTE-advanced downlink," IEICE Trans. on Commun., vol. E95, no. 4, pp. 1208–1217, April 2012.

[29] V. Chandrasekhar and J. G. Andrews, "Uplink capacity and interference avoidance for two-tier femtocell networks," IEEE Trans. on Wireless Commun., vol. 8, no. 7, July 2009.

[30] R. Bosisio and U. Spagnolini, "Collision model for the bit error rate analysis of multicell multiantenna OFDMA systems," IEEE ICC Proc., pp. 5732–5737, June 2007.

[31] H. Claussen, L. T. W. Ho and L. G. Samuel, "An overview of the femtocell concept," Bell Labs Tech. Journal, vol. 13, no. 1, pp. 221-245, 2008.

[32] 3GPP R1-073036, “Inter-cell uplink power control for E-UTRA – evaluation of fractional path loss compensation,” Erricson, June 2007.

[33] 3GPP TR 36.213 v9.3.0, “Evolved universal terrestrial radio access (E-UTRA); physical layer procedures,” Sept. 2010.

[34] 3GPP TR 36.921 v10.0.0, “Evolved universal terrestrial radio access (E-UTRA); FDD Home eNode B (HeNB) radio frequency (RF) requirements analysis,” April 2011.

[35] M. Yavuz, F. Meshkati, S. Nanda, A. Pokhariyal, N. Johnson, B. Raghothaman, and A. Richardson, “ Interference management and performance analysis of UMTS/HSPA+ femtocells,” IEEE Commun. Mag., pp. 102–109, Sept. 2009.

[36] Y. Tokgoz, F. Meshkati, Y. Zhou, M. Yavuz, and S. Nanda, “Uplink interference management for HSPA+ and 1XEVDO femtocells,” IEEE GLOBECOM Proc., pp. 1–7, Dec. 2009.

[37] J. Kim and D.-H Cho, “A joint power and subchannel allocation scheme maximizing system capacity in indoor dense mobile communication systems,” IEEE Trans. on Vehicular Tech., vol. 59, no. 9, pp. 4340–4353, Nov. 2010.

[38] K. C. Beh, S. Armour, and A. Doufexi, “Joint time-frequency domain proportional fair scheduler with HARQ for 3GPP LTE systems,” IEEE VTC Proc., pp. 1–5, Sept. 2008.

[39] M. Bohge, J. Gross, and A. Wolisz, “Optimal soft frequency reuse and dynamic sub-carrier assignments in cellular OFDMA networks,” European Trans. on Telecommun., vol. 21, no. 8, pp. 704–713, Dec. 2010.

[40] I. N. Stiakogiannakis and D. I Kaklamani, "Fractional frequency reuse techniques for multi-cellular WiMAX networks," IEEE PIMRC Proc., pp. 2432–2437, Sept. 2010.

[41] K. I. Perdersen, T. E. Kolding, F. Frederiksen, I. Z. Kovacs, D. Laselva, and P. E. Mogensen, "An overview of downlink radio resource management for UTRAN long-tem evolution," IEEE Commun. Mag., pp. 86–93, July 2009.

[42] H. Jia, Z. Zhang, G. Yu, P. Cheng, and S. Li, "On the performance of IEEE 802.16 OFDMA system under different frequency reuse and subcarrier permutation patterns," Proc. the IEEE ICC, pp. 5720–5725, June 2007.

[43] M. Rahman and H. Yanikomeroglu, "Enhancing cell-edge performance: a downlink dynamic interference avoidance scheme with inter-cell coordination," IEEE Trans. on Wireless Commun., vol. 9, no. 4, April 2010.

[44] L. Xu, K. Yamamoto, H. Murata, S. Yoshida, "Cell edge capacity improvement by using adaptive base station cooperation in cellular networks with fractional frequency reuse," IEICE Trans. on Comm. vol. E93-B, No. 7, pp. 1912–1918, July 2010.

[45] X. Mao, A. Maaref, and K. H. Teo, "Adaptive soft frequency reuse for inter-cell interference coordination in SC-FDMA based 3GPP LTE uplinks," IEEE GLOBECOM Proc., pp. 1–6, Nov./Dec. 2008.

[46] R. Y. Chang, Z. Tao, J. Zhang, and C.-C. J. Kuo, "A graph approach to dynamic fractional frequency reuse (FFR) in multi-cell OFDMA networks," IEEE ICC Proc., pp. 1–6, June 2009.

[47] Z. Xie, and B. Walke, “Enhanced fractional frequency reuse to increase capacity of OFDMA systems,” IEEE NTMS Proc., pp. 1–5, Dec. 2009.

[48] P. Lee, T. Lee, J. Jangkeun, and J. Shin, “Interference management in LTE femtocell systems using fractional frequency reuse,” IEEE ICACT Proc., pp. 1047–1051, Feb. 2010.

[49] I. Cho, S.-J. Kim, and C.-H. Cho, “Resource allocation for interference avoidance in OFDMA-TDD based femtocell networks,” IEICE. Trans. Commun., vol.E95-B, no. 5, pp. 1886-1889, May 2012.

[50] Z. Zhao, F. Zheng, A. Wilzeck, and T. Kaiser, “Femtocell spectrum access underlaid in fractional frequency reused macrocell,” IEEE ICC Proc., pp. 1–6, June 2011.

[51] A. S. Afolabi, E. Munkbat, C. Ohta, and H. Tamaki, “Fair resource partitioning between cell-center and cell-edge of FFR-based multi-tier wireless access networks,” IEEE WiCOM Proc., Sept. 2011.

[52] I. Katzela and M. Naghshineh, “Channel assignment schemes for cellular mobile telecommunication systems: a comprehensive survey,” IEEE Personal Commun., vol. 3, no. 2, pp. 10–31, June 1996.

[53] C. Lee, J.-H Huang, and L.-C. Wang, “Distributed channel selection principles for femtocells with two-tier interference,” IEEE VTC Proc., pp. 1–5, May 2010.

[54] 3GPP TR 25.892 v6.0.0, “Feasibility study for Orthogonal frequency division multiplexing (OFDM) for UTRAN enhancement,” June 2004.

[55] J. G. Andrews, A. Ghosh, and R. Muhamed, "Fundamentals of WiMAX: understanding broadband wireless networking," Prentice Hall, 2007.

[56] L. Chen, W. Chen, X. Zhang, and D. Yang, "Analysis and simulation for spectrum aggregation in LTE-advanced system," IEEE VTC Proc., pp. 1–6, Sept. 2009.

[57] B. Kaufman, E. Erkip, J. Lilleberg, and B. Aazhang, "Femtocells in cellular radio networks with successive interference cancellation," IEEE ICC Proc., pp 1–5, June 2011.

[58] K.-T. Cho, J. Kim, and G. Jeon, "Interference management for LTE femtocell system using power control," IEICE Trans. on Commun., vol. E95-B, no. 5, May 2012.

[59] L. G. U. Garcia, K. I. Perdersen, and P. E. Mogensen, "Autonomous component carrier selection: interference management in local area environments," IEEE Commun. Mag., vol. 47, no. 9, pp. 110-116, 2009.

[60] 3GPP R4-092042 , "Simulation assumptions and parameters for FDD HeNB RF requirements," Alcatel-Lucent, May 2009.

[61] G. de la Roche, A. Valcarce, and D. Lopez-Perez, "Access control mechanisms for femtocells," IEEE Commun. Mag., pp. 33–39, Jan. 2010.

[62] 3GPP TR 25.820, v8.2.0, "Technical specification group radio access networks; 3G home nodeB study item technical report," Sept. 2008.

[63] D. L-Perez, A. Ladanyi, A. Juttner, and J. Zhang, "Intracell handover for interference and handover mitigation in OFDMA two-tier macrocell-femtocell networks," EURASIP Journal on Wireless Commun. and Networking, vol. 2010, pp. 1–15, Feb. 2010.

[64] R. Jain, "The art of computer systems performance analysis: techniques for experimental design, measurement, simulation and modeling," John Wiley & Sons Inc., 1991.

[65] H. Claussen, L. T. W. Ho, and L. G. Samuel, "Self-optimization of coverage for femto cell deployments," Wireless Telecomm. Symposium, pp. 278–285, April 2008.

[66] X. Li, L. Qian, and D. Kataria, "Downlink power control in co-channel macrocell femto cell overlay," Conference on Information Science and Systems, pp. 383–388, March 2009.

[67] H.-S. Jo, J.-G. Yook, C. Mun, J. Moon, "A self-organized uplink power control for cross-tier interference management in femtocell networks," IEEE MILCOM Proc., pp. 1–6, Nov. 2008.

[68] S.-Y. Lien, C.-C Tseng, K.-C Chen, and C.-W Su, "Cognitive radio resource management for QoS guarantees in autonomous femtocell networks," IEEE ICC Proc., pp. 1–6, May 2010.

[69] K.C. Chen and R. Prasad, "Cognitive radio networks," John Wiley and Sons, 2009.

[70] Z. Bharucha, A. Saul, G. Auer, and H. Haas, "Dynamic resource partitioning for downlink femto-to-macro-cell interference avoidance", EURASIP Journal on Wireless Commun. and Networking, vol. 2010, April 2010.

[71] A. S. Afolabi, C. Ohta, and H. Tamaki, "Macrocell batch resource allocation for a closed access femto-macro cellular wireless network," IEEE WiOpt Proc., May 2011.

[72] 3GPP TR 36.211 v9.0.0, "Evolved universal terrestrial radio access (E-UTRA); Physical channels and modulation," Dec. 2009.

[73] C. Gessner,"UMTS long term evolution (LTE) technology introduction," `http://www2.rohde-schwarz.com/file_10948/1MA111_2E.pdf,` accessed on 18.2.2012, Sept., 2008.

[74] S.-B. Lee, I. Perfkianakis, A. Meyerson, S. Xu, and S. Lu, "Proportional fair frequency-domain packet scheduling for 3GPP LTE uplink," IEEE INFOCOM Proc., pp. 2611–2615, April 2009.

[75] 3GPP TR 36.942 v8.2.0, "Evolved universal terrestrial radio access (E-UTRA); radio frequency (RF) system scenarios," May 2009.

List of Publications

Publications in International Journals

A. S. Afolabi, E. Munkhbat, Y. Takaki, C. Ohta, H. Tamaki, Y. Tanaka, T. Yamamoto, and Y. Okada,“Fair partitioning of the downlink resources of an OFDMA-based multi-user multi-tier cellular network using fractional frequency reuse,” IEICE Transactions on Communications, vol. E95–B, no. 10, Oct. 2012 (printing in progress).

A. S. Afolabi, C. Ohta, and H. Tamaki, “A novel co-operative channel assignment scheme for indoor base stations,” Global Science and Technology Forum (GSTF) International Journal on Computing, vol. 1, no. 2, pp. 205–210, Feb 2011.

A. S. Afolabi, Y. Takaki, C. Ohta, and H. Tamaki, Y. Tanaka, T. Yamamoto, and Y. Okada, “A batch resource allocation scheme for co-channel interference reduction in macro-femto cell closed access networks,” IEICE Transactions on Communications (conditional acceptance).

Publication in the Proceedings of International Conferences

A. S. Afolabi, E. Munkhbat, C. Ohta, and H. Tamaki,“Fair resource partitioning between cell-center and cell-edge of FFR-based multi-tier wireless access networks,” IEEE WiCOM Proc., pp. 1–4, Sept. 2011.

A. S. Afolabi, C. Ohta, and H. Tamaki,“Macrocell batch resource allocation for a closed access femto-macro cellular wireless network,” IEEE WiOpt Proc., pp. 434–439, May 2011.

A. S. Afolabi, C. Ohta, and H. Tamaki,“A base station co-operation protocol for indoor base stations,” Global Science and Technology Forum (GSTF) NTC Proc., pp. N37–N42, Nov. 2010.